
DEFI'S CONCENTRATED LIQUIDITY FROM SCRATCH

REVIEW

Mark B. Richardson*
Bancor Protocol
Zug, Switzerland
mark@bancor.network

Stefan Loesch
Topaze Blue
London, United Kingdom
stefan@topaze.blue

Edited: August 25, 2024
Original: July 4, 2024

ABSTRACT

The scope of this article includes the three preminent descriptions of concentrated liquidity from Bancor (2020 and 2022), and Uniswap (2021), as well as three additional descriptions informed by trigonometric analysis of the same. The purpose of this contribution is to organize the seminal and derivative forms of this cornerstone DeFi technology, and algebraically and geometrically elaborate these descriptions to achieve an authoritative and near-exhaustive overview of the underlying theory powering the current state-of-the-art in decentralized exchange infrastructure.

This material was created for the Token Engineering Academy Study Season 2024,² a cohort-based online program scheduled for April–July 2024. The Study Season offers access to a bachelor-level online learning program, and complementary live tracks with the most influential practitioners and researchers in the sector – all provided as free, public goods.

Keywords Bonding Curve · Concentrated Liquidity · Automatic Market Maker · Decentralized Exchange · Blockchain · Smart Contracts · Bancor · Uniswap · Carbon DeFi

*To whom correspondence should be addressed.

²tokenengineering.net

Contents

1	Introduction	3
2	The Basics: Elementary Analysis of the Reference Curve	3
3	The Seminal Concentrated Liquidity Invariant	9
3.1	The Bancor v2 Virtual Curve	9
3.2	The Bancor v2 Real Curve	20
4	Other “Unnatural” Reparameterizations of the Concentrated Liquidity Invariant Function	31
4.1	The Uniswap v3 Real Curve	31
4.2	The Uniswap v3 Virtual Curve	41
4.3	The Uniswap v3 Reference Curve	45
4.4	The Carbon DeFi Real Curve	48
4.5	The Carbon DeFi Virtual Curve	58
4.6	The Carbon DeFi Reference Curve	64
5	The “Natural” Reparameterizations of the Concentrated Liquidity Invariant Function	67
5.1	Three “Pretty” Invariants	68
5.2	Transforming and Normalizing the Curves in a New Coordinate System	73
5.3	The Trigonometric Description of Liquidity Concentration	82
6	Conclusion	85

1 Introduction

The objective with this piece is to formally derive amplified (aka "concentrated liquidity") bonding curves from first principles, including their hyperbolic trigonometric descriptions. There are a plethora of white papers and research articles on the subject that do a fine job of elucidating these concepts with rigor. However, as often happens in pursuits of an academic nature, the literature has become somewhat piecemeal, and the establishing theory is no longer in vogue. Those steeped in the industry for several years have the benefit of experiencing the evolution of the technology over time, whereas new talent is left to contend with the patchy, unmaintained, and disorganized record that was left for them. Worse still, the lack of an editorial process combined with the conflation of research and marketing efforts has produced a sometimes confused, and often flawed knowledge base. More to the point of this article, even the high-quality papers are written for an exclusive audience, as evidenced by the skilled density of their composition which often sacrifices expository prose for brevity. As it should.

The impetus here is to take the opposite approach – one where the reader's erudition in DeFi is not assumed. Of course, these are technical concepts and so command a minimum working knowledge of algebra, calculus, and maybe a few other things. However, the presentation format is designed to resemble a study guide more than a technical disclosure. Therefore, those equipped with the necessary tools (e.g. undergraduate math, maybe high school!) can quickly orient themselves and get familiar with the theory and save some wasted effort.

The concentrated liquidity construction will begin from the description first published by Bancor in 2020, with an exclusive focus on the now familiar two-dimensional, equal weights variety, as this has now reached market saturation thanks largely to Uniswap v3. By itself, this is nothing to write home about. However, an additional step further is taken to arrive at a trigonometric description of these concepts and derive what we refer to as the three "natural" concentrated liquidity invariant equations. While these invariant equations have appeared previously in the Carbon DeFi Whitepaper³ and Invention Disclosure⁴, this may be the first time their trigonometric origins have been elaborated in a public forum.

2 The Basics: Elementary Analysis of the Reference Curve

This exercise begins truly from scratch, with an empty Cartesian plane (Figure 1).

Choose any point $(x = x_0, y = y_0)$. This point represents your beginning token balances. The choice of these token balances is not incidental, and we will revisit this in a moment. For now, let x_0 and y_0 be any positive real number (Figure 2).

Then, draw a rectangular hyperbola through this point. In its original 2017 form,⁵ the invariant was general, allowing for the x - and y -axis to be scaled independently (Equation 1).

$$x^\alpha \cdot y^\beta = x_0^\alpha \cdot y_0^\beta \quad (1)$$

Most of the industry has settled on the requirement for equal exponents, $\alpha = \beta$, which simplifies the invariant function a little (Equation 2).

$$\text{from} \quad x \cdot y = x_0 \cdot y_0 \quad (2)$$

While the general and multi-dimensional form is still very much in operation, the remainder of this exercise will focus exclusively on the two-dimensional equal-weights variety.

To constrain the complexity of our discussion, we will ignore the [poorly named] "fee" parameter, which deserves a dedicated exposé. Therefore, this curve represents all the allowed token balances for your liquidity pool, and anyone can change the token balances so long as those balances satisfy the predicate $x \cdot y = x_0 \cdot y_0$. This means that someone can add additional tokens to the liquidity pool in one dimension (e.g. Δx) and remove tokens from the other dimension (e.g. Δy), thus performing a trade with you. To satisfy the predicate, the token trade amounts Δx and Δy can be easily calculated as follows (Equations 3, 4 and 5).

$$\text{from} \quad (x + \Delta x) \cdot (y + \Delta y) = x_0 \cdot y_0 \quad (3)$$

³resources.carbondefi.xyz/pages/CarbonWhitepaper.pdf

⁴resources.carbondefi.xyz/pages/CarbonPatent.pdf

⁵Hertzog, E.; Benartzi, G.; Benartzi, G.; Levi, Y. Methods for Exchanging and Evaluating Virtual Currency

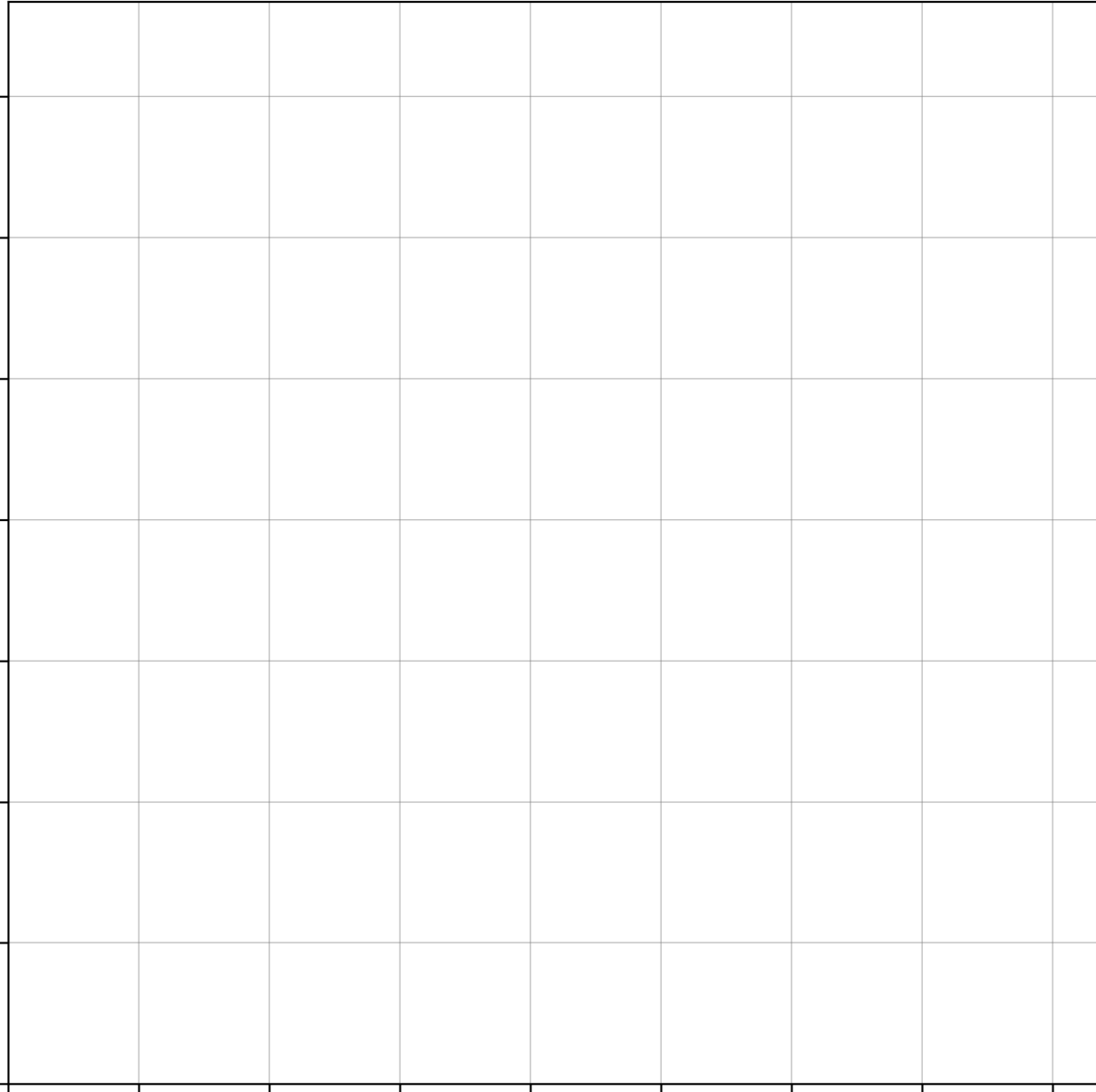


Fig. 1 An empty Cartesian plane.

from
(3)

$$\Delta x = \frac{x_0 \cdot y_0}{y + \Delta y} - x \quad (4)$$

from
(3)

$$\Delta y = \frac{x_0 \cdot y_0}{x + \Delta x} - y \quad (5)$$

The calculation can be made dependent on only one of either the x or y coordinates by substituting their identities in terms of each other (Equations 6 and 8), and the x_0 and y_0 constants (Equations 7 and 9).

from
(2)

$$x = \frac{x_0 \cdot y_0}{y} \quad (6)$$

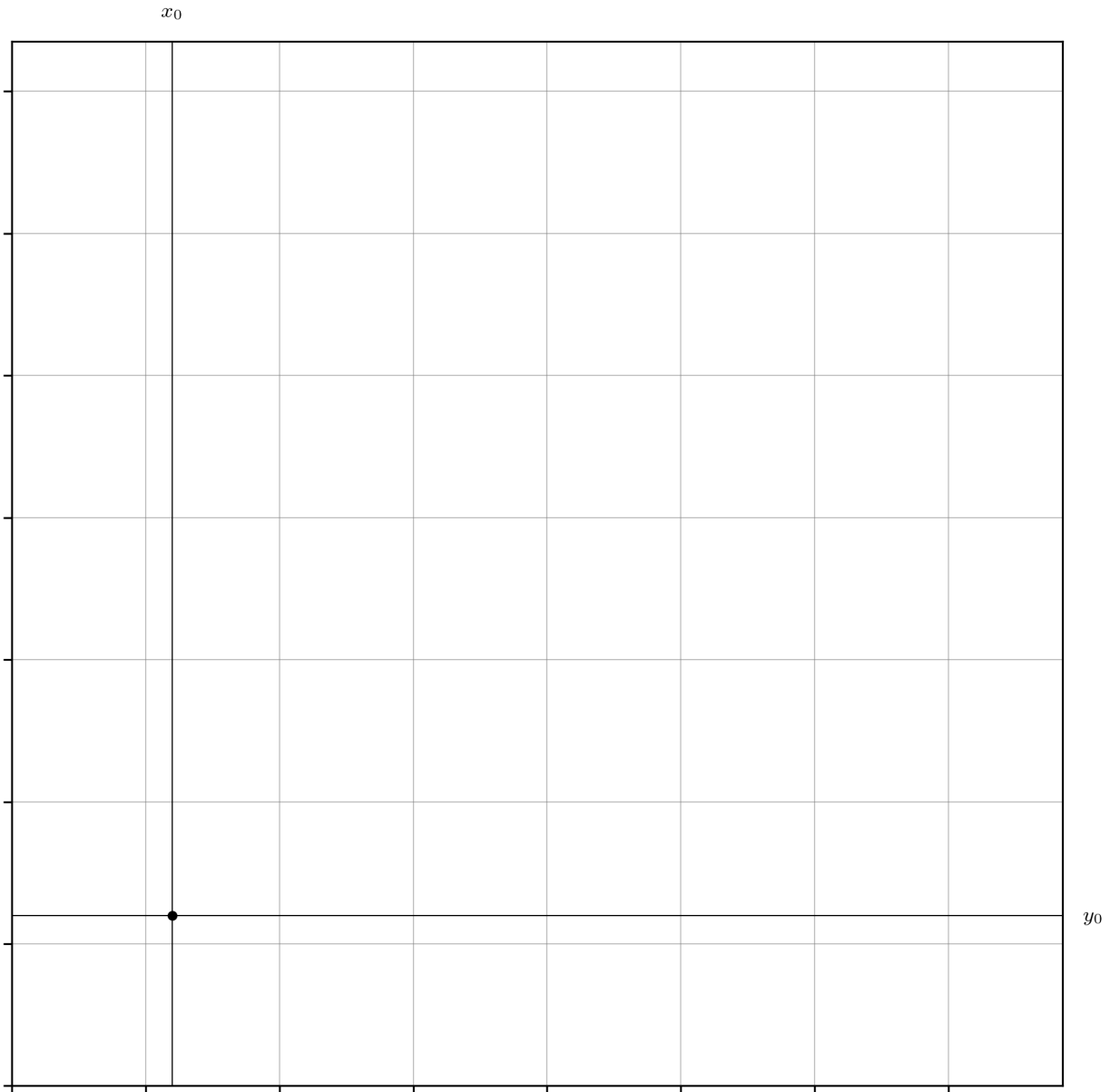


Fig. 2 The point $x = x_0, y = y_0$.

$$\begin{array}{l} \text{from} \\ (4) \\ (6) \end{array} \quad \Delta x = \frac{x_0 \cdot y_0}{y + \Delta y} - \frac{x_0 \cdot y_0}{y} = -\frac{\Delta y \cdot x_0 \cdot y_0}{y \cdot (y + \Delta y)} \quad (7)$$

$$\begin{array}{l} \text{from} \\ (2) \end{array} \quad y = \frac{x_0 \cdot y_0}{x} \quad (8)$$

$$\begin{array}{l} \text{from} \\ (5) \\ (8) \end{array} \quad \Delta y = \frac{x_0 \cdot y_0}{x + \Delta x} - \frac{x_0 \cdot y_0}{x} = -\frac{\Delta x \cdot x_0 \cdot y_0}{x \cdot (x + \Delta x)} \quad (9)$$

There are a few important notes here. First, it is important to remember that Δx and Δy have opposite signs with respect to each other; a positive change in one dimension is always coupled with a negative change in the opposite

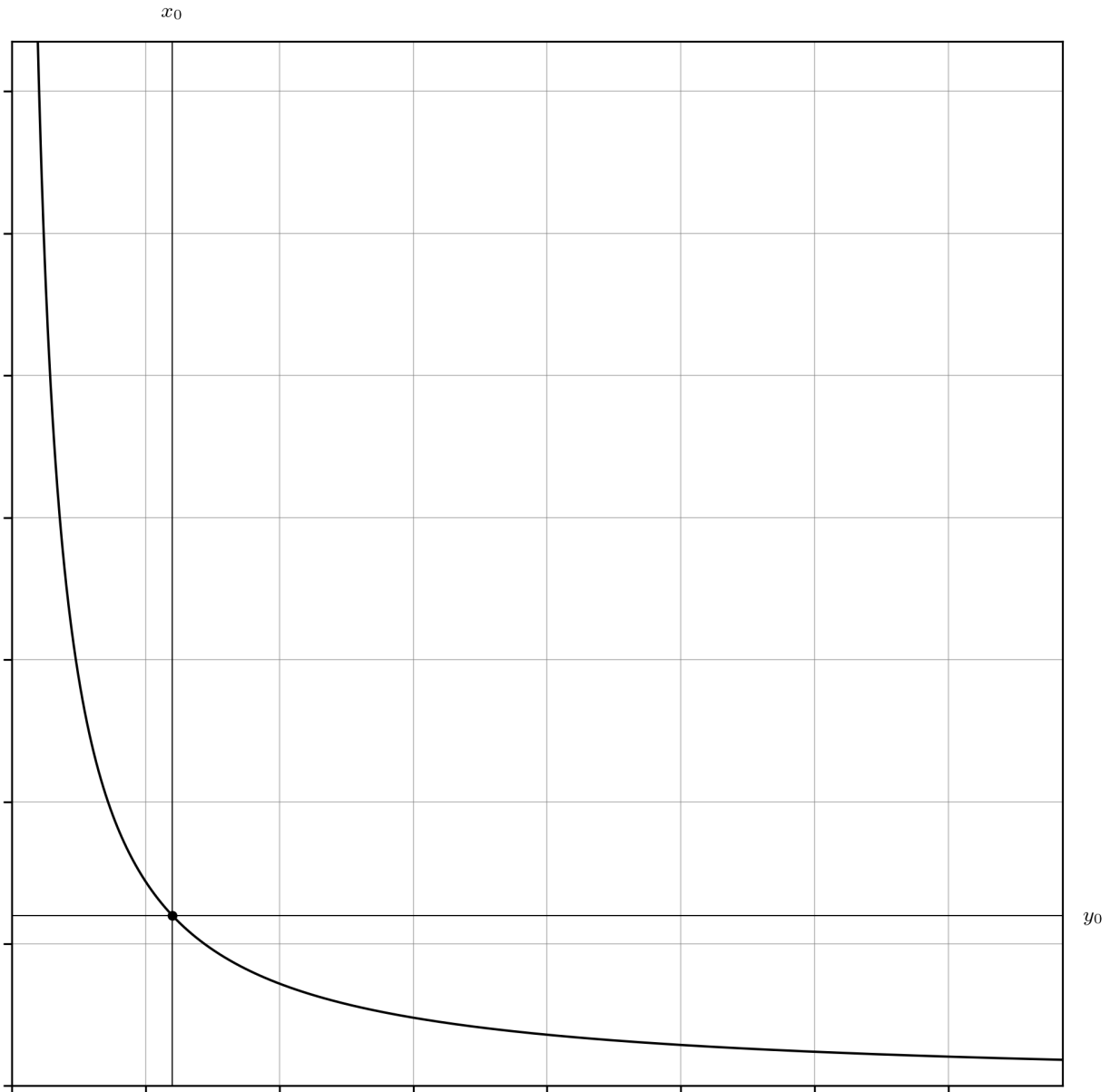


Fig. 3 The rectangular hyperbola $x \cdot y = x_0 \cdot y_0$ (Equation 2), necessarily passing through the point $x = x_0, y = y_0$.

dimension. If $\Delta x > 0$, then $\Delta y < 0$ and vice-versa. Secondly, these are not the familiar swap equations you will see elsewhere, but rest assured they are redundant forms. The representations chosen here have explicit x_0 and y_0 constants to help to maintain consistency with the rest of the theory as it is presented below. To derive the more common forms, consider that the $x_0 \cdot y_0$ term in Equations 4, and 5 can be substituted for $x \cdot y$, as implied by the invariant function (Equation 2), which allows for further simplification (Equations 10, and 11). Note that this refactoring makes the sign inversion of Δx and Δy explicit, which is appropriate given the liquidity pool's frame of reference and preserves consistency with some of the other manipulations we are going to explore. However, it is common to present these equations with a moving frame of reference, where both $\Delta x > 0$ and $\Delta y > 0$. While this is likely a reflection of their unsigned implementation in smart contracts, it also breaks a pleasing symmetry in the algebra and so is not the convention used here. Traversal upon the implicit curve representing a token swap is depicted in Figure 4.

from (7)
$$\Delta x = -\frac{\Delta y \cdot x \cdot y}{y \cdot (y + \Delta y)} = -\frac{\Delta y \cdot x}{y + \Delta y} \quad (10)$$

from (9)
$$\Delta y = -\frac{\Delta x \cdot x \cdot y}{x \cdot (x + \Delta x)} = -\frac{\Delta x \cdot y}{x + \Delta x} \quad (11)$$

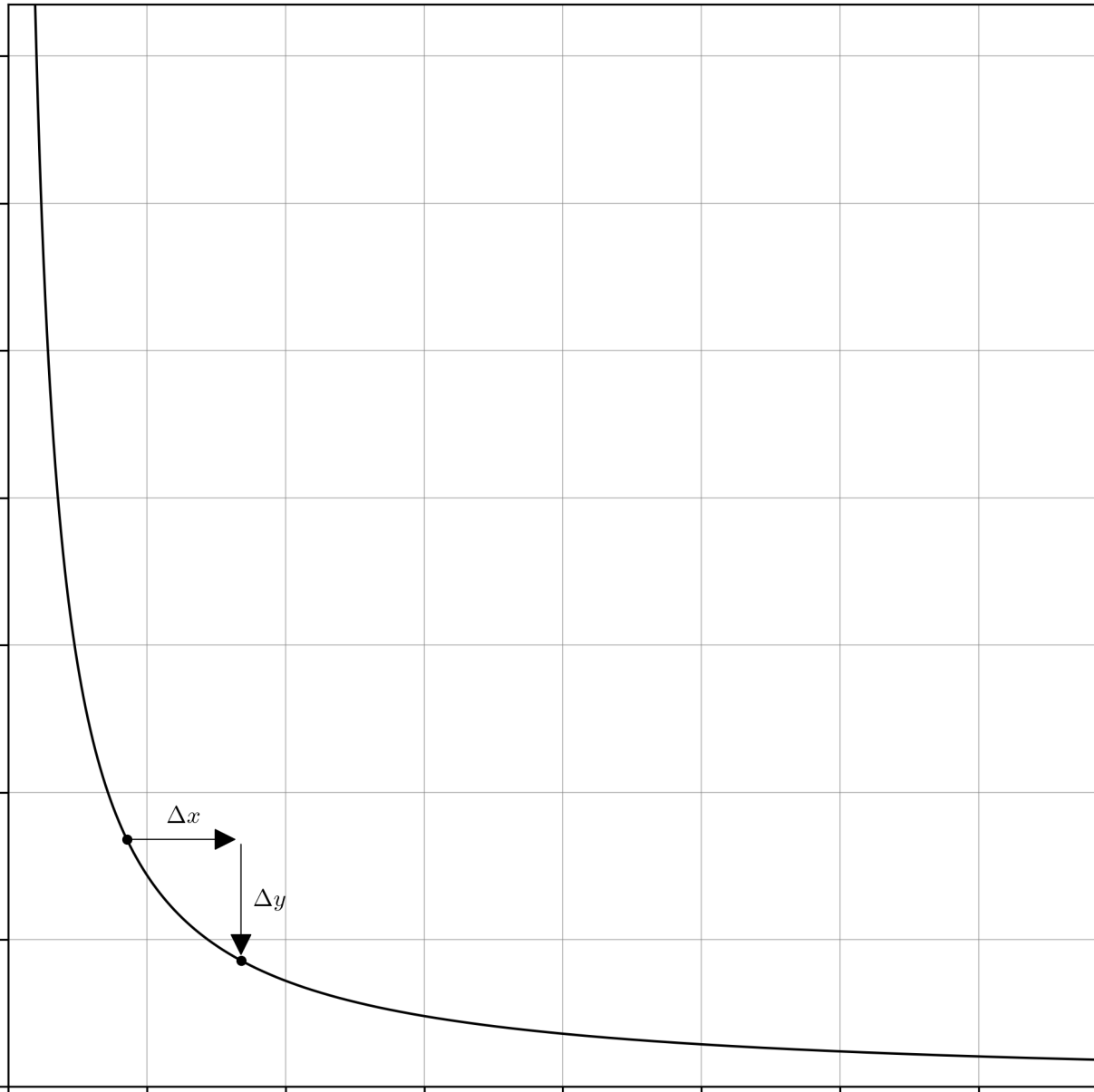


Fig. 4 The traversal upon the rectangular hyperbola $x \cdot y = x_0 \cdot y_0$ (Equation 2) representing a token swap against the liquidity pool, where $\Delta x > 0$ and $\Delta y < 0$.

From here, we can derive the marginal rate of exchange in two convenient ways. First, we can rearrange Equations 10 and 11 to get the *effective rate of exchange* (Equations 12 and 14), then take the limit as the denominator goes to zero (Equations 13 and 15) to determine the *instantaneous rate of exchange* (i.e. the marginal price).

$$\begin{array}{l} \text{from} \\ (10) \end{array} \quad \frac{\Delta x}{\Delta y} = -\frac{x}{y + \Delta y} \quad (12)$$

$$\begin{array}{l} \text{from} \\ (12) \end{array} \quad \frac{\partial x}{\partial y} = \lim_{\Delta y \rightarrow 0} \frac{\Delta x}{\Delta y} = -\frac{x}{y} \quad (13)$$

$$\begin{array}{l} \text{from} \\ (11) \end{array} \quad \frac{\Delta y}{\Delta x} = -\frac{y}{x + \Delta x} \quad (14)$$

$$\begin{array}{l} \text{from} \\ (14) \end{array} \quad \frac{\partial y}{\partial x} = \lim_{\Delta x \rightarrow 0} \frac{\Delta y}{\Delta x} = -\frac{y}{x} \quad (15)$$

Alternatively, rearrangement of Equation 2 to make either x or y the subject (Equations 6 and 8), followed by differentiation with respect to the other term while treating x_0 and y_0 as constants delivers an equivalent result (Equations 16 and 17). Again, this form is less familiar, but also more analytically robust and consistent with the bulk of the following presentation.

$$\begin{array}{l} \text{from} \\ (6) \end{array} \quad \frac{\partial x}{\partial y} = -\frac{x_0 \cdot y_0}{y^2}; \quad \frac{\partial y}{\partial x} = -\frac{y^2}{x_0 \cdot y_0} \quad (16)$$

$$\begin{array}{l} \text{from} \\ (8) \end{array} \quad \frac{\partial y}{\partial x} = -\frac{x_0 \cdot y_0}{x^2}; \quad \frac{\partial x}{\partial y} = -\frac{x^2}{x_0 \cdot y_0} \quad (17)$$

It is important to recognize that the marginal rates of exchange, $\partial x/\partial y$ and $\partial y/\partial x$, are commensurate with price quotes. These are the onchain oracle prices for the token pair (simplified, but close enough) and represent the current price for a trade value of zero, whereas the effective price experienced during a trade is dependent on the trade amounts and the token balances inside the liquidity pool (Equations 12 and 14).

To complete this part of the exercise, consider that the familiar implicit curve of the invariant function, or bonding curve, is the integrated form of the price function. Therefore, the swap equations can also be derived from explicit integration of Equations 16 and 17 over the interval representing the number of tokens being swapped (Equations 18 and 19, which yield results identical to Equations 7 and 9). The integration above $\partial y/\partial x = -x_0 \cdot y_0/x^2$ over the interval $x \rightarrow x + \Delta x$ representing a token swap is depicted in Figure 5.

$$\begin{array}{l} \text{from} \\ (16) \end{array} \quad \Delta x = -\int_y^{y+\Delta y} \frac{x_0 \cdot y_0}{y^2} \cdot \partial y = \left[\frac{x_0 \cdot y_0}{y} \right]_y^{y+\Delta y} \Rightarrow \text{Eqn. 7} \quad (18)$$

$$\begin{array}{l} \text{from} \\ (17) \end{array} \quad \Delta y = -\int_x^{x+\Delta x} \frac{x_0 \cdot y_0}{x^2} \cdot \partial x = \left[\frac{x_0 \cdot y_0}{x} \right]_x^{x+\Delta x} \Rightarrow \text{Eqn. 9} \quad (19)$$

Take special note that integration of the more familiar price functions over the same interval requires a more considered approach, as x and y vary with each other. Beginning from the previously obtained differential equations (Equations 13 and 15), first separate the x and y variables across the equality (Equation 20) then evaluate their definite integrals over $x \rightarrow x + \Delta x$ and $y \rightarrow y + \Delta y$, independently (Equations 21 and 22). Following that, the minuends and subtrahends resulting from integration of each variable are transformed into their corresponding quotients via the properties of logarithms (Equation 23). Then, rearrangement of the expressions thus obtained to isolate either Δx or Δy gives Equations 24 and 25, which can be further simplified to recreate the identities previously obtained (Equations 10 and 11).

$$\begin{array}{l} \text{from} \\ (13) \\ (15) \end{array} \quad \frac{1}{y} \cdot \partial y = -\frac{1}{x} \cdot \partial x \quad (20)$$

$$\text{from (20)} \quad \int_y^{y+\Delta y} \frac{1}{y} \cdot \partial y = - \int_x^{x+\Delta x} \frac{1}{x} \cdot \partial x = [\ln(y)]_y^{y+\Delta y} = - [\ln(x)]_x^{x+\Delta x} \quad (21)$$

$$\text{from (21)} \quad \ln(y + \Delta y) - \ln(y) = \ln(x) - \ln(x + \Delta x) \quad (22)$$

$$\text{from (22)} \quad \ln\left(\frac{y + \Delta y}{y}\right) = \ln\left(\frac{x}{x + \Delta x}\right) \Rightarrow \frac{y + \Delta y}{y} = \frac{x}{x + \Delta x} \quad (23)$$

$$\text{from (23)} \quad \Delta x = -x \cdot \left(1 - \frac{y}{y + \Delta y}\right) \Rightarrow \mathbf{Eqn. 10} \quad (24)$$

$$\text{from (23)} \quad \Delta y = -y \cdot \left(1 - \frac{x}{x + \Delta x}\right) \Rightarrow \mathbf{Eqn. 11} \quad (25)$$

Therefore, the implicit curve of the invariant function and its first derivative are equally valid expressions of the underlying theory, and the preference for presenting only one or the other is an arbitrary choice. You should expect to see a combination of both throughout the DeFi whitepaper literature.

Something important to note here is that the price equation is asymptotic at $\partial y/\partial x = 0$ and $\partial y/\partial x = -\infty$ for all real positive token balances, $\forall x, y \in \mathbb{R}^+$. Therefore, the $x \cdot y = x_0 \cdot y_0$ invariant can quote any price, regardless of the relative values of the underlying tokens. This property is sacrificed in the concentrated liquidity extension.

3 The Seminal Concentrated Liquidity Invariant

The original motivation for concentrated liquidity has been articulated in Bancor's announcement blog^{6,7} on April 29, 2020, and later in Uniswap's announcement blog⁸ on March 22, 2021.

Here is the short version. Two different liquidity pools will offer the same *marginal exchange rate* if the ratio of their token balances is identical (Equations 13, 15, 16 and 17); however, the liquidity pool with the larger absolute quantity of tokens can offer a better *effective exchange rate* for the same trade amount than the smaller pool (Equations 12 and 14). The improvement in the overall exchange rate on the larger pool for the same trade quantities is the same as observing that the larger pool has a reduced slippage compared to the smaller pool (these are equivalent statements).

Similarly, for the same effective exchange rate, or for the same relative move in the market price of the two tokens inside the liquidity pool, the larger pool can process a larger trade volume than the smaller one. In other words, it takes a larger trade volume to move the marginal price of the larger pool compared to the smaller one. If these characteristics of the larger pool are desirable, then the smaller pool can *pretend* to be equivalent in size, thereby achieving the same exchange rate profile and supporting larger trade volumes. The caveat is that emulation of the larger curve also restricts the price interval over which it operates.

3.1 The Bancor v2 Virtual Curve

To begin this part of the exercise, suppose that the starting coordinates chosen for Figure 3 are multiplied by an amplification constant, A , to give new virtual coordinates, x_v and y_v (Figure 6). Then, draw through this new point the same rectangular hyperbola as we have before (Equation 26) (Figure 7). The only difference between Equations 2 and 26 is that the invariant part of the latter is increased by the square of the amplification constant.

$$\text{from (2)} \quad x_v \cdot y_v = (A \cdot x_0) \cdot (A \cdot y_0) = A^2 \cdot x_0 \cdot y_0 \quad (26)$$

⁶Hertzog, E.; Levi, Y.; Manos, B.; Shachaf, A.; Benartzi, G. Smart Contract of a Blockchain for Management of Cryptocurrencies

⁷blog.bancor.network/announcing-bancor-v2-2f56b515e9d8

⁸blog.uniswap.org/uniswap-v3

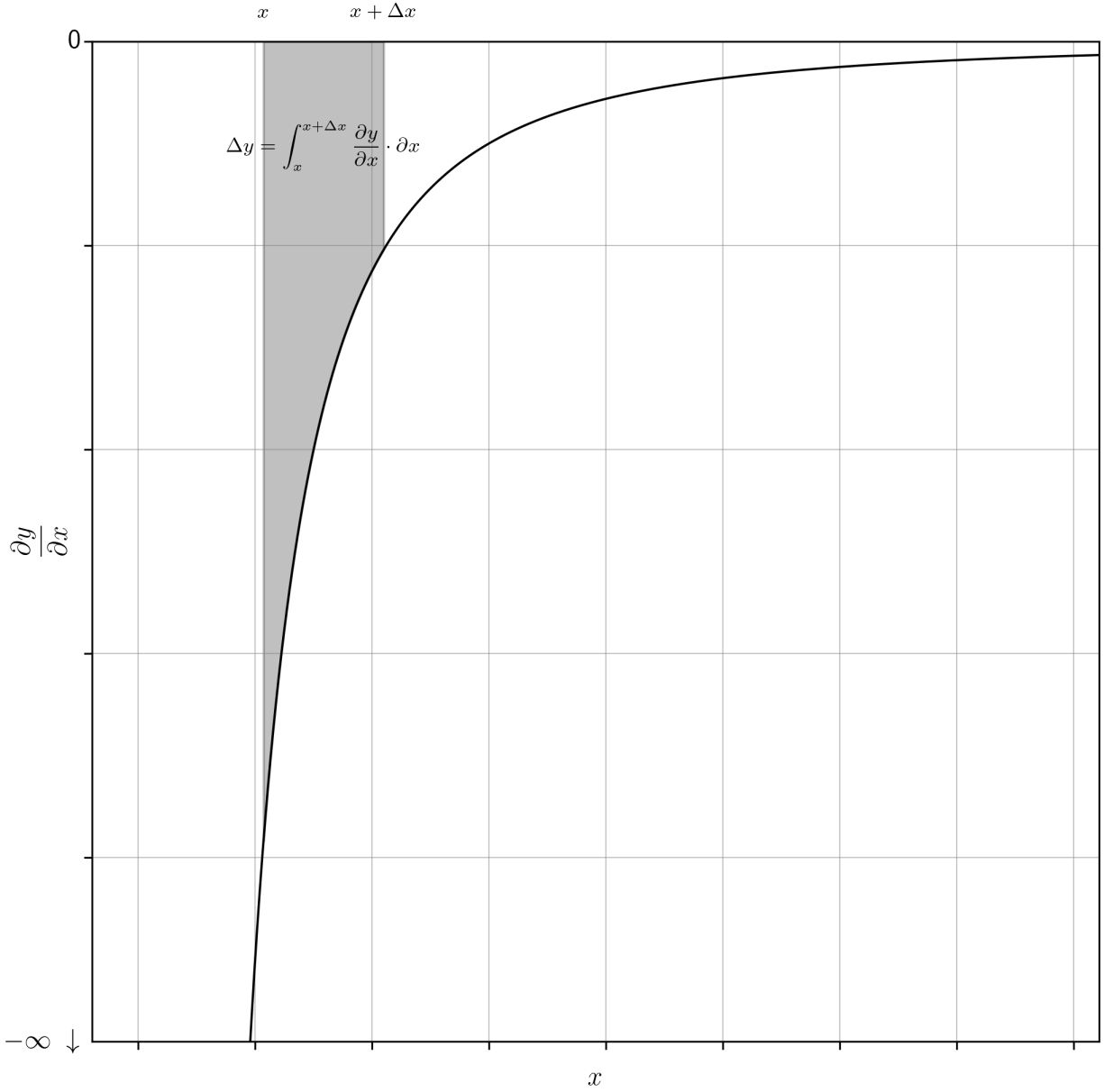


Fig. 5 The integration above $\frac{\partial y}{\partial x} = -x_0 \cdot y_0 / x^2$ (Equation 17) over the interval $x \rightarrow x + \Delta x$ representing a token swap against the liquidity pool, where $\Delta x > 0$ and $\Delta y < 0$.

The amplified $x_v \cdot y_v = A^2 \cdot x_0 \cdot y_0$ curve has the same properties as its $x \cdot y = x_0 \cdot y_0$ counterpart. The expressions above that explicitly refer to the constants x_0 and y_0 (Equations 3, 4, 5, 6, 7, 8, 9, 16, and 17) can be adapted easily by introducing the amplification constant as appropriate (Equations 27, 28, 29, 30, 31, 32, 33, 34 and 35).

$$\begin{array}{l} \text{from} \\ (8) \end{array} \quad y_v = \frac{A^2 \cdot x_0 \cdot y_0}{x_v} \quad (27)$$

$$\begin{array}{l} \text{from} \\ (6) \end{array} \quad x_v = \frac{A^2 \cdot x_0 \cdot y_0}{y_v} \quad (28)$$

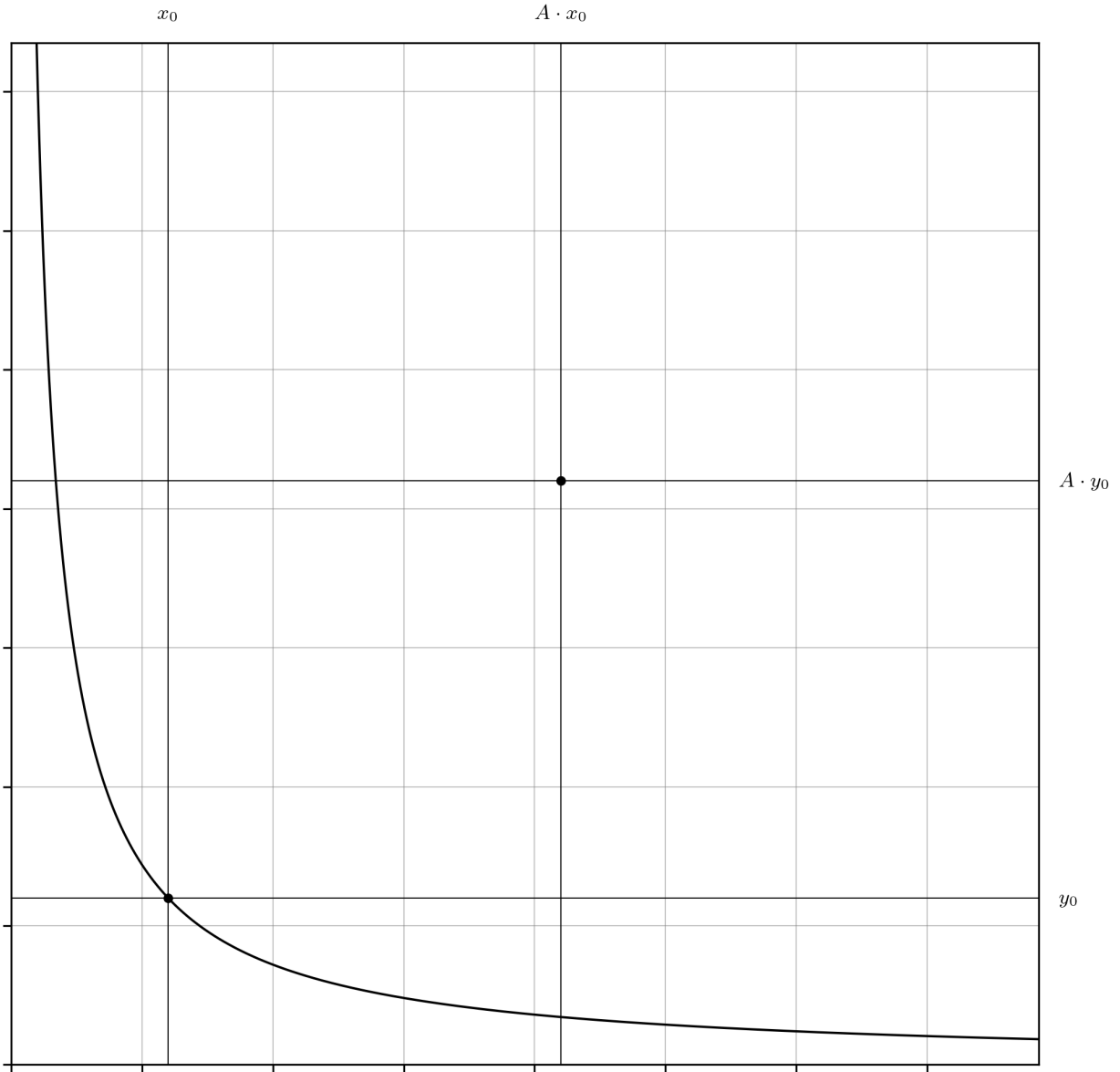


Fig. 6 The point $(x_v = A \cdot x_0, y_v = A \cdot y_0)$, appended to the plot depicted in Figure 3.

$$\begin{array}{l} \text{from} \\ (3) \end{array} \quad (x_v + \Delta x) \cdot (y_v + \Delta y) = A^2 \cdot x_0 \cdot y_0 \quad (29)$$

$$\begin{array}{l} \text{from} \\ (4) \end{array} \quad \Delta x = \frac{A^2 \cdot x_0 \cdot y_0}{y_v + \Delta y} - x_v \quad (30)$$

$$\begin{array}{l} \text{from} \\ (7) \end{array} \quad \Delta x = -\frac{\Delta y \cdot A^2 \cdot x_0 \cdot y_0}{y_v \cdot (y_v + \Delta y)} \quad (31)$$

$$\begin{array}{l} \text{from} \\ (5) \end{array} \quad \Delta y = \frac{A^2 \cdot x_0 \cdot y_0}{x_v + \Delta x} - y_v \quad (32)$$

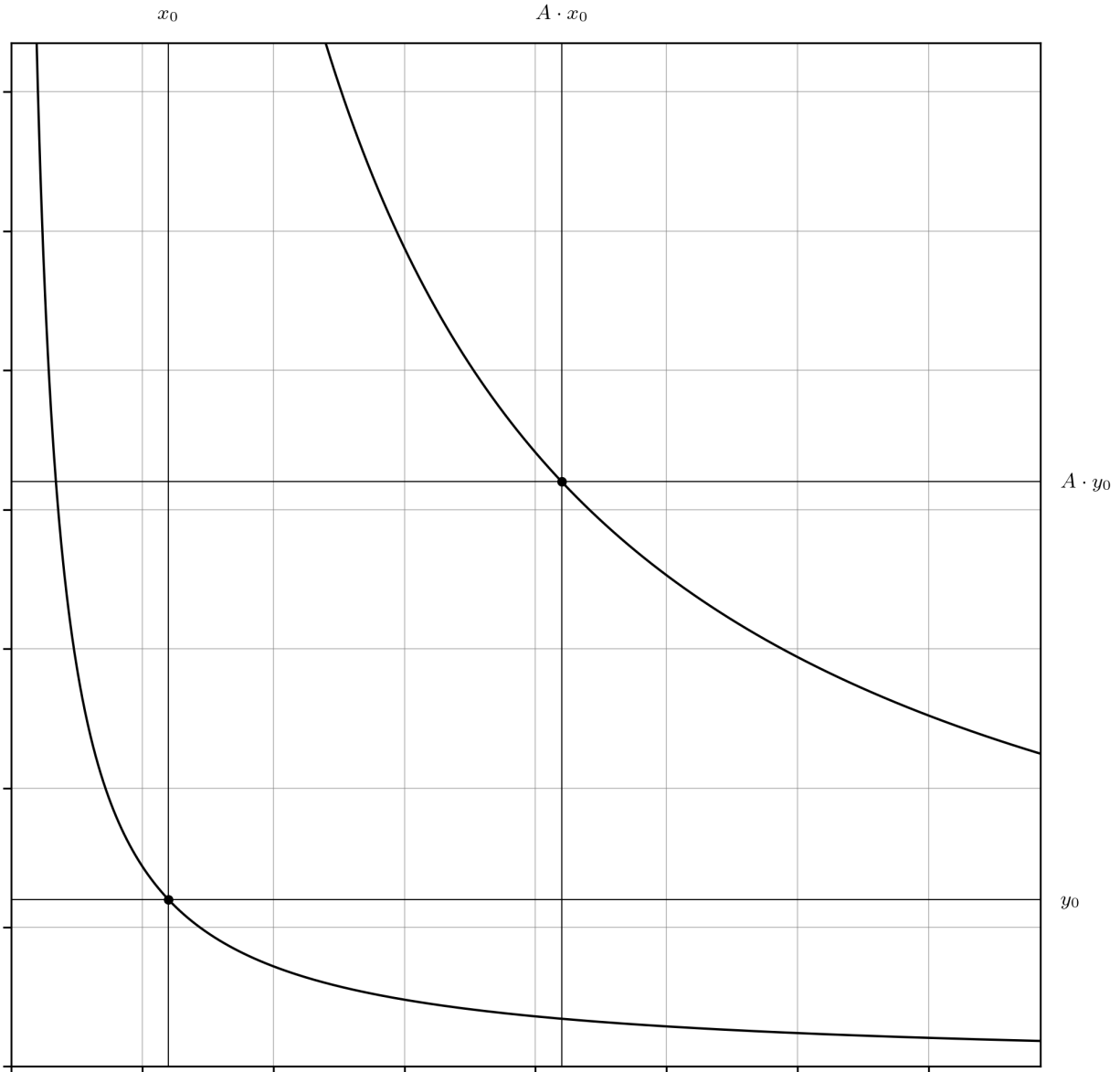


Fig. 7 The rectangular hyperbola $x_v \cdot y_v = A^2 \cdot x_0 \cdot y_0$ (Equation 26), necessarily passing through the point $(x_v = A \cdot x_0, y_v = A \cdot y_0)$.

$$\text{from (9)} \quad \Delta y = -\frac{\Delta x \cdot A^2 \cdot x_0 \cdot y_0}{x_v \cdot (x_v + \Delta x)} \quad (33)$$

$$\text{from (16)} \quad \frac{\partial x_v}{\partial y_v} = -\frac{A^2 \cdot x_0 \cdot y_0}{y_v^2}; \quad \frac{\partial y_v}{\partial x_v} = -\frac{y_v^2}{A^2 \cdot x_0 \cdot y_0} \quad (34)$$

$$\text{from (17)} \quad \frac{\partial y_v}{\partial x_v} = -\frac{A^2 \cdot x_0 \cdot y_0}{x_v^2}; \quad \frac{\partial x_v}{\partial y_v} = -\frac{x_v^2}{A^2 \cdot x_0 \cdot y_0} \quad (35)$$

More significantly, the expressions that ignore the x_0 and y_0 terms (Equations 10, 11, 12, 13, 14, and 15) can be used verbatim; they are intrinsically self-referential with respect to the size of the curve, emulated or not, and so no correction

is required. However, both the explicitly amplified and uncorrected expressions make no attempt to compensate for the fact that the emulated curve is only pretending to have the liquidity it represents. In the common vernacular, these emulated token balances are referred to as *virtual token balances*, and the amplified curve as the *virtual curve*.

Since the virtual curve has only the original tokens that were used to create it, x_0 and y_0 , then it is possible to completely deplete its real token balances, regardless of its virtual token balances. Therefore, there are two boundaries to discover: the virtual token balances when the real x token balance is depleted, and when the real y token balance is depleted.

The derivation is straightforward. The virtual curve begins with $A \cdot x_0$ virtual x_v tokens and will become depleted when x_0 tokens have been traded out of it (Equations 36) (Figure 8). Let this be the minimum virtual x-coordinate, $\min(x_v)$; which is necessarily coupled with the maximum virtual y-coordinate, $\max(y_v)$. The identity of $\max(y_v)$ can be found by substitution of $\min(x_v)$ into Equation 27 (Equation 37).

$$\min(x_v) = A \cdot x_0 - x_0 = x_0 \cdot (A - 1) \quad (36)$$

from
(27)
(36)

$$\max(y_v) = \frac{A^2 \cdot x_0 \cdot y_0}{\min(x_v)} = \frac{A^2 \cdot y_0}{A - 1} \quad (37)$$

This process is repeated to discover the identity of the other boundary, with coordinates at $\max(x_v)$ and $\min(y_v)$ (Figure 9). The virtual curve begins with $A \cdot y_0$ virtual y tokens and is depleted when y_0 tokens have been traded out of it (Equation 38). The identity of $\max(x_v)$ can be found by substitution of $\min(y_v)$ into Equation 28 (Equation 39).

$$\min(y_v) = A \cdot y_0 - y_0 = y_0 \cdot (A - 1) \quad (38)$$

from
(28)
(36)

$$\max(x_v) = \frac{A^2 \cdot x_0 \cdot y_0}{\min(y_v)} = \frac{A^2 \cdot x_0}{A - 1} \quad (39)$$

Turning our attention now to the exchange rates implied at these points of interest. It is trivial that the gradient of the curves at the points (x_0, y_0) on the reference curve and $(A \cdot x_0, A \cdot y_0)$ on the virtual curve are equal (Equation 40); this identity is proved by substitution of these values into Equation 15 for the reference curve, or any of Equations 15, 34, or 35 for the virtual curve (Figure 10).

from
(15)
(34)
(35)

$$\frac{\partial y_v}{\partial x_v} = -\frac{A \cdot y_0}{A \cdot x_0} = -\frac{(A \cdot y_0)^2}{A^2 \cdot x_0 \cdot y_0} = -\frac{A^2 \cdot x_0 \cdot y_0}{(A \cdot x_0)^2} = -\frac{y_0}{x_0} \quad (40)$$

The price boundaries represented by $(\min(x_v), \max(y_v))$ and $(\max(x_v), \min(y_v))$ can be defined via a similar process; substituting their identities into any of Equations 15, 34, or 35 yields the same result (Equations 41 and 42). Note that since the price curves implied by both the virtual and reference curves each encompass the same range, $-\infty < \partial y_v / \partial x_v < 0, \forall x_v, y_v \in \mathbb{R}^+$ and $-\infty < \partial y / \partial x < 0, \forall x, y \in \mathbb{R}^+$, there must exist points on the reference curve where evaluation of the first derivative of $x \cdot y = x_0 \cdot y_0$ at these points yields the same marginal prices as the boundaries of the virtual curve. Geometrically, these are the unique points where tangent lines drawn on the reference curve are parallel to the tangent lines drawn at the boundaries of the virtual curve (Figure 11).

from
(36)
(37)

$$\frac{\partial y_v}{\partial x_v} = -\frac{\max(y_v)}{\min(x_v)} = -\frac{\max^2(y_v)}{A^2 \cdot x_0 \cdot y_0} = -\frac{A^2 \cdot x_0 \cdot y_0}{\min^2(x_v)} = -\frac{A^2}{(A - 1)^2} \cdot \frac{y_0}{x_0} \quad (41)$$

from
(38)
(39)

$$\frac{\partial y_v}{\partial x_v} = -\frac{\min(y_v)}{\max(x_v)} = -\frac{\min^2(y_v)}{A^2 \cdot x_0 \cdot y_0} = -\frac{A^2 \cdot x_0 \cdot y_0}{\max^2(x_v)} = -\frac{(A - 1)^2}{A^2} \cdot \frac{y_0}{x_0} \quad (42)$$

Owing to their significance, let the marginal prices at the points $(\min(x_v), \max(y_v))$ and $(\max(x_v), \min(y_v))$ be represented by the variable names P_{high} , P_0 , and P_{low} , respectively. These variables are defined here to be the absolute value of the marginal exchange rates at these points as this renders some of the analysis performed later in this document

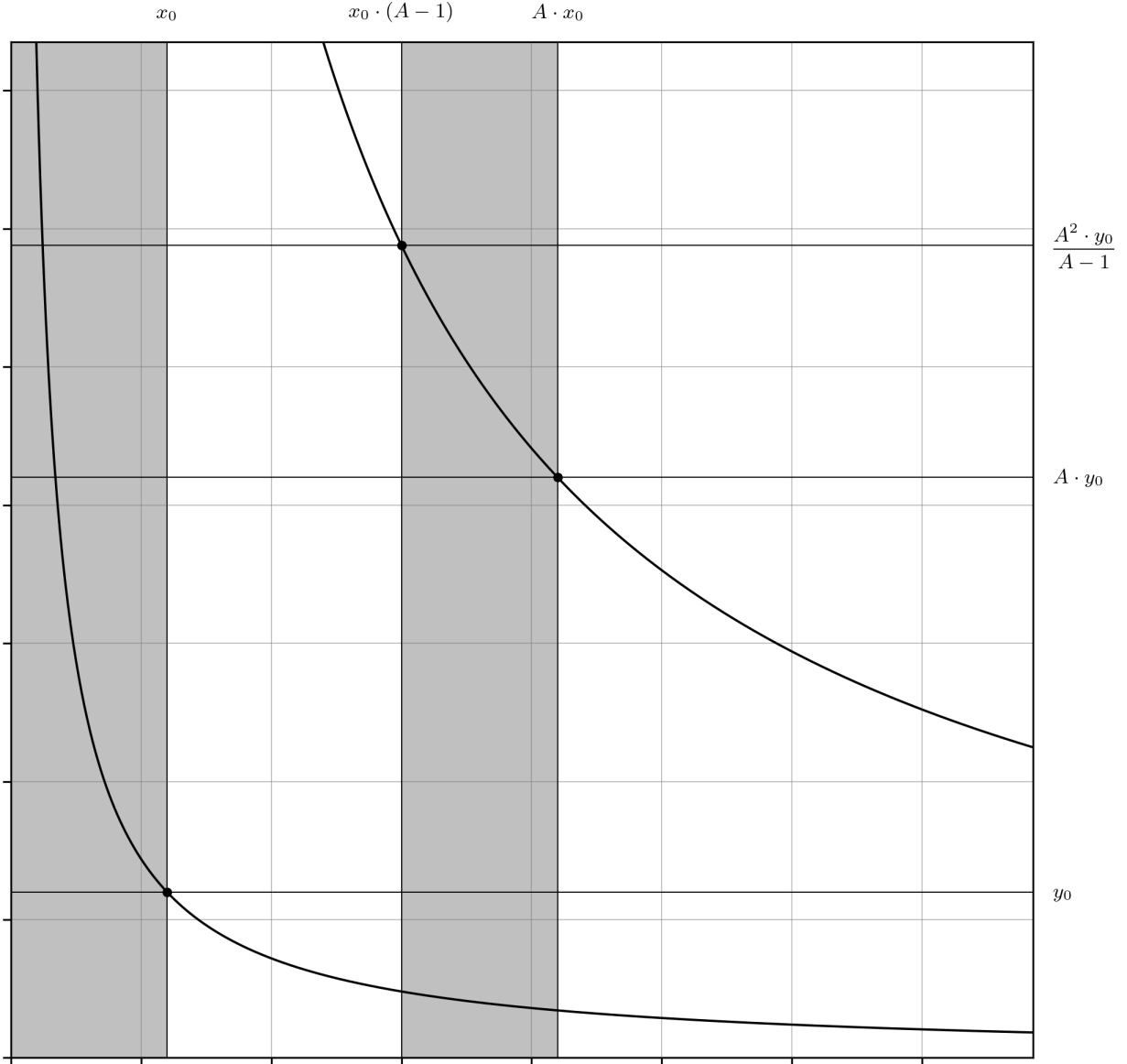


Fig. 8 The min (x_v) and max (y_v) coordinates (Equations 36 and 37). The correspondence between the virtual token balance and the real token balance is depicted with shaded areas for reference.

a little less complicated (Equations 43, 44 and 47). However, one ignores the implicit negative sign of the slopes on these curves at their own peril. To save face, this negation is stated plainly in Equations 44, 46 and 48.

$$\begin{array}{l} \text{from} \\ (41) \end{array} \quad P_{\text{high}} = \frac{A^2}{(A-1)^2} \cdot \frac{y_0}{x_0}; \quad \sqrt{P_{\text{high}}} = \frac{A}{A-1} \cdot \frac{\sqrt{y_0}}{\sqrt{x_0}} \quad (43)$$

$$\begin{array}{l} \text{from} \\ (41) \\ (43) \end{array} \quad \left. \frac{\partial y_v}{\partial x_v} \right|_{\min(x_v)} = -P_{\text{high}} \quad (44)$$

$$\begin{array}{l} \text{from} \\ (40) \end{array} \quad P_0 = \frac{y_0}{x_0}; \quad \sqrt{P_0} = \frac{\sqrt{y_0}}{\sqrt{x_0}} \quad (45)$$

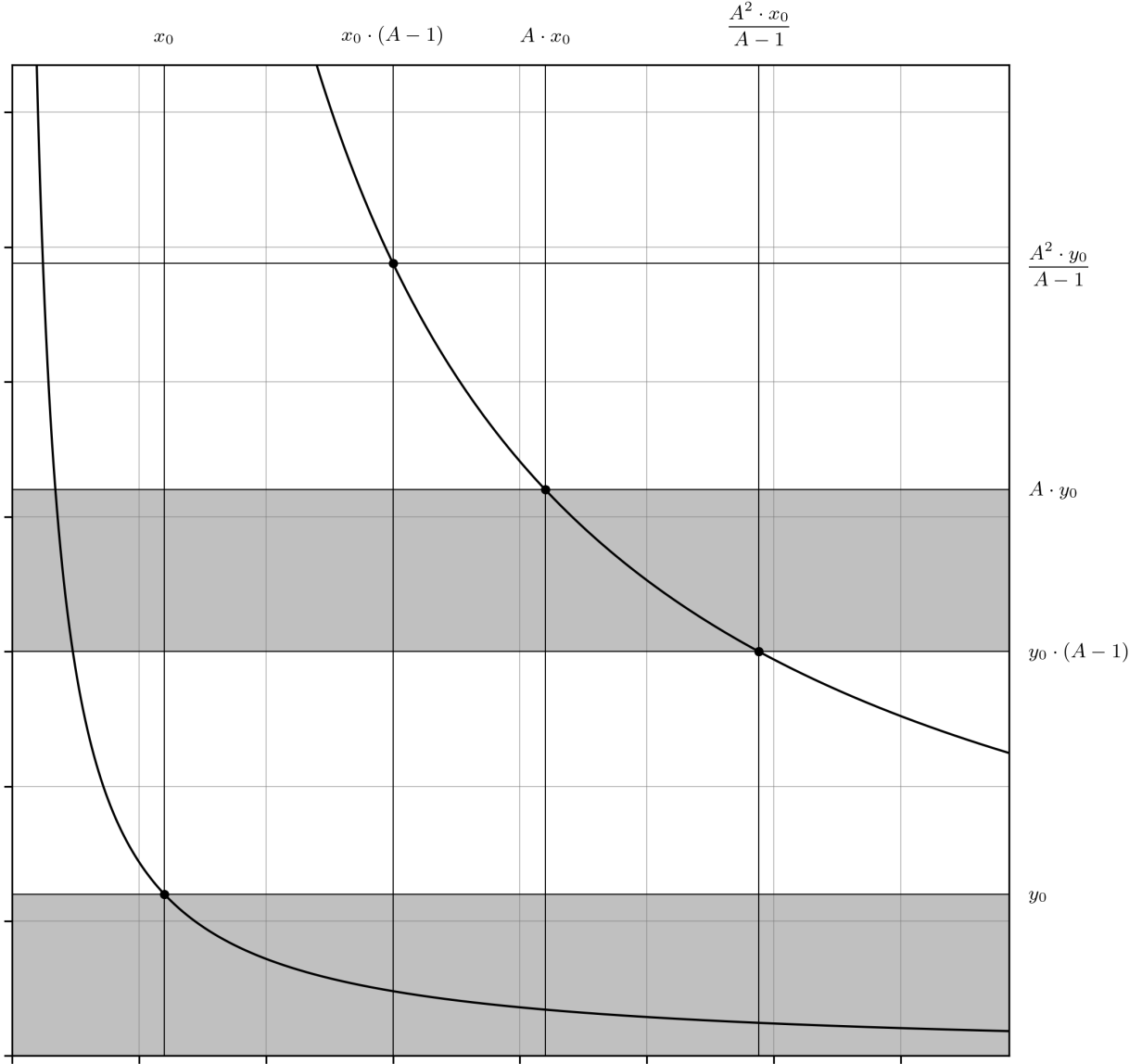


Fig. 9 The max (x_v) and min (y_v) coordinates (Equations 38 and 39). The correspondence between the virtual token balance and the real token balance is depicted with shaded areas for reference.

$$\begin{array}{l} \text{from} \\ (40) \\ (45) \end{array} \quad \left. \frac{\partial y_v}{\partial x_v} \right|_{A \cdot x_0} = -P_0 \quad (46)$$

$$\begin{array}{l} \text{from} \\ (42) \end{array} \quad P_{\text{low}} = \frac{(A - 1)^2}{A^2} \cdot \frac{y_0}{x_0}; \quad \sqrt{P_{\text{low}}} = \frac{A - 1}{A} \cdot \frac{\sqrt{y_0}}{\sqrt{x_0}} \quad (47)$$

$$\begin{array}{l} \text{from} \\ (42) \\ (47) \end{array} \quad \left. \frac{\partial y_v}{\partial x_v} \right|_{\max(x_v)} = -P_{\text{low}} \quad (48)$$

There are a few significant capstone identities that can be found at this juncture. Firstly, the geometric mean of P_{high} and P_{low} is equal to P_0 (Equations 49 and 50). Similarly, the geometric means of $\max(x_v)$ and $\min(x_v)$, and $\max(y_v)$ and

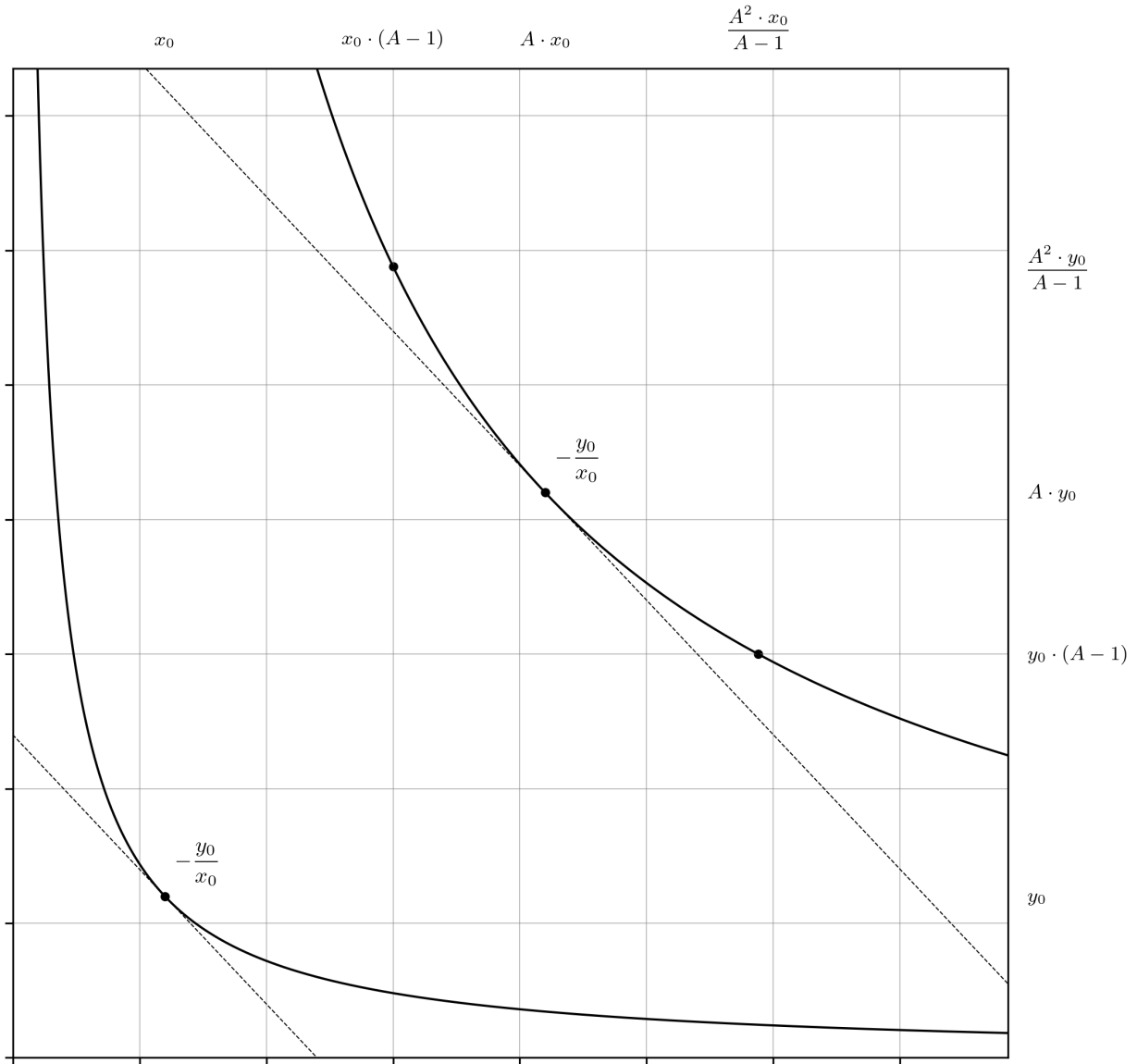


Fig. 10 It is trivial that the gradient of the curves at the points (x_0, y_0) on the reference curve and $(A \cdot x_0, A \cdot y_0)$ on the virtual curve are equal (Equations 15 and 40).

$\min(y_v)$ are equal to $A \cdot x_0$ and $A \cdot y_0$, respectively (which are the coordinates at which the first derivative evaluates to P_0) (Equations 49, 50, 51, 52, 53 and 54). These are expected results, and can be understood as a consequence of the Mean Value Theorem⁹ applied to the implicit curve and price curve over the closed interval defined by the bounds elucidated above. This is even more evident in the quotients of $\max(y_v)$ and $\max(x_v)$, and $\min(y_v)$ and $\min(x_v)$, which evaluate to y_0/x_0 and is equal to P_0 (Equations 55 and 56).

$$\begin{array}{l} \text{from} \\ (43) \\ (47) \end{array} \quad P_{\text{high}} \cdot P_{\text{low}} = \frac{(A-1)^2}{A^2} \cdot \frac{A^2}{(A-1)^2} \cdot \frac{y_0}{x_0} \cdot \frac{y_0}{x_0} = \frac{y_0^2}{x_0^2} \quad (49)$$

$$\begin{array}{l} \text{from} \\ (45) \\ (49) \end{array} \quad \sqrt{P_{\text{high}}} \cdot \sqrt{P_{\text{low}}} = P_0 = \frac{y_0}{x_0} \quad (50)$$

⁹wikipedia.org/wiki/Mean_value_theorem

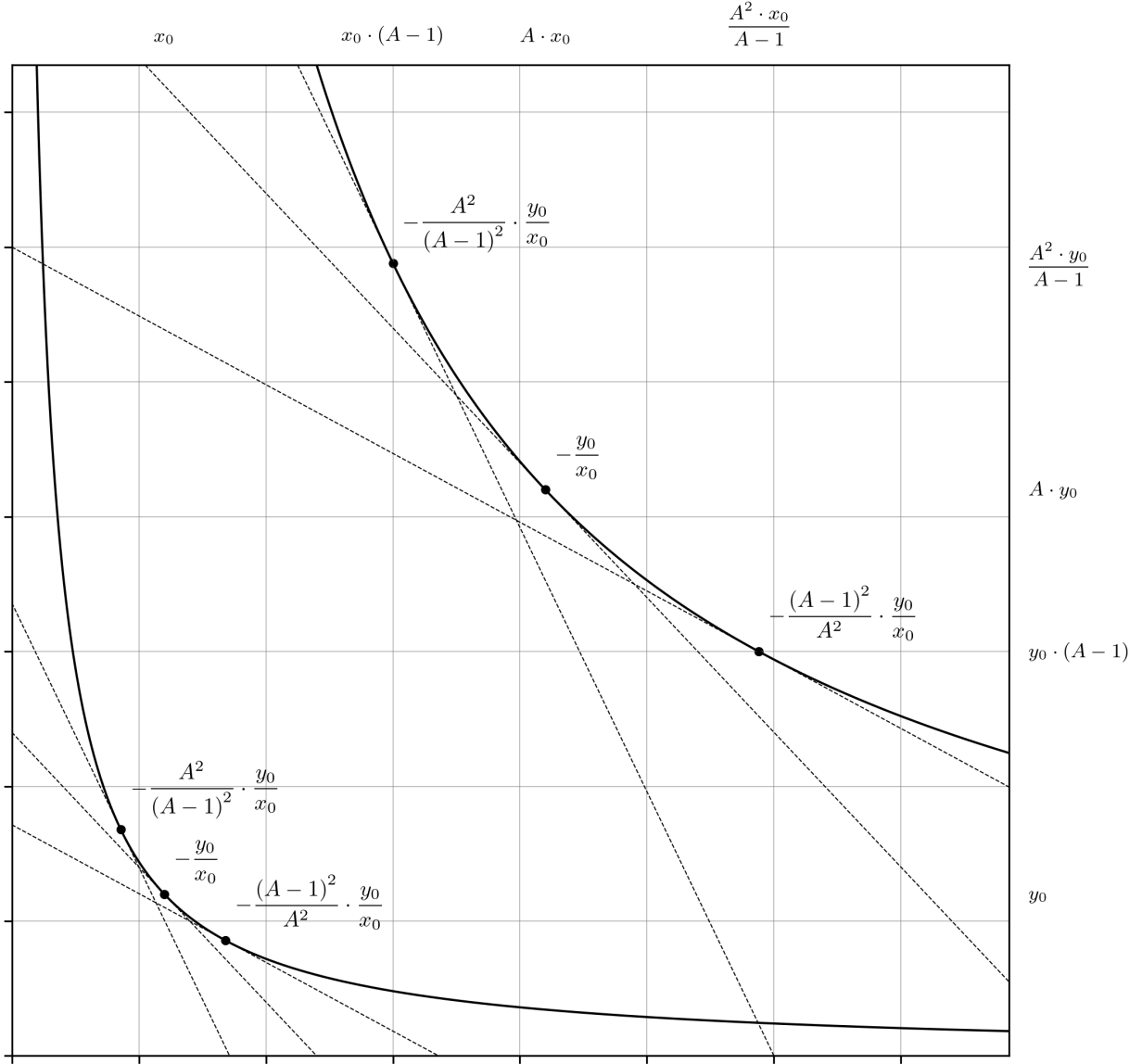


Fig. 11 The slope of tangent lines drawn at the points $(\min(x_v), \max(y_v))$ and $(\max(x_v), \min(y_v))$ on the virtual curve are commensurate with its price boundaries. Tangent lines are drawn on the reference curve parallel to those on the virtual curve; the algebraic identities of the points where these parallel tangents kiss the reference curve are elucidated later in this exercise (Equations 43, 45 and 47).

from
(36)
(39)

$$\max(x_v) \cdot \min(x_v) = \frac{A^2 \cdot x_0}{A-1} \cdot x_0 \cdot (A-1) = A^2 \cdot x_0^2 \quad (51)$$

from
(51)

$$\sqrt{\max(x_v)} \cdot \sqrt{\min(x_v)} = A \cdot x_0 \quad (52)$$

from
(37)
(38)

$$\max(y_v) \cdot \min(y_v) = \frac{A^2 \cdot y_0}{A-1} \cdot y_0 \cdot (A-1) = A^2 \cdot y_0^2 \quad (53)$$

from
(53)

$$\sqrt{\max(y_v)} \cdot \sqrt{\min(y_v)} = A \cdot y_0 \quad (54)$$

$$\begin{array}{l} \text{from} \\ (36) \\ (39) \end{array} \quad \frac{\max(y_v)}{\max(x_v)} = \frac{\frac{A^2 \cdot y_0}{A-1}}{\frac{A^2 \cdot x_0}{A-1}} = \frac{y_0}{x_0} = P_0 \quad (55)$$

$$\begin{array}{l} \text{from} \\ (37) \\ (38) \end{array} \quad \frac{\min(y_v)}{\min(x_v)} = \frac{y_0 \cdot (A-1)}{x_0 \cdot (A-1)} = \frac{y_0}{x_0} = P_0 \quad (56)$$

Secondly, and less trivially, the quotient of P_{high} and P_{low} can be expressed entirely as a function of A (Equations 57, 58 and 59). This result is commonly referred to as the “capital efficiency” identity without context or explanation but can now be understood through the lens of a smaller liquidity pool emulating a larger liquidity pool A times larger than itself.

$$\begin{array}{l} \text{from} \\ (43) \\ (47) \end{array} \quad \frac{P_{\text{high}}}{P_{\text{low}}} = \frac{\frac{A^2}{(A-1)^2} \cdot \frac{y_0}{x_0}}{\frac{A^2}{(A-1)^2} \cdot \frac{y_0}{x_0}} = \frac{A^4}{(A-1)^4} \quad (57)$$

$$\begin{array}{l} \text{from} \\ (57) \end{array} \quad \frac{\sqrt[4]{P_{\text{high}}}}{\sqrt[4]{P_{\text{low}}}} = \frac{A}{A-1} \quad (58)$$

$$\begin{array}{l} \text{from} \\ (58) \end{array} \quad A = \frac{1}{1 - \frac{\sqrt[4]{P_{\text{low}}}}{\sqrt[4]{P_{\text{high}}}}} = \frac{\sqrt[4]{P_{\text{high}}}}{\sqrt[4]{P_{\text{high}}} - \sqrt[4]{P_{\text{low}}}} \quad (59)$$

The so-called “capital efficiency” term receives a lot of attention, but it is ultimately a red herring. The more important observation is that the quotients of P_{high} and P_0 , and P_0 and P_{low} are equal to each other and to some other constant, also expressed in terms of A (Equations 60, 61 and 62). For now, let this constant be the symbol C ; its identity has a deep connection to the underlying hyperbolic trigonometry demonstrated later in this exercise. The constant C is also obtainable from the quotients of $\max(x_v)$ and $\min(x_v)$, and $\max(y_v)$ and $\min(y_v)$ (Equations 63 and 64).

$$\begin{array}{l} \text{from} \\ (43) \\ (45) \end{array} \quad \frac{P_{\text{high}}}{P_0} = \frac{\frac{A^2}{(A-1)^2} \cdot \frac{y_0}{x_0}}{\frac{y_0}{x_0}} = \frac{A^2}{(A-1)^2} = C \quad (60)$$

$$\begin{array}{l} \text{from} \\ (45) \\ (47) \end{array} \quad \frac{P_0}{P_{\text{low}}} = \frac{\frac{y_0}{x_0}}{\frac{A^2}{(A-1)^2} \cdot \frac{y_0}{x_0}} = \frac{A^2}{(A-1)^2} = C \quad (61)$$

$$\begin{array}{l} \text{from} \\ (57) \\ (60) \\ (61) \end{array} \quad \frac{P_{\text{high}}}{P_{\text{low}}} = \frac{A^4}{(A-1)^4} = C^2; \quad \frac{\sqrt[4]{P_{\text{high}}}}{\sqrt[4]{P_{\text{low}}}} = \frac{A^2}{(A-1)^2} = C \quad (62)$$

$$\begin{array}{l} \text{from} \\ (43) \\ (45) \end{array} \quad \frac{\max(x_v)}{\min(x_v)} = \frac{\frac{A^2 \cdot x_0}{A-1}}{x_0 \cdot (A-1)} = \frac{A^2}{(A-1)^2} = C \quad (63)$$

$$\begin{array}{l} \text{from} \\ (45) \\ (47) \end{array} \quad \frac{\max(y_v)}{\min(y_v)} = \frac{A^2 \cdot y_0}{y_0 \cdot (A-1)} = \frac{A^2}{(A-1)^2} = C \quad (64)$$

Turning our attention now to the tangents drawn on the reference curve, parallel to those on the virtual curve. There are two convenient methods to elucidate the algebraic identities of the points on the reference curve where the marginal prices are equal to the price boundaries of the virtual curve. The naïve method (which still works) is to simply reverse the amplification by taking the quotients of $\min(x_v)$, $\max(y_v)$, $\min(y_v)$, $\max(x_v)$, and the amplification constant A (Equations 65, 66, 67 and 68).

$$\begin{array}{l} \text{from} \\ (36) \end{array} \quad \min(x) = \frac{\min(x_v)}{A} = \frac{x_0 \cdot (A-1)}{A} \quad (65)$$

$$\begin{array}{l} \text{from} \\ (37) \end{array} \quad \max(y) = \frac{\max(y_v)}{A} = \frac{A^2 \cdot y_0}{A} = \frac{A \cdot y_0}{A-1} \quad (66)$$

$$\begin{array}{l} \text{from} \\ (38) \end{array} \quad \max(x) = \frac{\max(x_v)}{A} = \frac{A^2 \cdot x_0}{A} = \frac{A \cdot x_0}{A-1} \quad (67)$$

$$\begin{array}{l} \text{from} \\ (39) \end{array} \quad \min(y) = \frac{\min(y_v)}{A} = \frac{y_0 \cdot (A-1)}{A} \quad (68)$$

The other method is by way of the previously derived marginal rate expressions, Equations 16 and 17, after substituting the appropriate marginal rate identity from Equations 41 and 42. This method is demonstrated only for $\min(x)$ below (Equations 69 and 70) but can be used to confirm all identities in Equations 65, 66, 67 and 68, adding some rigor to the amplification reversal method used above.

$$\begin{array}{l} \text{from} \\ (17) \\ (41) \end{array} \quad \frac{\partial y}{\partial x} = -\frac{x_0 \cdot y_0}{\min^2(x)} = -\frac{A^2}{(A-1)^2} \cdot \frac{y_0}{x_0} \quad (69)$$

$$\begin{array}{l} \text{from} \\ (69) \end{array} \quad \frac{1}{\min^2(x)} = \frac{A^2}{(A-1)^2} \cdot \frac{1}{x_0^2} \Rightarrow \min(x) = \frac{x_0 \cdot (A-1)}{A} \quad (70)$$

These points have been appended to the evolving plot in Figure 12. For completeness, the shadow of the Mean Value Theorem can be observed here, too. The geometric means of $\min(x)$ and $\max(x)$, and $\max(y)$ and $\min(y)$ are equal to x_0 and y_0 , respectively (which are also the coordinates at which the first derivative evaluates to P_0) (Equations 71, 72, 73 and 74). The quotients of $\max(y)$ and $\max(x)$, and $\min(y)$ and $\min(x)$ also evaluate to y_0/x_0 and are equal to P_0 (Equations 75 and 76). Further foreshadowing the hyperbolic trigonometry discussion, the quotients of $\max(x)$ and $\min(x)$, and $\max(y)$ and $\min(y)$ also yield the previously observed constant, C (Equations 77 and 78).

$$\begin{array}{l} \text{from} \\ (65) \\ (67) \end{array} \quad \min(x) \cdot \max(x) = \frac{x_0 \cdot (A-1)}{A} \cdot \frac{A \cdot x_0}{A-1} = x_0^2 \quad (71)$$

$$\begin{array}{l} \text{from} \\ (71) \end{array} \quad \sqrt{\min(x)} \cdot \sqrt{\max(x)} = x_0 \quad (72)$$

$$\begin{array}{l} \text{from} \\ (66) \\ (68) \end{array} \quad \max(y) \cdot \min(y) = \frac{A \cdot y_0}{A-1} \cdot \frac{y_0 \cdot (A-1)}{A} = y_0^2 \quad (73)$$

$$\begin{array}{l} \text{from} \\ (73) \end{array} \quad \sqrt{\max(y)} \cdot \sqrt{\min(y)} = y_0 \quad (74)$$

$$\begin{array}{l} \text{from} \\ (66) \\ (67) \end{array} \quad \frac{\max(y)}{\max(x)} = \frac{\frac{A \cdot y_0}{A-1}}{\frac{A \cdot x_0}{A-1}} = \frac{y_0}{x_0} = P_0 \quad (75)$$

$$\begin{array}{l} \text{from} \\ (65) \\ (68) \end{array} \quad \frac{\min(y)}{\min(x)} = \frac{\frac{y_0 \cdot (A-1)}{A}}{\frac{x_0 \cdot (A-1)}{A}} = \frac{y_0}{x_0} = P_0 \quad (76)$$

$$\begin{array}{l} \text{from} \\ (65) \\ (67) \end{array} \quad \frac{\max(x)}{\min(x)} = \frac{\frac{A \cdot x_0}{A-1}}{\frac{x_0 \cdot (A-1)}{A}} = \frac{A^2}{(A-1)^2} = C \quad (77)$$

$$\begin{array}{l} \text{from} \\ (66) \\ (68) \end{array} \quad \frac{\max(y)}{\min(y)} = \frac{\frac{A \cdot y_0}{A-1}}{\frac{y_0 \cdot (A-1)}{A}} = \frac{A^2}{(A-1)^2} = C \quad (78)$$

A heuristic understanding of the token balance virtualization can now be attained. A section of the standard $x \cdot y = x_0 \cdot y_0$ implicit curve, defined by a geometric center with the reference coordinates (x_0, y_0) , and relative distances from this reference point defined by the amplification constant A , is mapped to the implicit curve of $x_v \cdot y_v = A^2 \cdot x_0 \cdot y_0$. Shaded areas and arrows which depict the mapping between the two curves have been added to the developing plot to visualize the overall process (Figure 13).

The capacity of the virtual curve to absorb higher trading volumes compared to the reference curve can also be interrogated by considering a token swap from one price bound to the other (Figures 14 and 15). Note that such an action will execute at the same effective price in both cases. While the marginal rates before and after the exchange (and therefore the overall exchange rate) are identical in both the reference and virtual curves, the trade amounts are significantly greater in the virtual curve. The improved trade volume can be inspected visually from the increased arrow lengths in Figure 14, and the integrated area in Figure 15.

While outside of the focus of the present discussion, the financial ramification of this process is worthy of consideration. The token swaps depicted in Figures 14 and 15 obscure the fact that the virtual curve has traded its entire reserve of one token for the other token, whereas the more conservative reference curve has only traded a small proportion of its reserves. This can have dramatic consequences¹⁰ on the portfolio value represented by the liquidity position of the virtual curve. In lieu of a more thorough investigation, the Medium articles^{11,12} authored by Peteris Erins and Ivan Vakhmyanin do an excellent job of elaborating this topic material further.

3.2 The Bancor v2 Real Curve

The objective of this part of the exercise is to translate the virtual invariant into a form where there is no recourse to virtual token balances. That is, to derive the real concentrated liquidity invariant which behaves identically to the virtual curve, but which correctly reports its own true token balances. This can be interpreted visually as a second mapping process which drives the boundaries of the virtual curve back to the x- and y-axes (Figure 16). Alternatively (and equivalently), this construction can also be interpreted as a direct mapping of the previously identified points and prices on the reference curve back to the x- and y-axes such that the geometric center remains stationary, and such that the marginal price at this point remains unchanged during the transformation (Figure 17).

¹⁰Loesch, S.; Hindman, N.; Richardson, M. B.; and Welch, N. Impermanent Loss in Uniswap v3. arxiv.org/abs/2111.09192, 2021.

¹¹medium.com/auditless/impermanent-loss-in-uniswap-v3-6c7161d3b445

¹²medium.com/coinmonks/top-5-mysterious-liquidity-providers-in-uniswap-v3-and-what-we-can-learn-from-them-1894bd27096f

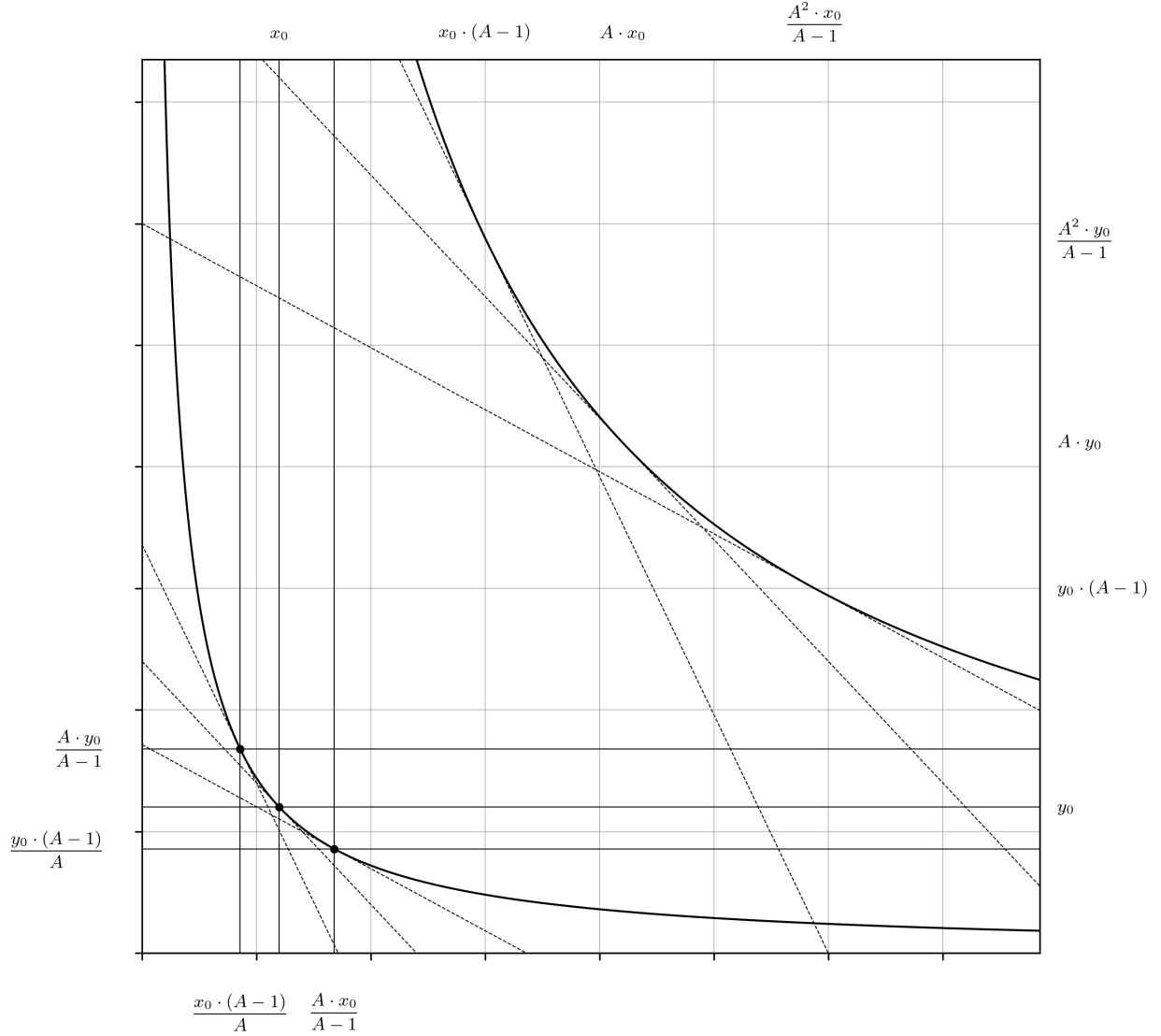


Fig. 12 The algebraic identities of the points where the lines tangent to the reference curve and parallel to the tangent lines at the price boundaries of the virtual curve are now elucidated (Equations 65, 66, 67 and 68).

Thankfully, this part is relatively easy. Introduction of horizontal, H , and vertical, V , shift parameters into the virtual invariant equation (Equation 26) yields Equation 79. These shifts are equal to the gap between the x - and y -axes, and the shaded areas representing the bounds of the virtual curve in Figure 16. Therefore, the horizontal shift is equal to $\min(x_v)$, and the vertical shift is equal to $\min(y_v)$; substitution of the algebraic identities for these terms (Equations 36 and 38) into H and V in Equation 79 yields the real concentrated liquidity invariant (Equation 80).

$$\begin{array}{l} \text{from} \\ (26) \end{array} \quad (x + H) \cdot (y + V) = A^2 \cdot x_0 \cdot y_0 \quad (79)$$

$$\begin{array}{l} \text{from} \\ (36) \\ (38) \\ (79) \end{array} \quad (x + x_0 \cdot (A - 1)) \cdot (y + y_0 \cdot (A - 1)) = A^2 \cdot x_0 \cdot y_0 \quad (80)$$

Algebraic manipulation of the real invariant (Equation 80) to derive the token swap identities, Δx and Δy , and the marginal rate equation is performed as follows. First, the expressions isolating x and y are derived (Equations 81 and 82).

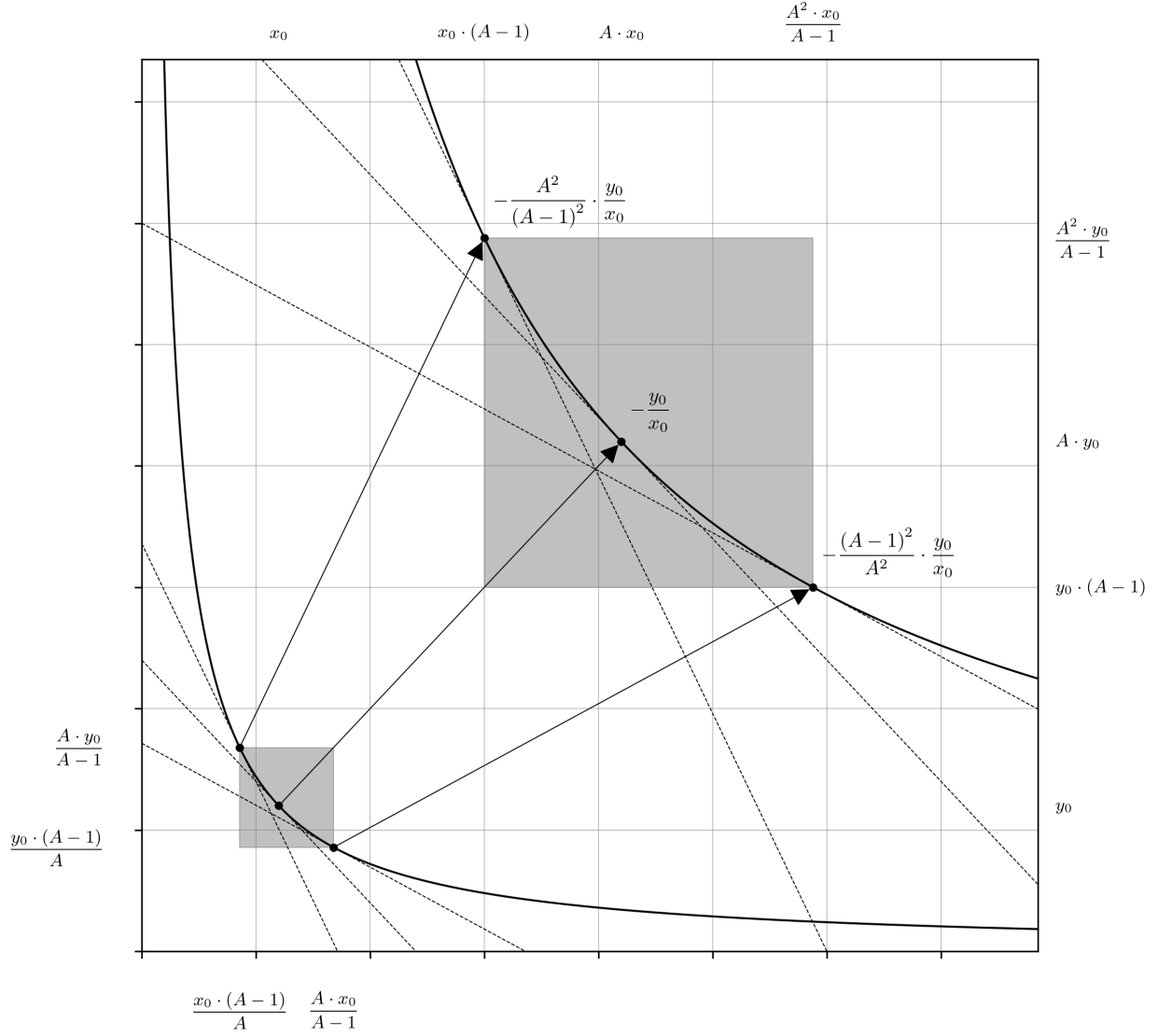


Fig. 13 The amplification process is depicted with corresponding shaded areas of the reference and virtual curves, respectively. Points where the first derivative of each curve evaluates to the same result are shown as white dots, and the mapping of these points is depicted with white arrows.

$$\begin{array}{l} \text{from} \\ (80) \end{array} \quad x = \frac{A^2 \cdot x_0 \cdot y_0}{y + y_0 \cdot (A - 1)} - x_0 \cdot (A - 1) \quad (81)$$

$$\begin{array}{l} \text{from} \\ (80) \end{array} \quad y = \frac{A^2 \cdot x_0 \cdot y_0}{x + x_0 \cdot (A - 1)} - y_0 \cdot (A - 1) \quad (82)$$

The token swap equations are constructed as before; the x and y terms in Equation 80 or Equations 81 and 82 are substituted for $x + \Delta x$ and $y + \Delta y$ (Equations 83, 84 and 85), then rearranged to make either Δx or Δy the subject.

$$\begin{array}{l} \text{from} \\ (80) \end{array} \quad (x + \Delta x + x_0 \cdot (A - 1)) \cdot (y + \Delta y + y_0 \cdot (A - 1)) = A^2 \cdot x_0 \cdot y_0 \quad (83)$$

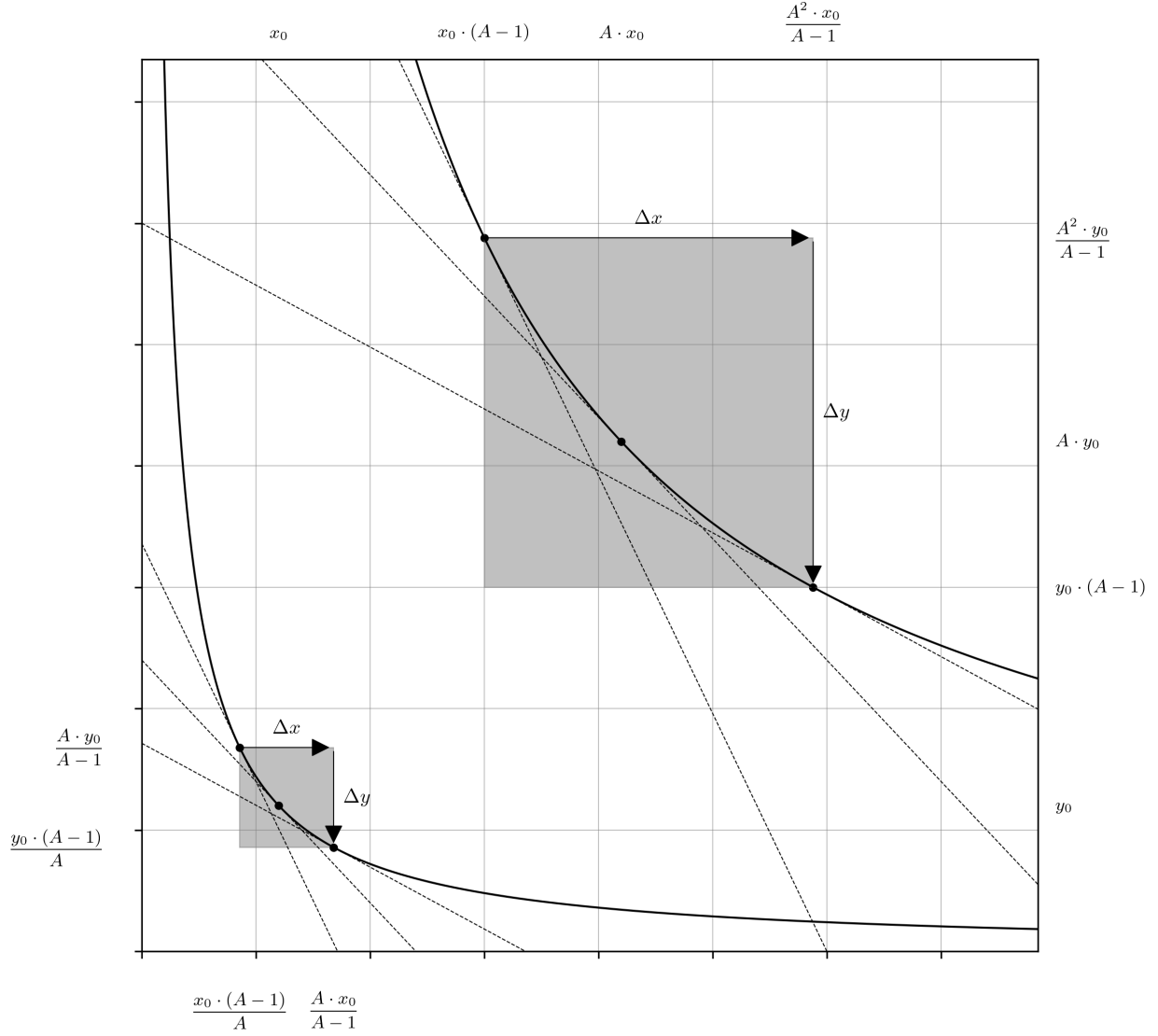


Fig. 14 Traversal upon the rectangular hyperbolas $x \cdot y = x_0 \cdot y_0$ and $x \cdot y = A^2 \cdot x_0 \cdot y_0$ (Equations 2 and 26), representing a token swap against the reference and amplified liquidity pools, where $\Delta x > 0$ and $\Delta y < 0$. The marginal rates of exchange before and after the swap are identical. The ratio of the Δx and Δy arrow lengths for each curve are also identical, and therefore the overall rate of exchange, $\Delta y/\Delta x$ is equal in both cases.

$$\begin{array}{l} \text{from} \\ (81) \\ (83) \end{array} \quad \Delta x = \frac{A^2 \cdot x_0 \cdot y_0}{y + \Delta y + y_0 \cdot (A - 1)} - x_0 \cdot (A - 1) - x \quad (84)$$

$$\begin{array}{l} \text{from} \\ (82) \\ (83) \end{array} \quad \Delta y = \frac{A^2 \cdot x_0 \cdot y_0}{x + \Delta x + x_0 \cdot (A - 1)} - y_0 \cdot (A - 1) - y \quad (85)$$

To reduce the number of dimensions, the identities for x and y in Equations 81 and 82 are substituted into Equations 84 and 85, respectively (Equations 86 and 88). Combining the minuends and subtrahends into a single fraction yields Equations 87 and 89.

$$\begin{array}{l} \text{from} \\ (81) \\ (84) \end{array} \quad \Delta x = \frac{A^2 \cdot x_0 \cdot y_0}{y + \Delta y + y_0 \cdot (A - 1)} - \frac{A^2 \cdot x_0 \cdot y_0}{y + y_0 \cdot (A - 1)} \quad (86)$$

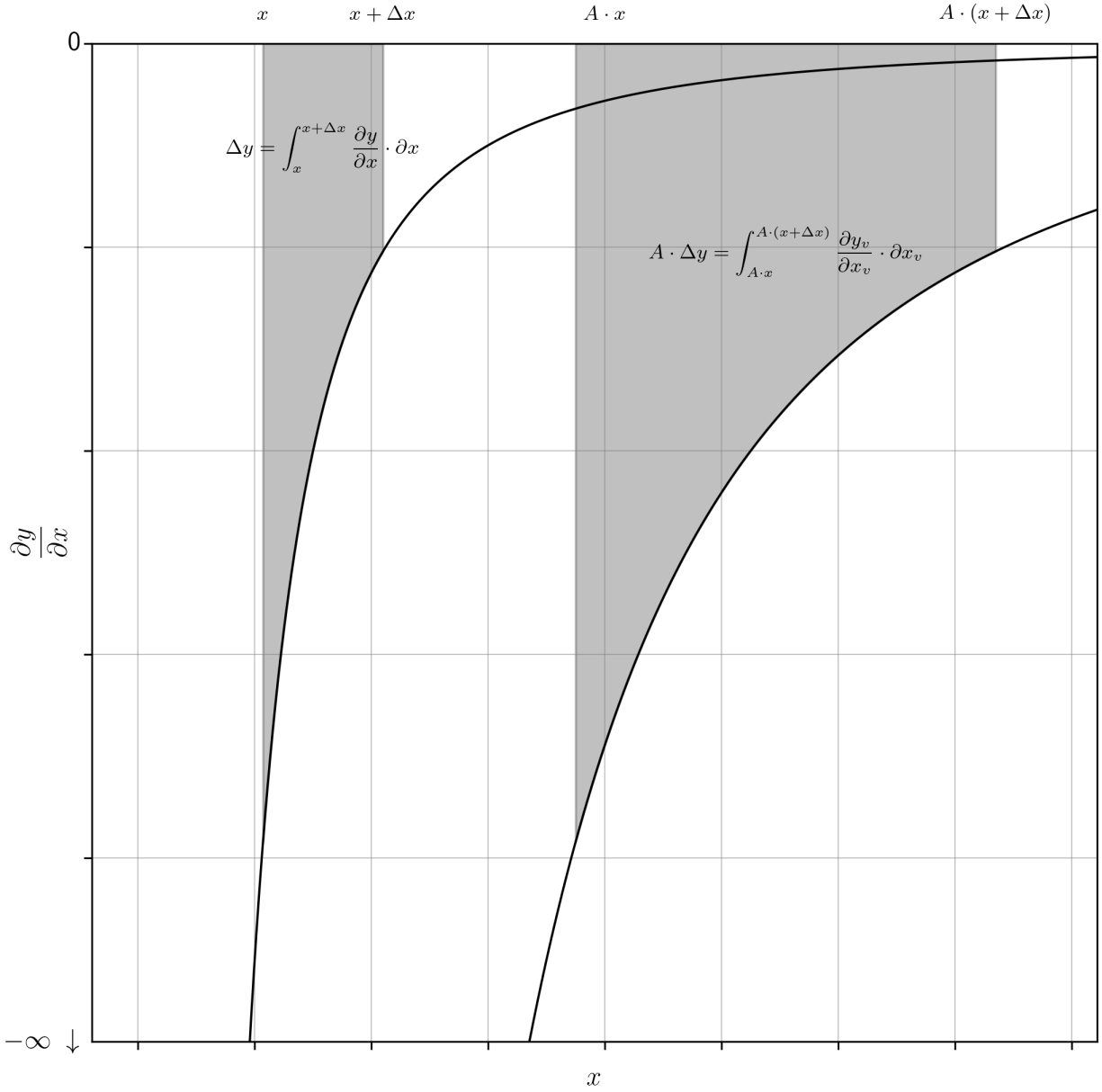


Fig. 15 The integration above $\partial y/\partial x = -x_0 \cdot y_0/x^2$ and $\partial y_v/\partial x_v = -A^2 \cdot x_0 \cdot y_0/x_v^2$ (Equations 17 and 35) over the intervals $x \rightarrow x + \Delta x$ and $A \cdot x \rightarrow A \cdot (x + \Delta x)$ (i.e. $x_v \rightarrow x_v + \Delta x$) representing a token swap against both the reference and amplified liquidity pools, where $\Delta x > 0$ and $\Delta y < 0$. Note that the integration areas for the reference and virtual curves are Δy and $A \cdot \Delta y$, respectively. By inference, any token swap against the virtual curve can be calculated from the reference curve by multiplying the output by the amplification constant.

from
(86)

$$\Delta x = -\frac{\Delta y \cdot A^2 \cdot x_0 \cdot y_0}{(y + y_0 \cdot (A - 1)) \cdot (y + \Delta y + y_0 \cdot (A - 1))} \quad (87)$$

from
(82)
(85)

$$\Delta y = \frac{A^2 \cdot x_0 \cdot y_0}{x + \Delta x + x_0 \cdot (A - 1)} - \frac{A^2 \cdot x_0 \cdot y_0}{x + x_0 \cdot (A - 1)} \quad (88)$$

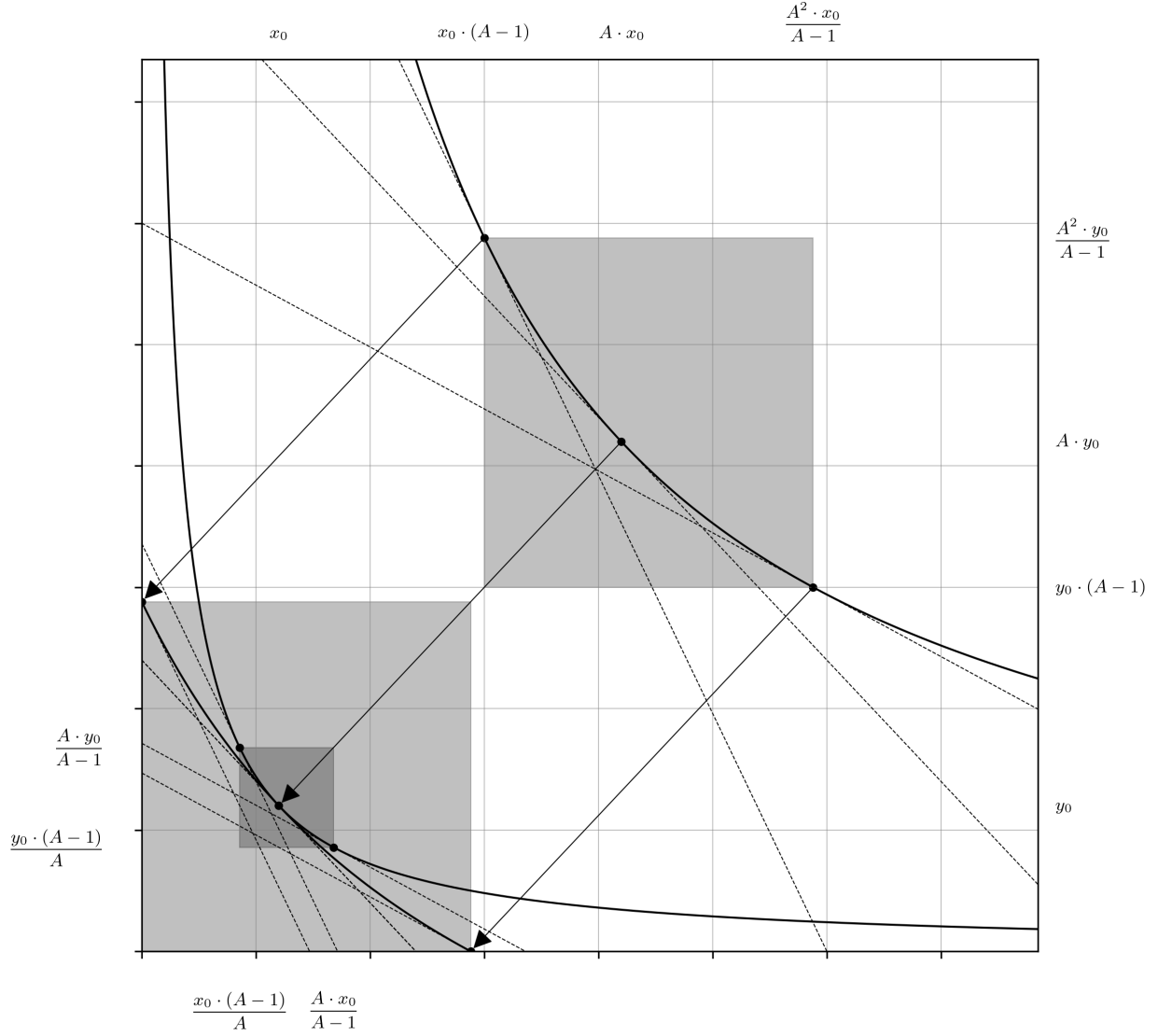


Fig. 16 Construction of the real concentrated liquidity curve is depicted as a map of the virtual curve back to the x- and y-axes.

$$\text{from (88)} \quad \Delta y = -\frac{\Delta x \cdot A^2 \cdot x_0 \cdot y_0}{(x + x_0 \cdot (A - 1)) \cdot (x + \Delta x + x_0 \cdot (A - 1))} \quad (89)$$

As done previously for Equations 10 and 11, the invariant term $A^2 \cdot x_0 \cdot y_0$ in Equations 87 and 89 can be substituted for its identity, $(x + x_0 \cdot (A - 1)) \cdot (y + y_0 \cdot (A - 1))$ (i.e. the LHS of Equation 80). This process yields the familiar two-dimensional swap equations which depend on both the x and y coordinates (Equations 90 and 91).

$$\text{from (87)} \quad \Delta x = -\frac{\Delta y \cdot (x + x_0 \cdot (A - 1))}{y + \Delta y + y_0 \cdot (A - 1)} \quad (90)$$

$$\text{from (89)} \quad \Delta y = -\frac{\Delta x \cdot (y + y_0 \cdot (A - 1))}{x + \Delta x + x_0 \cdot (A - 1)} \quad (91)$$

Again, the marginal price equations can be derived in several ways. Repeating the process demonstrated in Equations 12, 13, 14 and 15, rearrangement of Equations 87 and 89 to get the *effective rate of exchange*, followed by determination

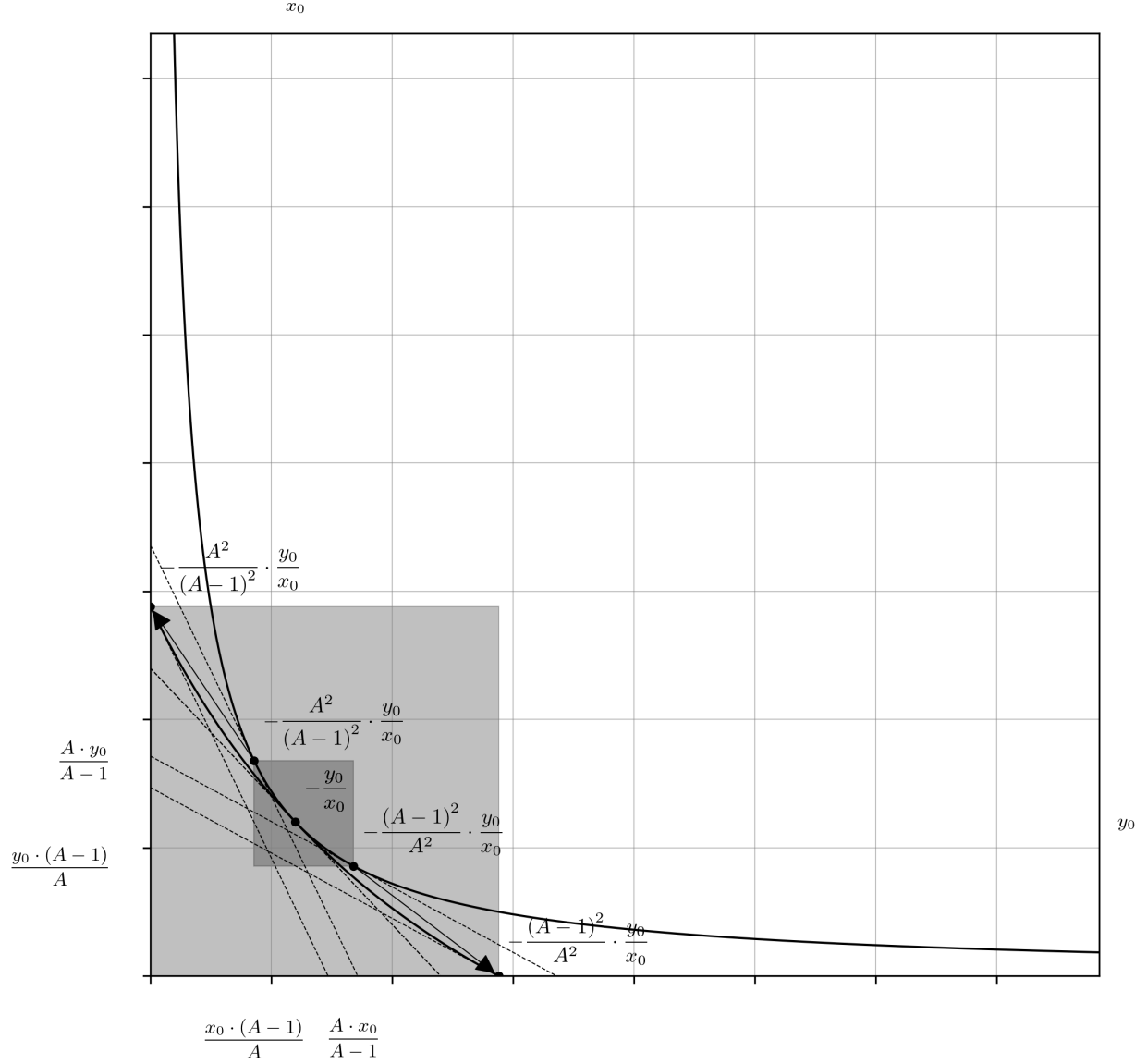


Fig. 17 Construction of the real concentrated liquidity curve is depicted as a map of the reference curve section to new coordinates such that the previously defined price boundaries occur at the x- and y-intercepts, the geometric center remains stationary, and the marginal exchange rate at its coordinates remains unchanged.

of the limit as the denominator goes to zero gives the *instantaneous rate of exchange*. It should be apparent that direct differentiation of Equations 81 and 82 via the quotient rule yields the same results.

$$\text{from (87)} \quad \frac{\Delta x}{\Delta y} = -\frac{A^2 \cdot x_0 \cdot y_0}{(y + y_0 \cdot (A - 1)) \cdot (y + \Delta y + y_0 \cdot (A - 1))} \quad (92)$$

$$\text{from (92)} \quad \frac{\partial x}{\partial y} = \lim_{\Delta y \rightarrow 0} \frac{\Delta x}{\Delta y} = -\frac{A^2 \cdot x_0 \cdot y_0}{(y + y_0 \cdot (A - 1))^2}; \quad \frac{\partial y}{\partial x} = -\frac{(y + y_0 \cdot (A - 1))^2}{A^2 \cdot x_0 \cdot y_0} \quad (93)$$

$$\text{from (89)} \quad \frac{\Delta y}{\Delta x} = -\frac{A^2 \cdot x_0 \cdot y_0}{(x + x_0 \cdot (A - 1)) \cdot (x + \Delta x + x_0 \cdot (A - 1))} \quad (94)$$

$$\begin{array}{l} \text{from} \\ (94) \end{array} \quad \frac{\partial y}{\partial x} = \lim_{\Delta x \rightarrow 0} \frac{\Delta y}{\Delta x} = -\frac{A^2 \cdot x_0 \cdot y_0}{(x + x_0 \cdot (A - 1))^2}; \quad \frac{\partial x}{\partial y} = -\frac{(x + x_0 \cdot (A - 1))^2}{A^2 \cdot x_0 \cdot y_0} \quad (95)$$

Lastly, the marginal rate equations can also be expressed in terms of both token balances via substitution of the x and y terms in Equations 13 and 15 with their horizontally- or vertically-shifted transformations (Equation 96). If that seems like a leap, the truth of this identity can also be proved by substituting the $A^2 \cdot x_0 \cdot y_0$ term in Equations 93 and 95 for its identity, the LHS of Equation 80.

$$\begin{array}{l} \text{from} \\ (80) \\ (93) \\ (95) \end{array} \quad \frac{\partial x}{\partial y} = -\frac{x + x_0 \cdot (A - 1)}{y + y_0 \cdot (A - 1)}; \quad \frac{\partial y}{\partial x} = -\frac{y + y_0 \cdot (A - 1)}{x + x_0 \cdot (A - 1)} \quad (96)$$

The token swap equations can now be independently derived, and further understood, from the continuous summation over the price curves. Explicit integration of Equations 93 and 95 over the interval representing the number of tokens being swapped yields results identical to Equations 86, 87, 88 and 89 (Equations 97 and 98). The integration above $\partial y/\partial x = -A^2 \cdot x_0 \cdot y_0 / (x + x_0 \cdot (A - 1))^2$ over the interval $x \rightarrow x + \Delta x$ representing a token swap is depicted in due course.

$$\begin{array}{l} \text{from} \\ (86) \\ (87) \\ (93) \end{array} \quad \Delta x = -\int_y^{y+\Delta y} \frac{A^2 \cdot x_0 \cdot y_0}{(y + y_0 \cdot (A - 1))^2} \cdot \partial y = \left[\frac{A^2 \cdot x_0 \cdot y_0}{y + y_0 \cdot (A - 1)} \right]_y^{y+\Delta y} \Rightarrow \text{Eqns. 86 and 87} \quad (97)$$

$$\begin{array}{l} \text{from} \\ (88) \\ (89) \\ (95) \end{array} \quad \Delta y = -\int_x^{x+\Delta x} \frac{A^2 \cdot x_0 \cdot y_0}{(x + x_0 \cdot (A - 1))^2} \cdot \partial x = \left[\frac{A^2 \cdot x_0 \cdot y_0}{x + x_0 \cdot (A - 1)} \right]_x^{x+\Delta x} \Rightarrow \text{Eqns. 88 and 89} \quad (98)$$

Be reminded that since x and y are dependent on each other, trying to obtain the token swap equation from direct integration of Equation 96 requires separation of the x and y variables first (Equations 99 and 100). Evaluation of the definite integrals over $x \rightarrow x + \Delta x$ and $y \rightarrow y + \Delta y$ (Equations 101, 102 and 103) followed by rearrangement of the resulting expression to isolate either Δx or Δy gives the familiar two-dimensional swap equations (Equations 104 and 105), which are redundant with those previously obtained (Equations 90 and 91).

$$\begin{array}{l} \text{from} \\ (96) \end{array} \quad \frac{1}{y + y_0 \cdot (A - 1)} \cdot \partial y = -\frac{1}{x + x_0 \cdot (A - 1)} \cdot \partial x \quad (99)$$

$$\begin{array}{l} \text{from} \\ (99) \end{array} \quad \int_y^{y+\Delta y} \frac{1}{y + y_0 \cdot (A - 1)} \cdot \partial y = -\int_x^{x+\Delta x} \frac{1}{x + x_0 \cdot (A - 1)} \cdot \partial x \quad (100)$$

$$\begin{array}{l} \text{from} \\ (100) \end{array} \quad [\ln(y + y_0 \cdot (A - 1))]_y^{y+\Delta y} = -[\ln(x + x_0 \cdot (A - 1))]_x^{x+\Delta x} \quad (101)$$

$$\begin{array}{l} \text{from} \\ (101) \end{array} \quad \ln\left(\frac{y + \Delta y + y_0 \cdot (A - 1)}{y + y_0 \cdot (A - 1)}\right) = \ln\left(\frac{x + x_0 \cdot (A - 1)}{x + \Delta x + x_0 \cdot (A - 1)}\right) \quad (102)$$

$$\begin{array}{l} \text{from} \\ (102) \end{array} \quad \frac{y + \Delta y + y_0 \cdot (A - 1)}{y + y_0 \cdot (A - 1)} = \frac{x + x_0 \cdot (A - 1)}{x + \Delta x + x_0 \cdot (A - 1)} \quad (103)$$

$$\begin{array}{l} \text{from} \\ (90) \\ (103) \end{array} \quad \Delta x = -(x + x_0 \cdot (A - 1)) \cdot \left(1 - \frac{y + y_0 \cdot (A - 1)}{y + \Delta y + y_0 \cdot (A - 1)}\right) \Rightarrow \text{Eqn. 90} \quad (104)$$

$$\begin{array}{l} \text{from} \\ (91) \\ (103) \end{array} \quad \Delta y = -(y + y_0 \cdot (A - 1)) \cdot \left(1 - \frac{x + x_0 \cdot (A - 1)}{x + \Delta x + x_0 \cdot (A - 1)} \right) \Rightarrow \mathbf{Eqn. 91} \quad (105)$$

Turning our attention back to the plot, the intercepts of the real curve (i.e. the points where it cuts either the x- or y-axes) can be determined easily (Figure 18). There are two convenient methods to achieve this. Substitution of y and x for zero in Equations 81 and 82, respectively, services the same result as taking the difference between $\max(x_v)$ and $\min(x_v)$, and $\max(y_v)$ and $\min(y_v)$, respectively (Equations 106 and 107). The latter approach is more geometrically intuitive given the construction thus far, but to each their own.

$$\begin{array}{l} \text{from} \\ (36) \\ (39) \\ (81) \end{array} \quad x_{\text{int}} = \max(x_v) - \min(x_v) = \frac{A^2 \cdot x_0}{A - 1} - x_0 \cdot (A - 1) = \frac{x_0 \cdot (2A - 1)}{A - 1} \quad (106)$$

$$\begin{array}{l} \text{from} \\ (37) \\ (38) \\ (82) \end{array} \quad y_{\text{int}} = \max(y_v) - \min(y_v) = \frac{A^2 \cdot y_0}{A - 1} - y_0 \cdot (A - 1) = \frac{y_0 \cdot (2A - 1)}{A - 1} \quad (107)$$

Since the real curve is shifted wholesale relative to the origin, so are its horizontal and vertical asymptotes. Again, the geometric intuition is to simply subtract from the origin the magnitude of the shift in the x- and y-dimensions, whereas the analytic approach is to substitute the y- or x-component of Equations 81 and 82 as required to set the denominator of the curve's equation to zero (Equations 108 and 109). In either case you get the same result for about the same effort (Figure 19).

$$\begin{array}{l} \text{from} \\ (36) \\ (82) \end{array} \quad x_{\text{asym}} = -x_0 \cdot (A - 1) \quad (108)$$

$$\begin{array}{l} \text{from} \\ (38) \\ (81) \end{array} \quad y_{\text{asym}} = -y_0 \cdot (A - 1) \quad (109)$$

The quotient properties of x_{int} , y_{int} , x_{asym} and y_{asym} are preserved with respect to P_0 (Equations 110 and 111), analogous to that previously observed for the virtual and reference curves (Equations 55, 56, 75 and 76).

$$\begin{array}{l} \text{from} \\ (106) \\ (107) \end{array} \quad \frac{y_{\text{int}}}{x_{\text{int}}} = \frac{\frac{y_0 \cdot (2A - 1)}{A - 1}}{\frac{x_0 \cdot (2A - 1)}{A - 1}} = \frac{y_0}{x_0} = P_0 \quad (110)$$

$$\begin{array}{l} \text{from} \\ (108) \\ (109) \end{array} \quad \frac{y_{\text{asym}}}{x_{\text{asym}}} = \frac{-y_0 \cdot (A - 1)}{-x_0 \cdot (A - 1)} = \frac{y_0}{x_0} = P_0 \quad (111)$$

The geometric means of the significant x- and y-coordinates is also preserved, but the perspective needs to be generalized to be their distances from the asymptotes, instead of implicitly their distance relative to the origin (which was the case previously). While many of the manipulations in this document may be [justly] criticized for their mathematical redundancy, this one is especially so (Equations 112, 113, 114 and 115). Measuring the distance of the intercepts and the origin from the asymptotes is literally the same as reversing the shift of the real curve back to the virtual curve, making these identities and the process of acquiring them identical to Equations 51, 52, 53 and 54. The mysterious constant C shows up again here for the same reason (Equations 116 and 117). This part of the exercise is not entirely without merit, though; these symbolic representations provide a convenient handle for further algebraic abstraction when reparametrizing the curve, as will be discussed shortly.

$$\begin{array}{l} \text{from} \\ (88) \\ (92) \end{array} \quad (x_{\text{int}} - x_{\text{asym}}) \cdot (0 - x_{\text{asym}}) = \max(x_v) \cdot \min(x_v) = A^2 \cdot x_0^2 \quad (112)$$

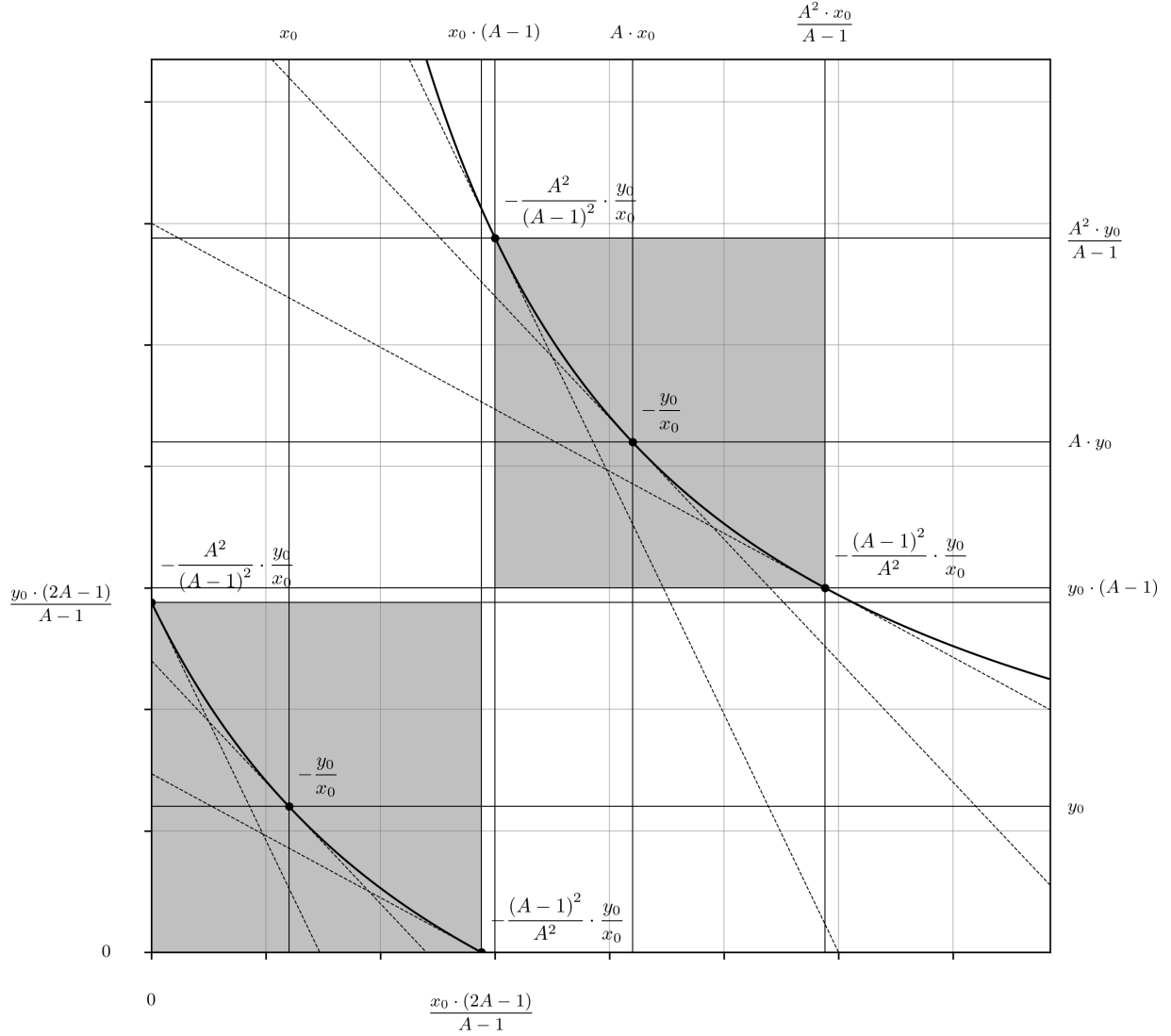


Fig. 18 The x- and y-intercepts of the real curve (Equations 106 and 107) are annotated, which completes its characterization. The real and virtual curves are depicted with the capstone algebraic identities elucidated thus far, including the value of the derivative evaluated at these points, illustrated with annotated tangent lines to the curve.

$$\begin{array}{l} \text{from} \\ (112) \end{array} \quad \sqrt{(x_{\text{int}} - x_{\text{asym}})} \cdot \sqrt{(0 - x_{\text{asym}})} = \sqrt{\max(x_v)} \cdot \sqrt{\min(x_v)} = A \cdot x_0 \quad (113)$$

$$\begin{array}{l} \text{from} \\ (89) \\ (93) \end{array} \quad (y_{\text{int}} - y_{\text{asym}}) \cdot (0 - y_{\text{asym}}) = \max(y_v) \cdot \min(y_v) = A^2 \cdot y_0^2 \quad (114)$$

$$\begin{array}{l} \text{from} \\ (114) \end{array} \quad \sqrt{(y_{\text{int}} - y_{\text{asym}})} \cdot \sqrt{(0 - y_{\text{asym}})} = \sqrt{\max(y_v)} \cdot \sqrt{\min(y_v)} = A \cdot y_0 \quad (115)$$

$$\begin{array}{l} \text{from} \\ (88) \\ (92) \end{array} \quad \frac{(x_{\text{int}} - x_{\text{asym}})}{(0 - x_{\text{asym}})} = \frac{\max(x_v)}{\min(x_v)} = \frac{A^2}{(A-1)^2} = C \quad (116)$$

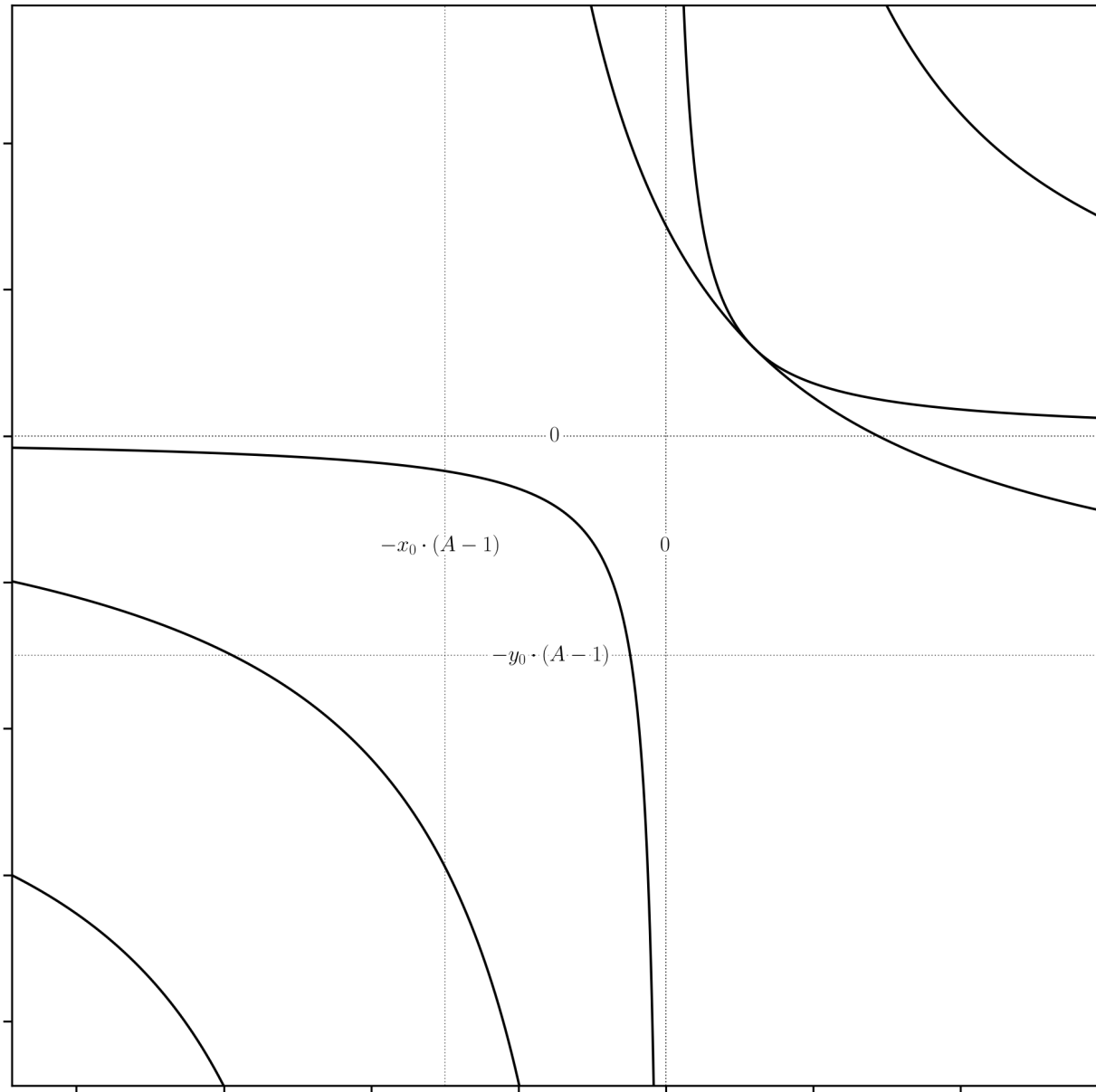


Fig. 19 The horizontal and vertical asymptotes of the virtual (Equations 108 and 109) and reference curves, and the real curve are depicted with dotted lines, and their coordinates are annotated appropriately.

$$\begin{array}{l} \text{from} \\ (89) \\ (93) \end{array} \quad \frac{(y_{\text{int}} - y_{\text{asym}})}{(0 - y_{\text{asym}})} = \frac{\max(y_v)}{\min(y_v)} = \frac{A^2}{(A - 1)^2} = C \quad (117)$$

Tying up loose ends, the same simulated token swap performed in Figures 14 and 15 is repeated for the real curve and compared with the virtual curve in Figures 19 and 20. The important thing to note is that the change in the coordinates conventions makes zero difference with respect to the outcome of the swap. The magnitudes of the Δx and Δy arrows in Figure 19, and the integrated area in Figure 20 are identical; only the position on the plane where the algorithm is performed has changed, which has no effect on either the marginal or effective rates of exchange. Therefore, they are equivalent in every way that matters to us.

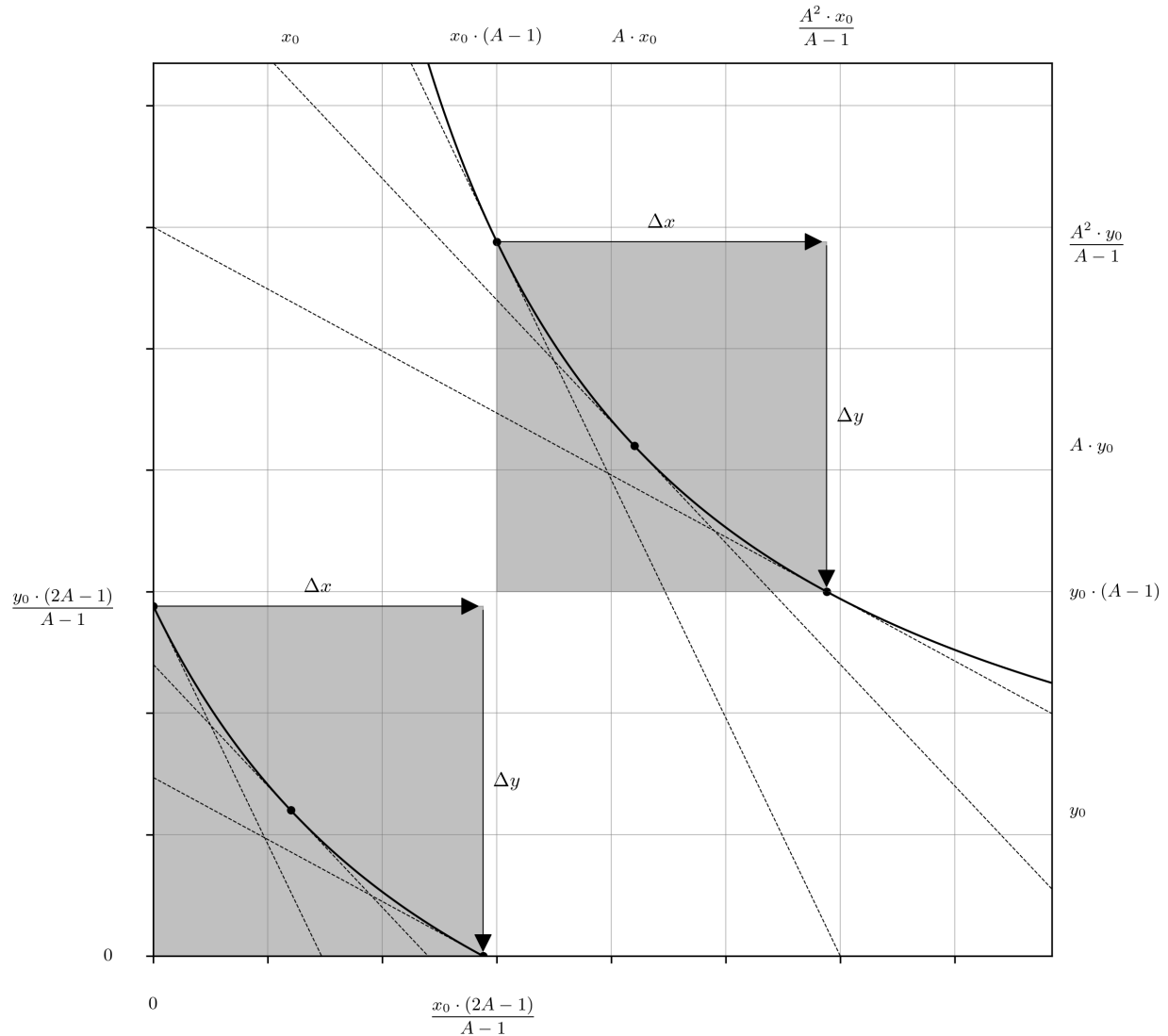


Fig. 20 Traversal upon the rectangular hyperbolas $x_v \cdot y_v = A^2 \cdot x_0 \cdot y_0$ and $(x + x_0 \cdot (A - 1)) \cdot (y + y_0 \cdot (A - 1)) = A^2 \cdot x_0 \cdot y_0$ (Equations 26 and 80), representing a token swap against the virtual and real depictions of the amplified liquidity pools, where $\Delta x > 0$ and $\Delta y < 0$. The swap quantities Δx and Δy , and marginal rates of exchange before and after the swap are identical. Therefore, with respect to the outcome of the exchange the difference between the two curve implementations is nothing.

4 Other “Unnatural” Reparameterizations of the Concentrated Liquidity Invariant Function

4.1 The Uniswap v3 Real Curve

The most common reparameterization of the real concentrated liquidity invariant (Equation 80) is that popularized by Uniswap v3 in its whitepaper.¹³ To construct this form, first obtain the identities of $(A - 1)$ in terms of the square roots of the price bounds via Equations 43 and 47 (Equations 118, 119, 120 and 121). Then, substitute the obtained $(A - 1)$ identities into the horizontal and vertical shift components of Equation 80 as appropriate (Equation 122); the substitution pattern must be such that the coefficient of the shift (x_0 or y_0) simplifies to its square root ($\sqrt{x_0}$ or $\sqrt{y_0}$) as shown in Equation 123. Substitution of the constant term $A \cdot \sqrt{x_0} \cdot \sqrt{y_0}$ for L (Equation 124) yields the Uniswap v3 real curve equation (Equation 125).

¹³Adams, H.; Zinmeister, N.; Salem, M.; Keefer, R.; Robinson, D. Uniswap v3 Core uniswap.org/whitepaper-v3.pdf

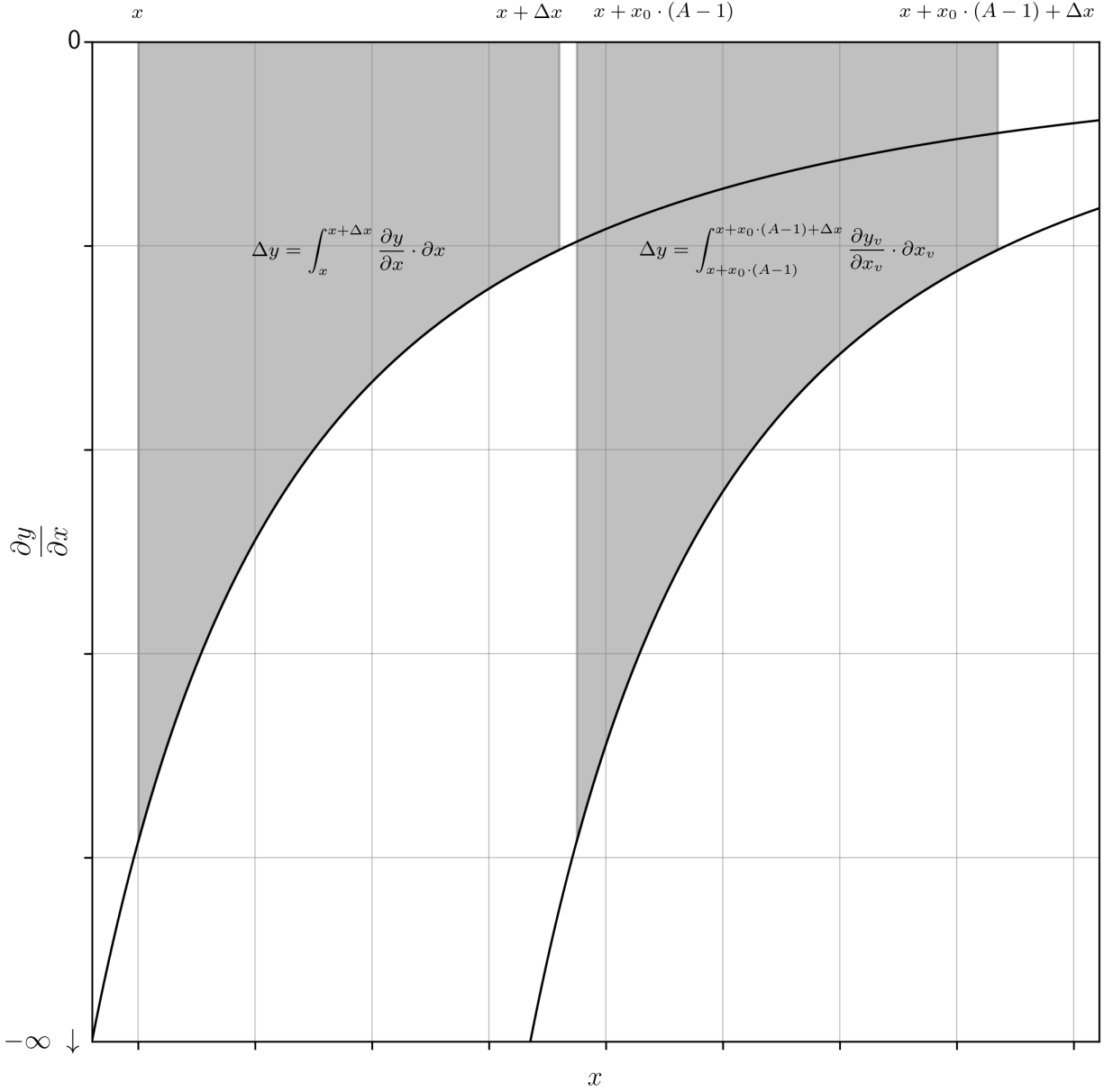


Fig. 21 The integration above $\partial y_v/\partial x_v = -A^2 \cdot x_0 \cdot y_0/x_v^2$ and $\partial y/\partial x = -A^2 \cdot x_0 \cdot y_0/(x + x_0 \cdot (A - 1))^2$ (Equations 35 and 95) over the intervals $x \rightarrow x + \Delta x$ and $x + x_0 \cdot (A - 1) \rightarrow x + x_0 \cdot (A - 1) + \Delta x$ representing a token swap against both the real and virtual curves, where $\Delta x > 0$ and $\Delta y < 0$. Apart from the shift along the x-axis, these are identical in every other aspect. Note that whereas the relationship between the reference and virtual price curves in Figure 15 was multiplicative (x and Δx , versus $A \cdot x$ and $A \cdot (x + \Delta x)$), the relationship between the real and virtual price curves depicted here is additive (x and Δx versus $x + x_0 \cdot (A - 1)$ and $x + x_0 \cdot (A - 1) + \Delta x$).

from
(43)

$$\sqrt{P_{\text{high}}} = \frac{A}{A - 1} \cdot \frac{\sqrt{y_0}}{\sqrt{x_0}} \quad (118)$$

from
(118)

$$A - 1 = \frac{A}{\sqrt{P_{\text{high}}}} \cdot \frac{\sqrt{y_0}}{\sqrt{x_0}} \quad (119)$$

$$\begin{array}{l} \text{from} \\ (47) \end{array} \quad \sqrt{P_{\text{low}}} = \frac{A-1}{A} \cdot \frac{\sqrt{y_0}}{\sqrt{x_0}} \quad (120)$$

$$\begin{array}{l} \text{from} \\ (120) \end{array} \quad A-1 = A \cdot \sqrt{P_{\text{low}}} \cdot \frac{\sqrt{x_0}}{\sqrt{y_0}} \quad (121)$$

$$\begin{array}{l} \text{from} \\ (80) \\ (119) \\ (121) \end{array} \quad \left(x + x_0 \cdot \left(\frac{A}{\sqrt{P_{\text{high}}}} \cdot \frac{\sqrt{y_0}}{\sqrt{x_0}} \right) \right) \cdot \left(y + y_0 \cdot \left(A \cdot \sqrt{P_{\text{low}}} \cdot \frac{\sqrt{x_0}}{\sqrt{y_0}} \right) \right) = A^2 \cdot x_0 \cdot y_0 \quad (122)$$

$$\begin{array}{l} \text{from} \\ (119) \end{array} \quad \left(x + \frac{A \cdot \sqrt{y_0} \cdot \sqrt{x_0}}{\sqrt{P_{\text{high}}}} \right) \cdot \left(y + A \cdot \sqrt{y_0} \cdot \sqrt{x_0} \cdot \sqrt{P_{\text{low}}} \right) = A^2 \cdot x_0 \cdot y_0 \quad (123)$$

$$\begin{array}{l} \text{from} \\ (123) \end{array} \quad A \cdot \sqrt{y_0} \cdot \sqrt{x_0} = L \quad (124)$$

$$\begin{array}{l} \text{from} \\ (123) \\ (124) \end{array} \quad \left(x + \frac{L}{\sqrt{P_{\text{high}}}} \right) \cdot \left(y + L \cdot \sqrt{P_{\text{low}}} \right) = L^2 \quad (125)$$

This process affords a new expression for the same mathematical object; fundamentally, Equations 80 and 125 are one and the same thing. However, this does not mean that they are equally useful given their context in smart contract implementations. For example, Equation 125 conveniently lists its own price bounds in the invariant itself but requires one to perform a little extra work to deduce its reference coordinates and relative scaling. On the other hand, Equation 80 reports its own reference coordinates and relative scaling at the expense of the price bounds. From an analytical perspective the difference is meaningless, but from an implementation perspective the difference could be important. In the case of Uniswap v3, the price bounds are commensurate with an overall smart contract architecture decision that requires these parameters (i.e. the tick boundaries) to be available and reliable. While on-the-fly calculations can recreate these parameters in situ, these operations add more computational overhead and rounding errors which may present gas efficiency issues, or even smart contract security concerns. Therefore, the expression used (Equation 125) reflects the overall systems design and serves as an abstraction of how to interpret and use the data one is likely to find stored there.

This is an important discussion point, because the difference between well and poorly designed systems can come down to the choice of how to parameterize the equations that describe it, even if those descriptions are analytically redundant. In the case of Uniswap v3, Equation 125 is in some sense the *correct parameterization for that system*; however, it is a dangerous idea to consider it a catch all that should be used by any concentrated liquidity system.

The Uniswap v3 real curve (Equation 125) is plotted in Figure 22 and annotated with the slopes of the tangent lines at the intercepts, which is the only information presently available at this stage of the analysis.

Returning to the objective of this part of the exercise, we will now fully elucidate the reparametrized version of the model beginning from the Uniswap v3 invariant function (Equation 125), characterise the real, virtual, and reference curves, and re-contextualize them in terms of the general theory as outlined in the previous sections. Manipulation of the Uniswap v3 invariant (Equation 125) is performed using the same methods as before. First, the expressions isolating x and y are derived (Equations 126 and 127).

$$\begin{array}{l} \text{from} \\ (125) \end{array} \quad x = \frac{L^2}{(y + L \cdot \sqrt{P_{\text{low}}})} - \frac{L}{\sqrt{P_{\text{high}}}} \quad (126)$$

$$\begin{array}{l} \text{from} \\ (125) \end{array} \quad y = \frac{L^2}{x + \frac{L}{\sqrt{P_{\text{high}}}}} - L \cdot \sqrt{P_{\text{low}}} \quad (127)$$

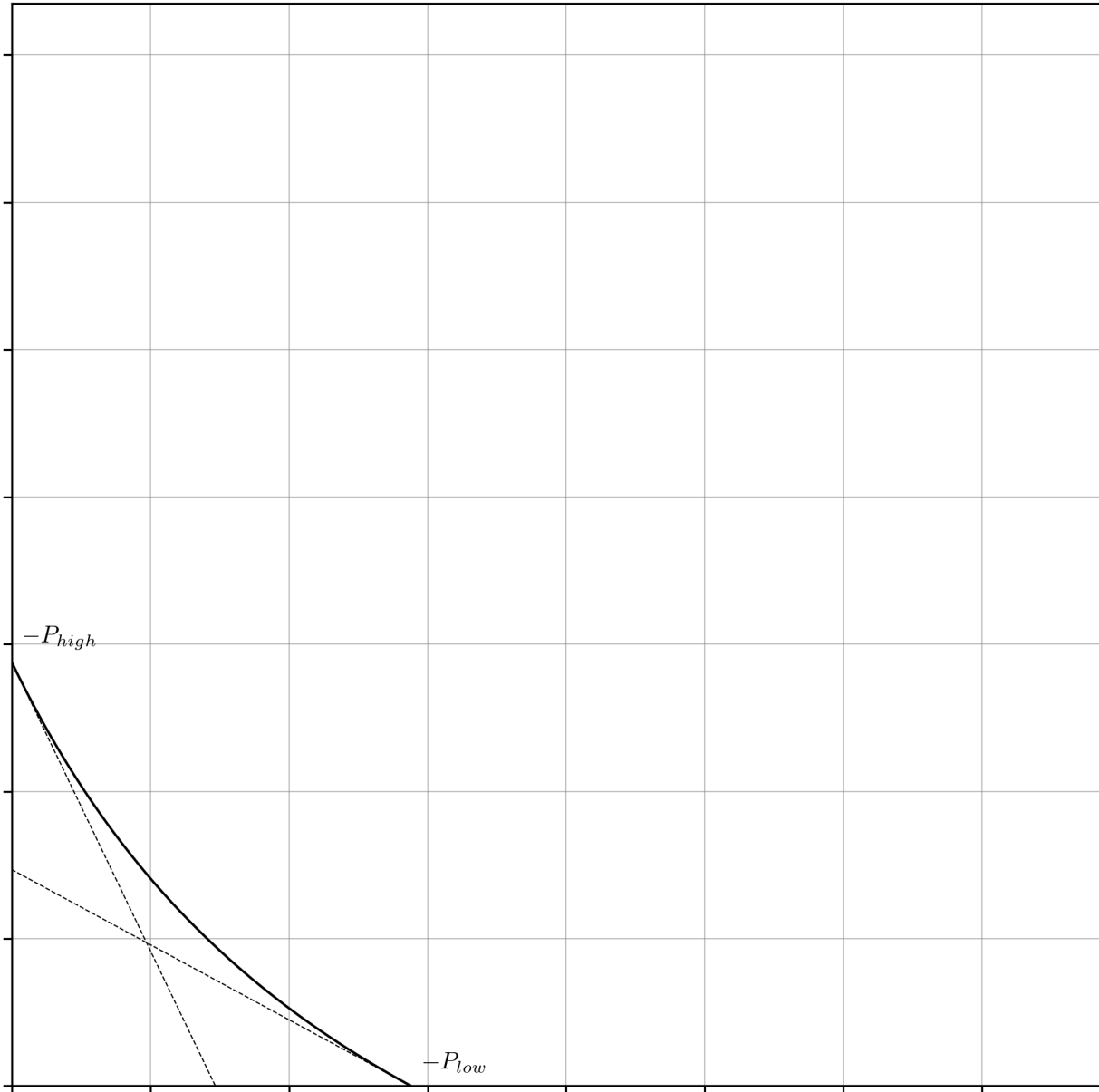


Fig. 22 Initial Uniswap v3 real curve. Due to its parameterisation and prior to performing any additional analysis, only the slopes of the tangent lines at the intercepts are known ($-P_{high}$ and $-P_{low}$).

Then, the token swap equations are constructed as normal; the x and y terms in Equation 125 or Equations 126 and 127 are substituted for $x + \Delta x$ and $y + \Delta y$ then rearranged to make either Δx or Δy the subject (Equations 128, 129 and 130).

$$\begin{array}{l} \text{from} \\ (125) \end{array} \quad \left(x + \Delta x + \frac{L}{\sqrt{P_{high}}} \right) \cdot \left(y + \Delta y + L \cdot \sqrt{P_{low}} \right) = L^2 \quad (128)$$

$$\begin{array}{l} \text{from} \\ (126) \\ (128) \end{array} \quad \Delta x = \frac{L^2}{(y + \Delta y + L \cdot \sqrt{P_{low}})} - \frac{L}{\sqrt{P_{high}}} - x \quad (129)$$

$$\begin{array}{l} \text{from} \\ (127) \\ (128) \end{array} \quad \Delta y = \frac{L^2}{x + \Delta x + \frac{L}{\sqrt{P_{\text{high}}}}} - L \cdot \sqrt{P_{\text{low}}} - y \quad (130)$$

Dimension reduction is achieved via the same process as previously demonstrated; the identities for x and y in Equations 126 and 127 are substituted into Equations 129 and 130, respectively (Equations 131 and 133). Simplifying these expressions into single fractions yields Equations 132 and 134.

$$\begin{array}{l} \text{from} \\ (126) \\ (129) \end{array} \quad \Delta x = \frac{L^2}{(y + \Delta y + L \cdot \sqrt{P_{\text{low}}})} - \frac{L}{\sqrt{P_{\text{high}}}} - \frac{L^2}{(y + L \cdot \sqrt{P_{\text{low}}})} + \frac{L}{\sqrt{P_{\text{high}}}} \quad (131)$$

$$\begin{array}{l} \text{from} \\ (128) \end{array} \quad \Delta x = -\frac{\Delta y \cdot L^2}{(y + L \cdot \sqrt{P_{\text{low}}}) \cdot (y + \Delta y + L \cdot \sqrt{P_{\text{low}}})} \quad (132)$$

$$\begin{array}{l} \text{from} \\ (127) \\ (130) \end{array} \quad \Delta y = \frac{L^2}{x + \Delta x + \frac{L}{\sqrt{P_{\text{high}}}}} - L \cdot \sqrt{P_{\text{low}}} - \frac{L^2}{x + \frac{L}{\sqrt{P_{\text{high}}}}} + L \cdot \sqrt{P_{\text{low}}} \quad (133)$$

$$\begin{array}{l} \text{from} \\ (133) \end{array} \quad \Delta y = -\frac{\Delta x \cdot L^2}{\left(x + \frac{L}{\sqrt{P_{\text{high}}}}\right) \cdot \left(x + \Delta x + \frac{L}{\sqrt{P_{\text{high}}}}\right)} \quad (134)$$

Note that Equations 132 and 134 can also be obtained directly from their predecessors, Equations 87 and 89, by substituting the scaling term, $A^2 \cdot x_0 \cdot y_0$, and the horizontal and vertical shift terms, $x_0 \cdot (A - 1)$ and $y_0 \cdot (A - 1)$, for their implicit identities, L^2 , $L/\sqrt{P_{\text{high}}}$, and $L \cdot \sqrt{P_{\text{low}}}$, respectively (Equations 118, 119, 120, 121, 122, 123, 124 and 125). This substitution pattern can also be used to obtain the effective and marginal price equations, but for consistency with the previous work, these identities will be elaborated below according to the previously established methods.

Repeating the process demonstrated in Equations 12, 13, 14, 15 and Equations 92, 93, 94, 95, rearrangement of Equations 129, and 131 to get the *effective rate of exchange*, followed by determination of the limit as the denominator goes to zero gives the *instantaneous rate of exchange* (i.e. the marginal price)(Equations 135, 136, 137, 138).

$$\begin{array}{l} \text{from} \\ (132) \end{array} \quad \frac{\Delta x}{\Delta y} = -\frac{L^2}{(y + L \cdot \sqrt{P_{\text{low}}}) \cdot (y + \Delta y + L \cdot \sqrt{P_{\text{low}}})} \quad (135)$$

$$\begin{array}{l} \text{from} \\ (135) \end{array} \quad \frac{\partial x}{\partial y} = \lim_{\Delta y \rightarrow 0} \frac{\Delta x}{\Delta y} = -\frac{L^2}{(y + L \cdot \sqrt{P_{\text{low}}})^2}; \quad \frac{\partial y}{\partial x} = -\frac{(y + L \cdot \sqrt{P_{\text{low}}})^2}{L^2} \quad (136)$$

$$\begin{array}{l} \text{from} \\ (134) \end{array} \quad \frac{\Delta y}{\Delta x} = -\frac{L^2}{\left(x + \frac{L}{\sqrt{P_{\text{high}}}}\right) \cdot \left(x + \Delta x + \frac{L}{\sqrt{P_{\text{high}}}}\right)} \quad (137)$$

$$\begin{array}{l} \text{from} \\ (137) \end{array} \quad \frac{\partial y}{\partial x} = \lim_{\Delta x \rightarrow 0} \frac{\Delta y}{\Delta x} = -\frac{L^2}{\left(x + \frac{L}{\sqrt{P_{\text{high}}}}\right)^2}; \quad \frac{\partial x}{\partial y} = -\frac{\left(x + \frac{L}{\sqrt{P_{\text{high}}}}\right)^2}{L^2} \quad (138)$$

The Uniswap v3 marginal rate equations can also be expressed in terms of both token balances via substitution of the x and y terms in Equations 13, and 15 with their horizontally or vertically shifted transformations (Equation 139), or via substitution of the identity of L^2 from the LHS of Equation 125 into Equations 136, and 138. Simplifying the fractions in Equation 139 yields Equation 140.

$$\begin{array}{l} \text{from} \\ (125) \\ (136) \\ (138) \end{array} \quad \frac{\partial x}{\partial y} = -\frac{x + \frac{L}{\sqrt{P_{\text{high}}}}}{y + L \cdot \sqrt{P_{\text{low}}}}; \quad \frac{\partial y}{\partial x} = -\frac{y + L \cdot \sqrt{P_{\text{low}}}}{x + \frac{L}{\sqrt{P_{\text{high}}}}} \quad (139)$$

$$\begin{array}{l} \text{from} \\ (139) \end{array} \quad \frac{\partial x}{\partial y} = -\frac{x \cdot \sqrt{P_{\text{high}}} + L}{\sqrt{P_{\text{high}}} \cdot (y + L \cdot \sqrt{P_{\text{low}}})}; \quad \frac{\partial y}{\partial x} = -\frac{\sqrt{P_{\text{high}}} \cdot (y + L \cdot \sqrt{P_{\text{low}}})}{x \cdot \sqrt{P_{\text{high}}} + L} \quad (140)$$

Continuous summation over the price curves (Equations 136 and 138) over the interval representing the number of tokens being swapped yields results identical to Equations 131, 132, 133 and 134. Again, do not be tempted to ignore the dependence of x and y on each other and attempt an integration of Equations 139 and 140, without separating these variables first (not shown).

$$\begin{array}{l} \text{from} \\ (131) \\ (132) \\ (136) \end{array} \quad \Delta x = -\int_y^{y+\Delta y} \frac{L^2}{(y + L \cdot \sqrt{P_{\text{low}}})^2} \cdot \partial y = \left[\frac{L^2}{y + L \cdot \sqrt{P_{\text{low}}}} \right]_y^{y+\Delta y} \Rightarrow \text{Eqns. 131 and 132} \quad (141)$$

$$\begin{array}{l} \text{from} \\ (133) \\ (134) \\ (138) \end{array} \quad \Delta y = -\int_x^{x+\Delta x} \frac{L^2}{\left(x + \frac{L}{\sqrt{P_{\text{high}}}}\right)^2} \cdot \partial x = \left[\frac{L^2}{x + \frac{L}{\sqrt{P_{\text{high}}}}} \right]_x^{x+\Delta x} \Rightarrow \text{Eqns. 133 and 134} \quad (142)$$

Both the direct token swap by traversal upon the bonding curve $(x + L/\sqrt{P_{\text{high}}}) \cdot (y + L \cdot \sqrt{P_{\text{low}}}) = L^2$ and the integration above $\partial y/\partial x = -L^2/(x + L/\sqrt{P_{\text{high}}})^2$ over the interval $x \rightarrow x + \Delta x$ are depicted in Figures 23 and 24.

The x - and y -intercepts under the Uniswap v3 parameterization are afforded by direct substitution of y and x for zero in Equations 126, and 127 (Equations 143, 144, and 145) (Figure 25). As expected, the quotient of y_{int} and x_{int} is equal to P_0 as previously observed in Equation 110 (Equation 146). The x - and y -asymptotes can again be derived geometrically or analytically (Figure 26). Since the Uniswap v3 curve makes use of the same horizontal and vertical shift parameters as previously discussed, albeit expressed in terms of L and either $\sqrt{P_{\text{high}}}$ or $\sqrt{P_{\text{low}}}$, the same geometric intuition can be applied here. Simply subtract from the origin these shift terms to obtain the asymptotes. Alternatively, substitute the y - or x -component of Equations 126 and 127 as required to set the denominator of the curve's equation to zero (Equations 147 and 148). Again, as seen previously (Equation 111), the quotient of the y - and x -asymptotes is equal to P_0 (Equation 149).

$$\begin{array}{l} \text{from} \\ (126) \end{array} \quad x_{\text{int}} = \frac{L}{\sqrt{P_{\text{low}}}} - \frac{L}{\sqrt{P_{\text{high}}}} = \frac{L}{\sqrt{P_{\text{high}}} \cdot \sqrt{P_{\text{low}}}} \cdot (\sqrt{P_{\text{high}}} - \sqrt{P_{\text{low}}}) \quad (143)$$

$$\begin{array}{l} \text{from} \\ (143) \end{array} \quad x_{\text{int}} = \frac{L}{P_0} \cdot (\sqrt{P_{\text{high}}} - \sqrt{P_{\text{low}}}) \quad (144)$$

$$\begin{array}{l} \text{from} \\ (127) \end{array} \quad y_{\text{int}} = L \cdot \sqrt{P_{\text{high}}} - L \cdot \sqrt{P_{\text{low}}} = L \cdot (\sqrt{P_{\text{high}}} - \sqrt{P_{\text{low}}}) \quad (145)$$

$$\begin{array}{l} \text{from} \\ (143) \\ (144) \\ (145) \end{array} \quad \frac{y_{\text{int}}}{x_{\text{int}}} = \sqrt{P_{\text{high}}} \cdot \sqrt{P_{\text{low}}} = P_0 \quad (146)$$

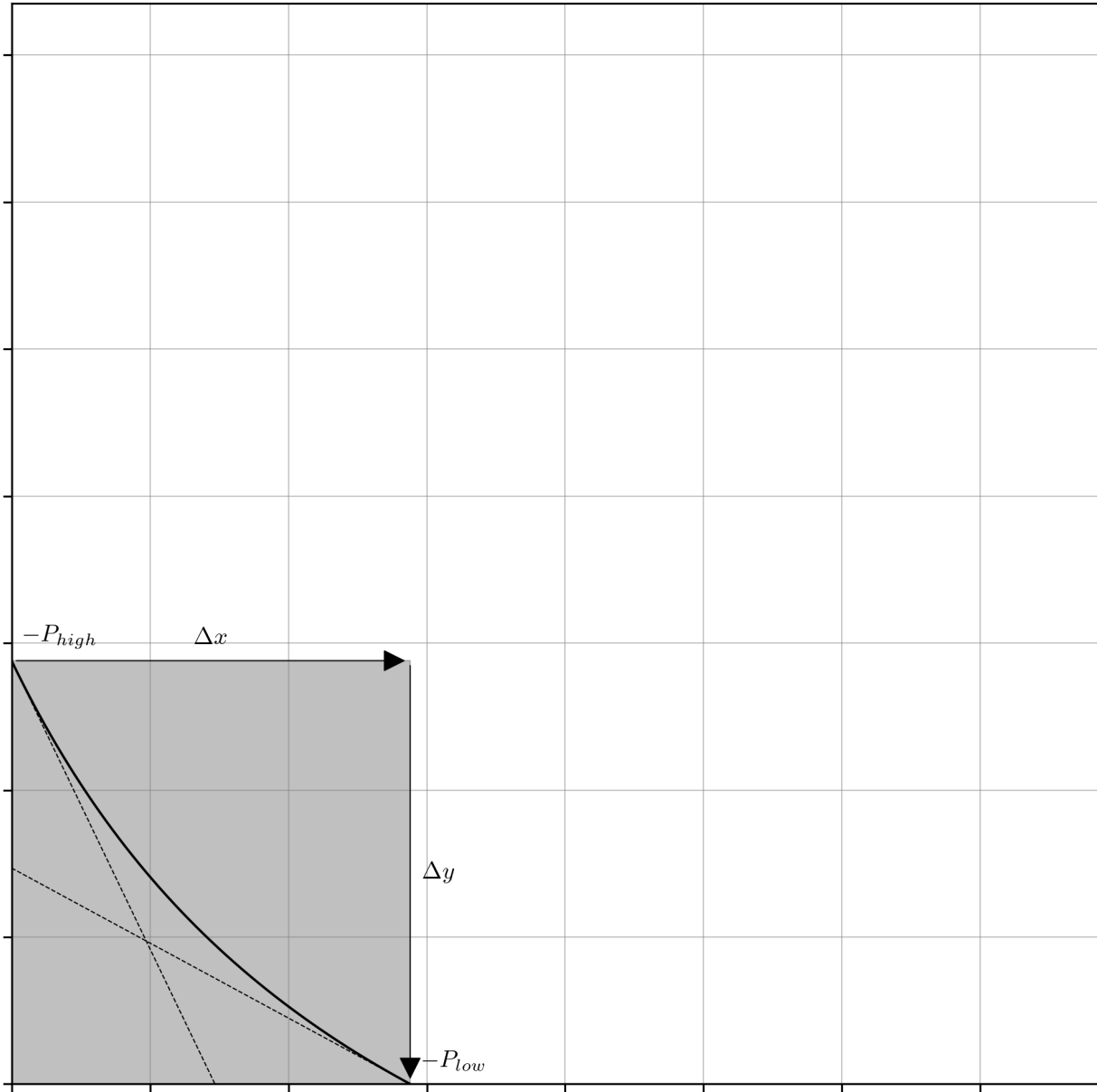


Fig. 23 Traversal upon the rectangular hyperbola $(x + L/\sqrt{P_{\text{high}}}) \cdot (y + L \cdot \sqrt{P_{\text{low}}}) = L^2$ (Equation 125), representing a token swap against the Uniswap v3 real curve, where $\Delta x > 0$ and $\Delta y < 0$.

$$\begin{array}{l} \text{from} \\ (127) \end{array} \quad x_{\text{asym}} = -\frac{L}{\sqrt{P_{\text{high}}}} \quad (147)$$

$$\begin{array}{l} \text{from} \\ (126) \end{array} \quad y_{\text{asym}} = -L \cdot \sqrt{P_{\text{low}}} \quad (148)$$

$$\begin{array}{l} \text{from} \\ (147) \\ (148) \end{array} \quad \frac{y_{\text{asym}}}{x_{\text{asym}}} = \sqrt{P_{\text{high}}} \cdot \sqrt{P_{\text{low}}} = P_0 \quad (149)$$

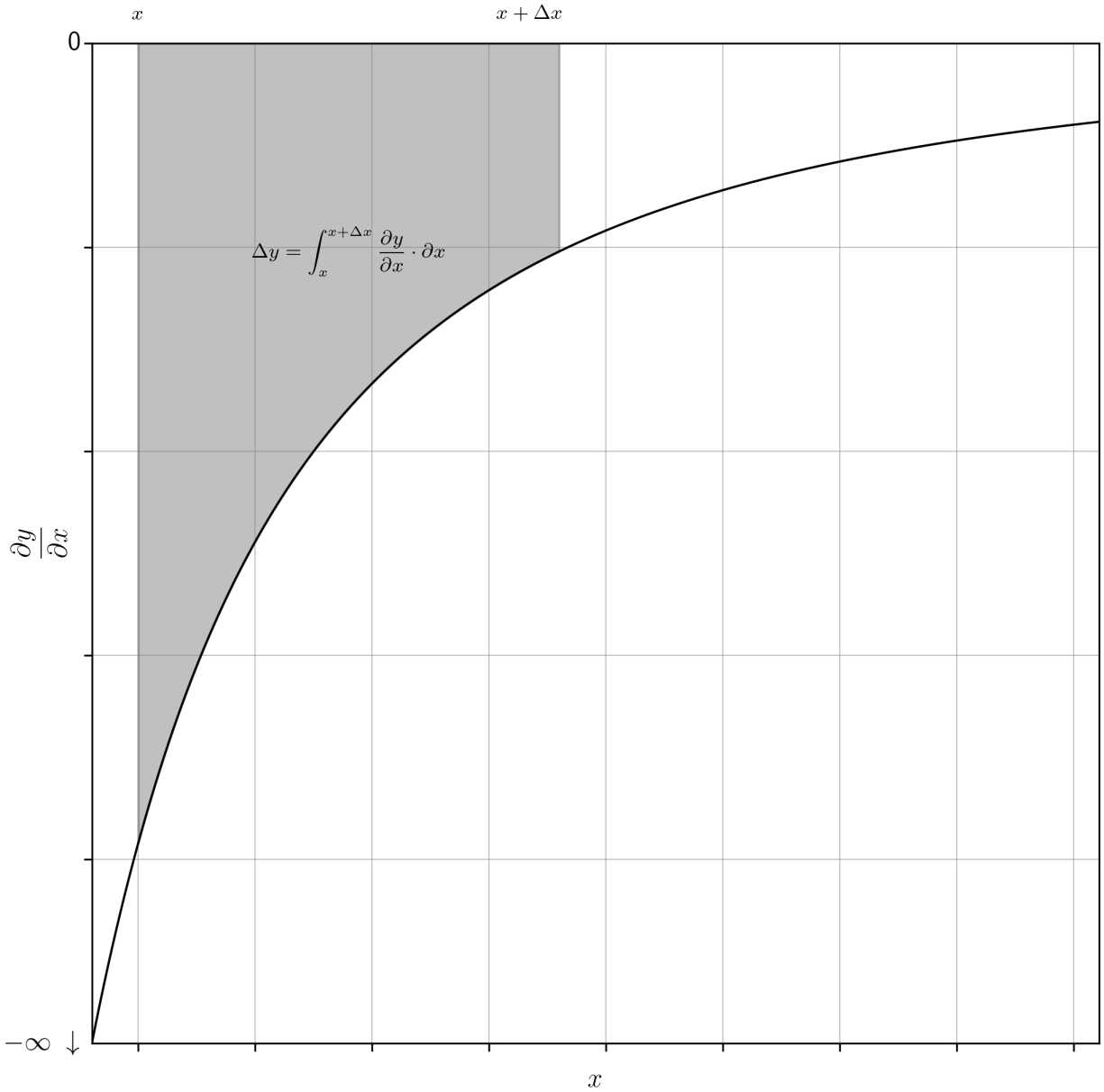


Fig. 24 The integration above $\partial y/\partial x = -L^2 / (x + L/\sqrt{P_{\text{high}}})^2$ (Equation 138) over the interval $x \rightarrow x + \Delta x$ representing a token swap against the Uniswap v3 real curve, where $\Delta x > 0$ and $\Delta y < 0$.

The remainder of this section is not strictly necessary – the algebra does not lie; however, as we are now several layers of abstraction above the original construction, this cross-referencing also helps to re-contextualize the derivation and connect back to some of the establishing theory.

The truth of the x- and y-intercept identities, x_{int} and y_{int} , derived in Equations 143, 144 and 145 can be verified with reference to work already completed. Since Equations 106 and 144 refer to the same object (i.e. the x-intercept of the real curve), we can assert their equivalence (Equation 150). Substitution of the P_0 and L terms via their definitions (Equations 45 and 124) results in Equation 151, which after handling the radicals yields a new relationship between A and the quotient of the difference of the square roots of the price bounds, $\sqrt{P_{\text{high}}}$ and $\sqrt{P_{\text{low}}}$, and the square root of their geometric mean, $\sqrt{P_0}$ (Equation 152). Similar algebraic manipulations of Equations 107 and 145 (i.e. the y-intercepts) produce the same result (Equations 153, 154 and 155). The independent verification of these expressions

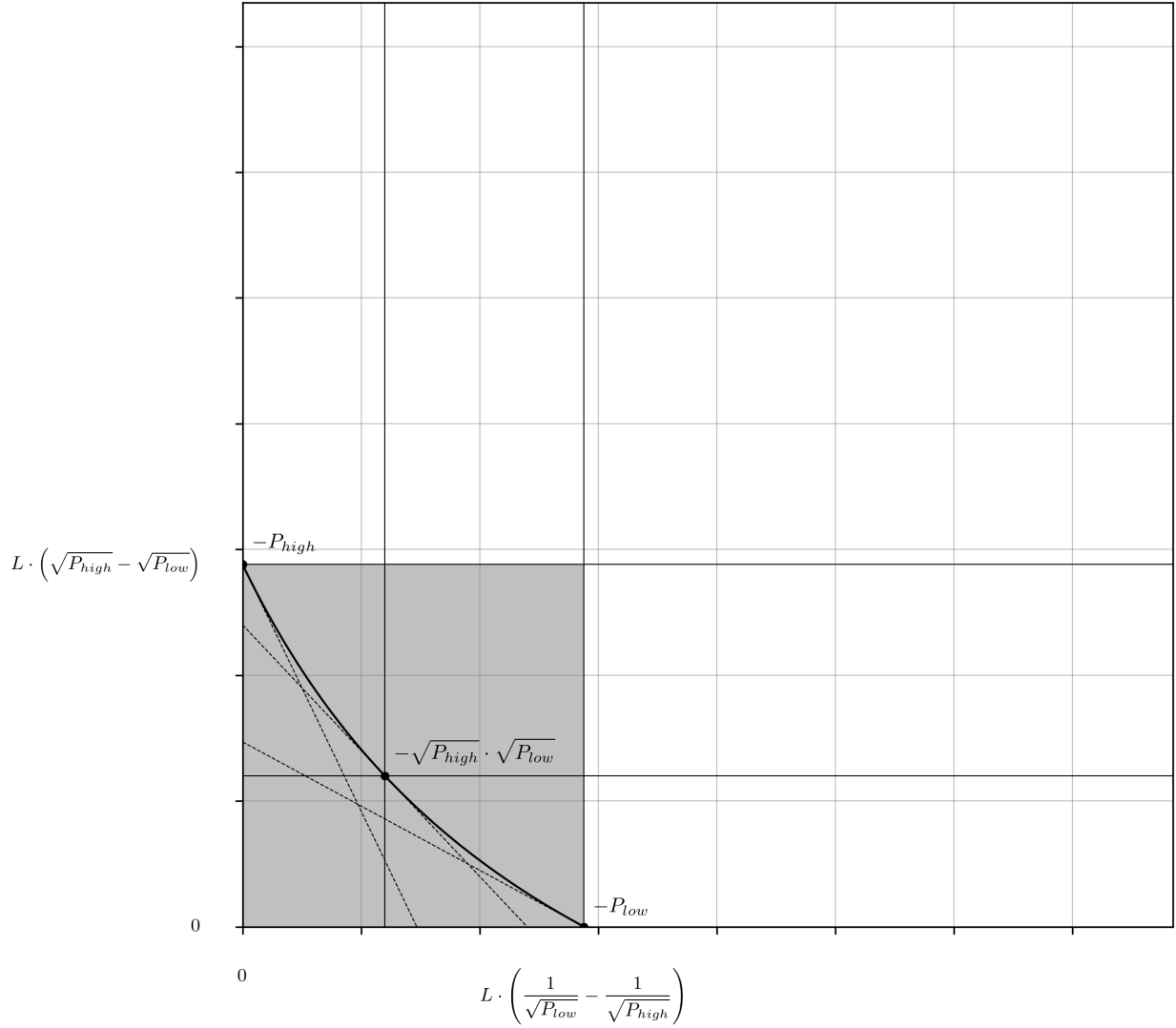


Fig. 25 The x- and y-intercepts of the Uniswap v3 real curve are annotated on the appropriate axes (Equations 143, 144 and 145).

can then be obtained directly from Equations 43, 45 and 47, which affords additional proof that these parameterizations are indeed describing the same object (Equations 156 and 157).

$$\begin{array}{l} \text{from} \\ (107) \\ (144) \end{array} \quad \frac{x_0 \cdot (2A - 1)}{A - 1} = \frac{L}{P_0} \cdot \left(\sqrt{P_{\text{high}}} - \sqrt{P_{\text{low}}} \right) \quad (150)$$

$$\begin{array}{l} \text{from} \\ (45) \\ (124) \\ (150) \end{array} \quad \frac{x_0 \cdot (2A - 1)}{A - 1} = \frac{A \cdot \sqrt{x_0} \cdot \sqrt{y_0}}{\frac{y_0}{x_0}} \cdot \left(\sqrt{P_{\text{high}}} - \sqrt{P_{\text{low}}} \right) \quad (151)$$

$$\begin{array}{l} \text{from} \\ (45) \\ (151) \end{array} \quad \frac{2A - 1}{A \cdot (A - 1)} = \frac{\sqrt{x_0}}{\sqrt{y_0}} \cdot \left(\sqrt{P_{\text{high}}} - \sqrt{P_{\text{low}}} \right) = \frac{\sqrt{P_{\text{high}}} - \sqrt{P_{\text{low}}}}{\sqrt{P_0}} \quad (152)$$

$$\begin{array}{l} \text{from} \\ (107) \\ (145) \end{array} \quad \frac{y_0 \cdot (2A - 1)}{A - 1} = L \cdot \left(\sqrt{P_{\text{high}}} - \sqrt{P_{\text{low}}} \right) \quad (153)$$

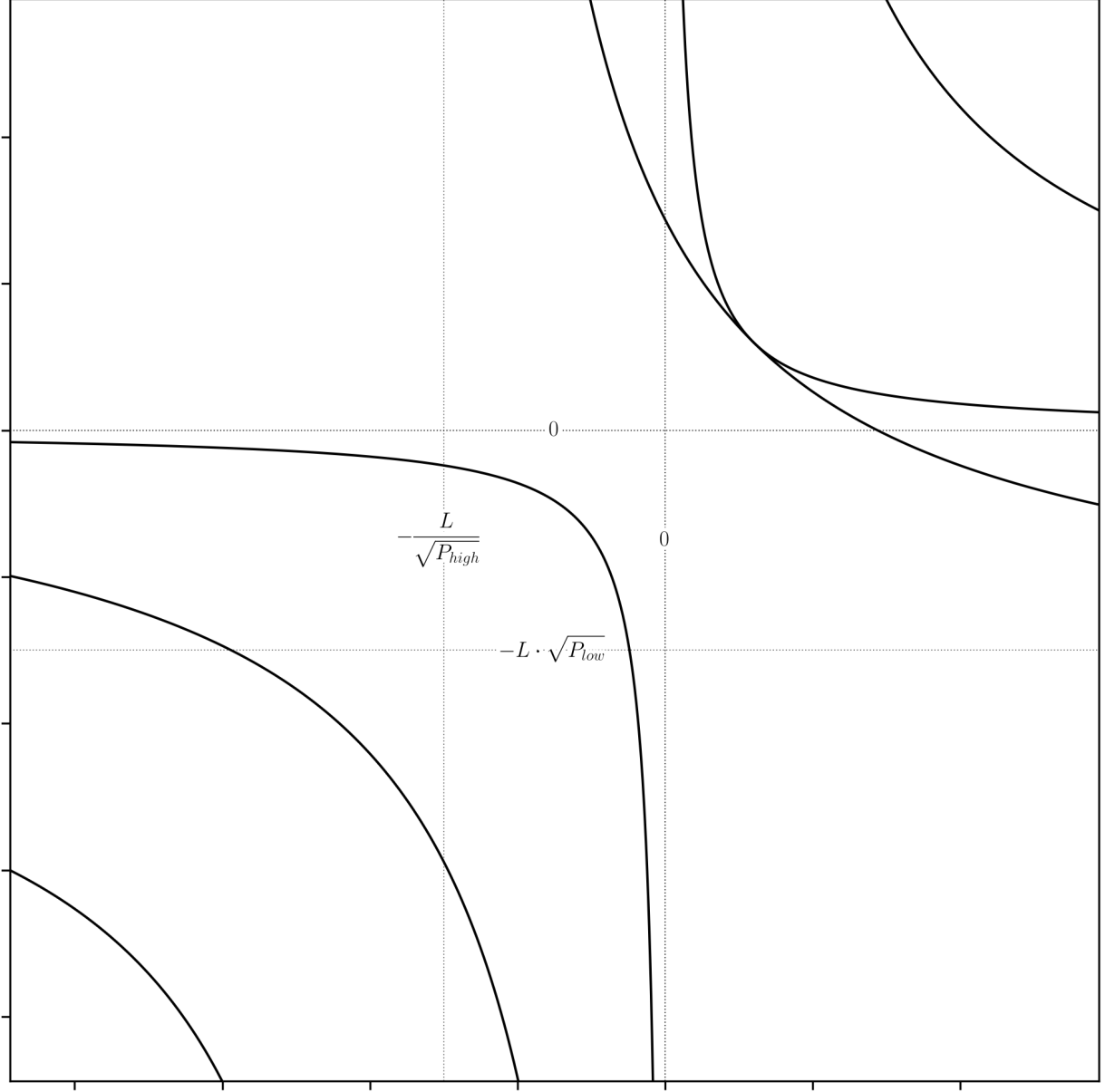


Fig. 26 The horizontal and vertical asymptotes of the Uniswap v3 virtual and reference curves, and its real curve (Equations 147 and 148), are depicted with dotted lines and their coordinates are annotated appropriately. While we have not yet approached the characterization of the reference and virtual curves, it is trivial that their asymptotes are at zero.

$$\begin{array}{l} \text{from} \\ (124) \\ (153) \end{array} \quad \frac{y_0 \cdot (2A - 1)}{A - 1} = A \cdot \sqrt{x_0} \cdot \sqrt{y_0} \cdot (\sqrt{P_{\text{high}}} - \sqrt{P_{\text{low}}}) \quad (154)$$

$$\begin{array}{l} \text{from} \\ (45) \\ (154) \end{array} \quad \frac{(2A - 1)}{A \cdot (A - 1)} = \frac{\sqrt{x_0}}{\sqrt{y_0}} \cdot (\sqrt{P_{\text{high}}} - \sqrt{P_{\text{low}}}) = \frac{\sqrt{P_{\text{high}}} - \sqrt{P_{\text{low}}}}{\sqrt{P_0}} \quad (155)$$

$$\begin{array}{l} \text{from} \\ (43) \\ (45) \\ (47) \end{array} \quad \sqrt{P_{\text{high}}} - \sqrt{P_{\text{low}}} = \frac{A}{A - 1} \cdot \frac{\sqrt{y_0}}{\sqrt{x_0}} - \frac{A - 1}{A} \cdot \frac{\sqrt{y_0}}{\sqrt{x_0}} = \frac{(2A - 1)}{A \cdot (A - 1)} \cdot \frac{\sqrt{y_0}}{\sqrt{x_0}} \quad (156)$$

$$\begin{array}{l} \text{from} \\ (45) \\ (156) \end{array} \quad \frac{\sqrt{P_{\text{high}}} - \sqrt{P_{\text{low}}}}{\sqrt{P_0}} = \frac{(2A - 1)}{A \cdot (A - 1)} \quad (157)$$

Further confirmation is possible via analysis of the x- and y-asymptotes, via Equations 108 and 147, and 109 and 148, respectively, which produce the identities previously obtained in Equations 43 and 47 for P_{high} and P_{low} (Equations 158 and 159).

$$\begin{array}{l} \text{from} \\ (108) \\ (124) \\ (147) \end{array} \quad x_0 \cdot (A - 1) = \frac{L}{\sqrt{P_{\text{high}}}} \Rightarrow \frac{A^2}{(A - 1)^2} \cdot \frac{y_0}{x_0} = P_{\text{high}} \quad (158)$$

$$\begin{array}{l} \text{from} \\ (109) \\ (124) \\ (148) \end{array} \quad y_0 \cdot (A - 1) = L \cdot \sqrt{P_{\text{low}}} \Rightarrow \frac{(A - 1)^2}{A^2} \cdot \frac{y_0}{x_0} = P_{\text{low}} \quad (159)$$

4.2 The Uniswap v3 Virtual Curve

The objective of this next section is to derive the same identities as was done for Equations 112, 113, 114, 115, 116 and 117, then prove these identities by way of substitution with previously obtained relationships.

Recall that the geometric means of the x- and y-bounds of the virtual curve have a correspondence with the amplified coordinates of the reference curve (to which its size is being compared). To perform this process for the Uniswap v3 reparametrized real curve, as before, we are comparing the bounds with respect to the asymptotes of the shifted curve, which is equivalent to reversing the shift before measuring these geometric means (Equations 160, 161, 162, 163, 164, 165, 166, 167, 168 and 169), thus recreating the virtual curve coordinates from the corresponding real curve coordinates (Figure 27). Consistent with prior work, the quotient of the maximum and minimum bounds in both dimensions are equal to the [yet] unexplained mystery constant, C (Equations 170 and 171). However, unlike last time it is now presented in terms of $\sqrt{P_{\text{high}}}$ and $\sqrt{P_{\text{low}}}$, instead of A . This identity has already been proven via Equation 62.

$$\begin{array}{l} \text{from} \\ (143) \\ (147) \end{array} \quad \max(x_v) = (x_{\text{int}} - x_{\text{asym}}) = \frac{L}{\sqrt{P_{\text{low}}}} - \frac{L}{\sqrt{P_{\text{high}}}} + \frac{L}{\sqrt{P_{\text{high}}}} \quad (160)$$

$$\begin{array}{l} \text{from} \\ (160) \end{array} \quad \max(x_v) = \frac{L}{\sqrt{P_{\text{low}}}} \quad (161)$$

$$\begin{array}{l} \text{from} \\ (147) \end{array} \quad \min(x_v) = (0 - x_{\text{asym}}) = \frac{L}{\sqrt{P_{\text{high}}}} \quad (162)$$

$$\begin{array}{l} \text{from} \\ (161) \\ (162) \end{array} \quad \max(x_v) \cdot \min(x_v) = \frac{L^2}{\sqrt{P_{\text{high}}} \cdot \sqrt{P_{\text{low}}}} = \frac{L^2}{P_0} \quad (163)$$

$$\begin{array}{l} \text{from} \\ (163) \end{array} \quad \sqrt{\max(x_v)} \cdot \sqrt{\min(x_v)} = \frac{L}{\sqrt[4]{P_{\text{high}}} \cdot \sqrt[4]{P_{\text{low}}}} = \frac{L}{\sqrt{P_0}} \quad (164)$$

$$\begin{array}{l} \text{from} \\ (145) \\ (148) \end{array} \quad \max(y_v) = (y_{\text{int}} - y_{\text{asym}}) = L \cdot (\sqrt{P_{\text{high}}} - \sqrt{P_{\text{low}}}) + L \cdot \sqrt{P_{\text{low}}} \quad (165)$$

$$\begin{array}{l} \text{from} \\ (165) \end{array} \quad \max(y_v) = L \cdot \sqrt{P_{\text{high}}} \quad (166)$$

$$\begin{array}{l} \text{from} \\ (148) \end{array} \quad \min(y_v) = (0 - y_{\text{asym}}) = L \cdot \sqrt{P_{\text{low}}} \quad (167)$$

$$\begin{array}{l} \text{from} \\ (166) \\ (167) \end{array} \quad \max(y_v) \cdot \min(y_v) = L^2 \cdot \sqrt{P_{\text{high}}} \cdot \sqrt{P_{\text{low}}} = L^2 \cdot P_0 \quad (168)$$

$$\begin{array}{l} \text{from} \\ (168) \end{array} \quad \sqrt{\max(y_v)} \cdot \sqrt{\min(y_v)} = L \cdot \sqrt[4]{P_{\text{high}}} \cdot \sqrt[4]{P_{\text{low}}} = L \cdot \sqrt{P_0} \quad (169)$$

$$\begin{array}{l} \text{from} \\ (161) \\ (162) \end{array} \quad \frac{\max(x_v)}{\min(x_v)} = \frac{\sqrt{P_{\text{high}}}}{\sqrt{P_{\text{low}}}} = C \quad (170)$$

$$\begin{array}{l} \text{from} \\ (166) \\ (167) \end{array} \quad \frac{\max(y_v)}{\min(y_v)} = \frac{\sqrt{P_{\text{high}}}}{\sqrt{P_{\text{low}}}} = C \quad (171)$$

Finally, validation of the geometric means of $\max(x_v)$ and $\min(x_v)$, and $\max(y_v)$ and $\min(y_v)$ (i.e. the x- and y-bounds of the implied virtual curve) (Equations 164 and 169) can be found by asserting their equivalence to the identities previously attained (Equations 113 and 115), and then deriving the identity of P_0 from this relationship (Equations 172 and 173).

$$\begin{array}{l} \text{from} \\ (113) \\ (124) \\ (164) \end{array} \quad A \cdot x_0 = \frac{L}{\sqrt{P_0}} \Rightarrow \frac{y_0}{x_0} = P_0 \quad (172)$$

$$\begin{array}{l} \text{from} \\ (115) \\ (124) \\ (169) \end{array} \quad A \cdot y_0 = L \cdot \sqrt{P_0} \Rightarrow \frac{y_0}{x_0} = P_0 \quad (173)$$

To complete the characterisation of the real curve and begin reconstructing the reparametrized reference curve, recall that the point at the coordinates (x_0, y_0) has two useful properties: the derivative of the reference curve evaluated at this point is equal to P_0 , and its position relative to the point on the virtual curve with the same derivative is uniquely determined by the same horizontal and vertical shift parameters as the real curve (none of the other points on the reference curve align with the virtual curve after performing the shift). Moreover, this is the one unique point that is shared by both the reference and the real curve, and their derivative evaluated at this point is also equal.

To obtain the identities of x_0 and y_0 , the shift parameter (equivalent to x_{asym} and y_{asym}) is applied as appropriate to the corresponding coordinates on the reference curve (i.e. the geometric means of $\min(x_v)$ and $\max(x_v)$, and $\min(y_v)$ and $\max(y_v)$) (Equations 174 and 176). In both cases, the expressions can be homogenized by distributing a lone radical into the square of its fourth root before factoring (Equations 175 and 177). There are two different representations apiece for the x_0 and y_0 identities included in Equations 175 and 177, respectively. One of these is a “better fit” for the real curve and the other for the reference curve, and both are used as appropriate when annotating the plots. With these coordinates, the characterization of the real curve is now complete (Figure 28).

$$\begin{array}{l} \text{from} \\ (147) \\ (164) \end{array} \quad x_0 = \sqrt{\max(x_v)} \cdot \sqrt{\min(x_v)} + x_{\text{asym}} = \frac{L}{\sqrt[4]{P_{\text{high}}} \cdot \sqrt[4]{P_{\text{low}}}} - \frac{L}{\sqrt{P_{\text{high}}}} \quad (174)$$

$$\begin{array}{l} \text{from} \\ (174) \end{array} \quad x_0 = L \cdot \left(\frac{1}{\sqrt[4]{P_{\text{high}}}} \cdot \left(\frac{1}{\sqrt[4]{P_{\text{low}}}} - \frac{1}{\sqrt[4]{P_{\text{high}}}} \right) \right) = \frac{L}{\sqrt[4]{P_{\text{high}}} \cdot \sqrt[4]{P_{\text{low}}}} \cdot \left(1 - \frac{\sqrt[4]{P_{\text{low}}}}{\sqrt[4]{P_{\text{high}}}} \right) \quad (175)$$

$$\begin{array}{l} \text{from} \\ (148) \\ (169) \end{array} \quad y_0 = \sqrt{\max(y_v)} \cdot \sqrt{\min(y_v)} + y_{\text{asym}} = L \cdot \sqrt[4]{P_{\text{high}}} \cdot \sqrt[4]{P_{\text{low}}} - L \cdot \sqrt{P_{\text{low}}} \quad (176)$$

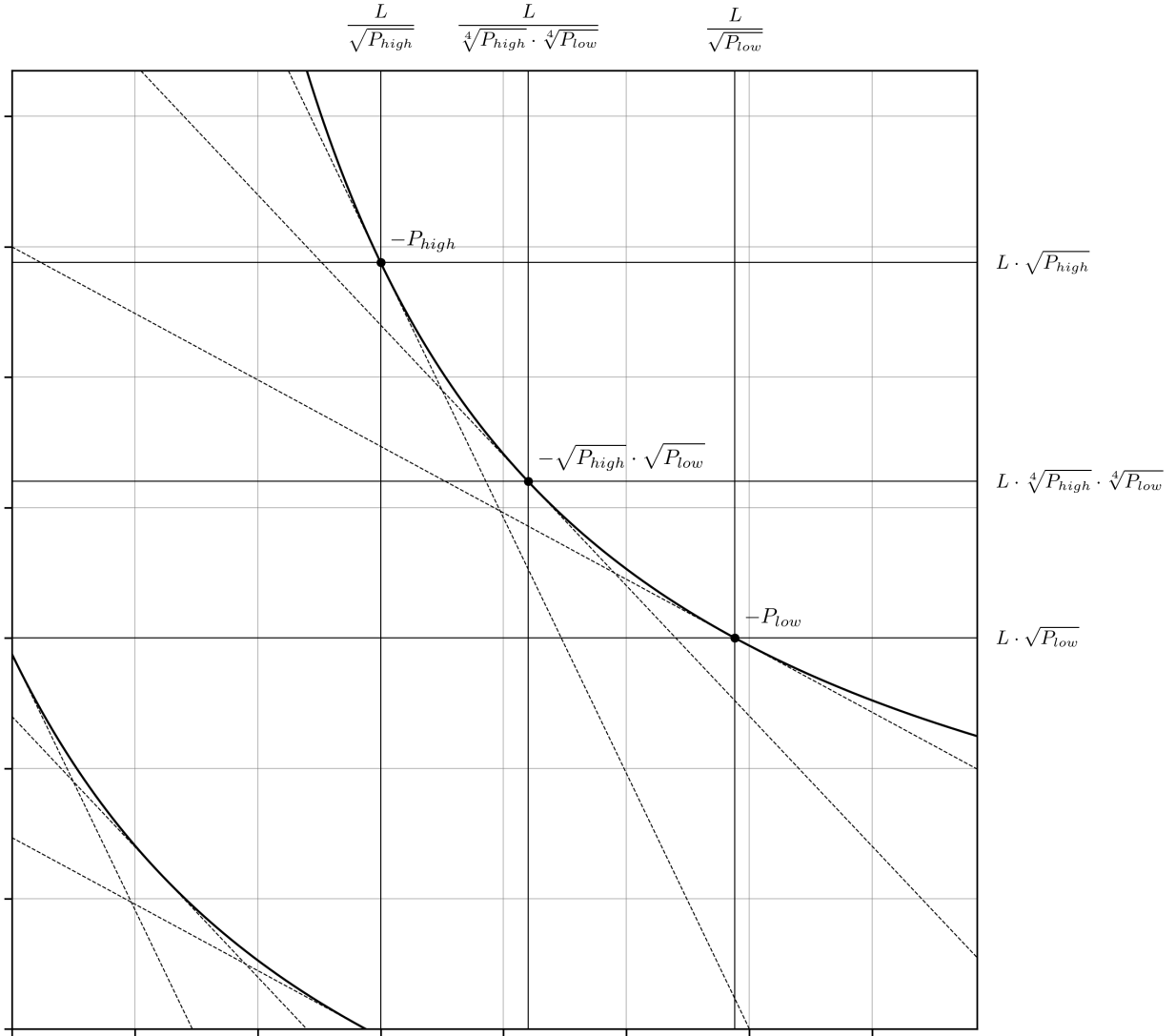


Fig. 27 The completed characterisation of the Uniswap v3 virtual curve, with the coordinates at its price bounds and geometric mean of the price bounds annotated as appropriate (Equations 161, 162, 166 and 167).

$$\text{from (176)} \quad y_0 = L \cdot \left(\sqrt[4]{P_{\text{low}}} \cdot \left(\sqrt[4]{P_{\text{high}}} - \sqrt[4]{P_{\text{low}}} \right) \right) = L \cdot \sqrt[4]{P_{\text{high}}} \cdot \sqrt[4]{P_{\text{low}}} \cdot \left(1 - \frac{\sqrt[4]{P_{\text{low}}}}{\sqrt[4]{P_{\text{high}}}} \right) \quad (177)$$

In contrast to the prior construction, which began with a reference curve followed by its virtual amplification and then horizontal and vertical shifts to arrive at the real curve, here, we have derived the virtual curve beginning from the shifted real curve. While the process is backwards, the result is the same, and it is still appropriate to define the real curve in terms of the virtual curve and the horizontal and vertical shifts (Figure 29).

Recall that the amplified virtual curve is just a regular rectangular hyperbola. The only important piece of information is its scaling constant, previously defined as $A^2 \cdot x_0 \cdot y_0$; none of these terms are native parameters in this case. However, the same scaling constant can be obtained directly from inspection of the RHS of Equation 125, or from the product of any set of coordinates along the curve, for which we have already elucidated three unique pairs. It does not matter which you use, the result will be the same (Equation 178). After that, the elaboration of the marginal price and token swap equations is performed as was done for Equations 26, 27, 28, 29, 30, 31, 32, 33, 34, and 35 (Equations 178, 179, 180, 181, 182, 183, 184, and 185).

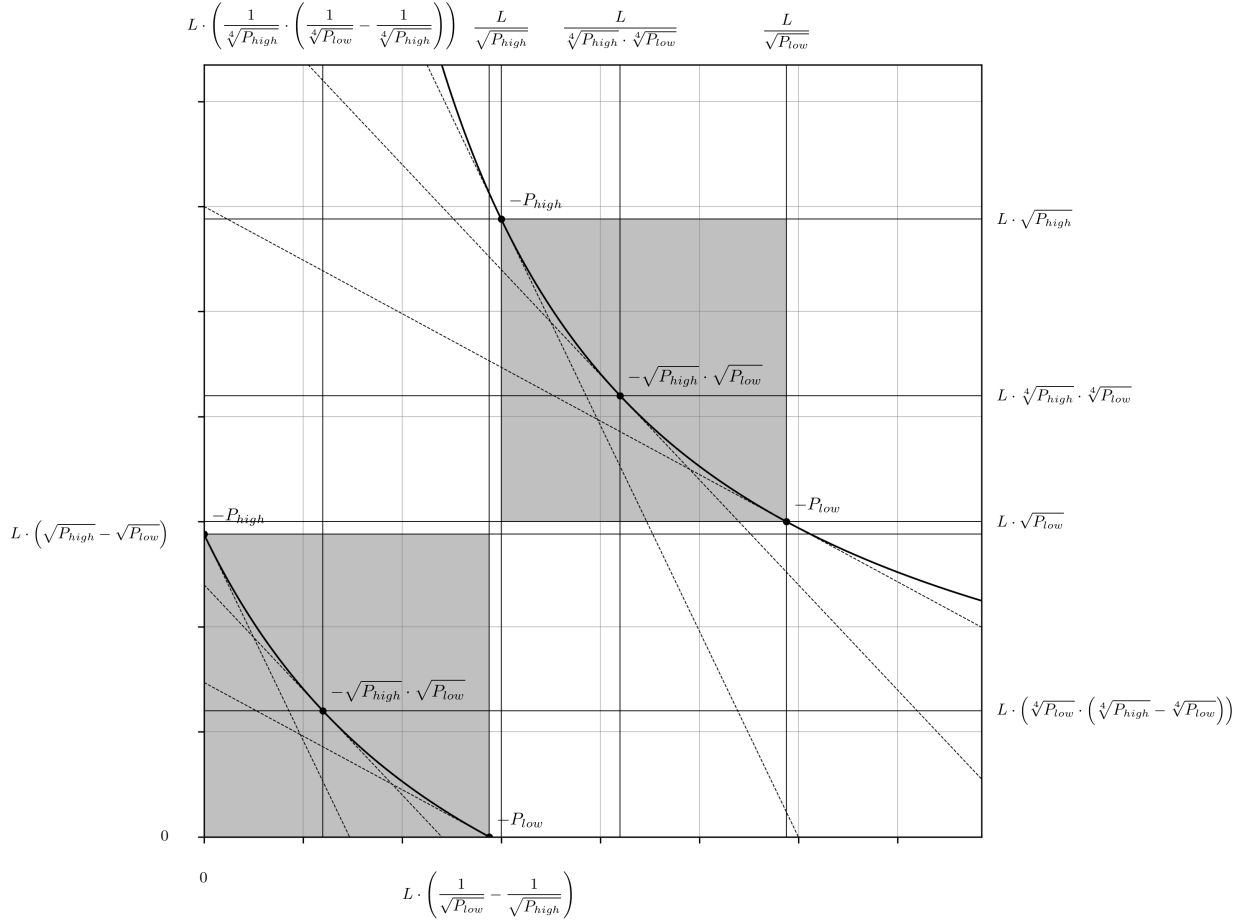


Fig. 28 Completed characterizations of the Uniswap v3 real and virtual curves are depicted and annotated appropriately (Equations 143, 145, 161, 162, 164, 166, 167, 169, 175, 177).

$$\begin{array}{l} \text{from} \\ (2) \end{array} \quad x_v \cdot y_v = \frac{L}{\sqrt[4]{P_{\text{high}}} \cdot \sqrt[4]{P_{\text{low}}}} \cdot L \cdot \sqrt[4]{P_{\text{high}}} \cdot \sqrt[4]{P_{\text{low}}} = L^2 \quad (178)$$

$$\begin{array}{l} \text{from} \\ (8) \end{array} \quad y_v = \frac{L^2}{x_v} \quad (179)$$

$$\begin{array}{l} \text{from} \\ (6) \end{array} \quad x_v = \frac{L^2}{y_v} \quad (180)$$

$$\begin{array}{l} \text{from} \\ (3) \end{array} \quad (x_v + \Delta x) \cdot (y_v + \Delta y) = L^2 \quad (181)$$

$$\begin{array}{l} \text{from} \\ (4) \\ (7) \end{array} \quad \Delta x = \frac{L^2}{y_v + \Delta y} - x_v = -\frac{\Delta y \cdot L^2}{y_v \cdot (y_v + \Delta y)} \quad (182)$$

$$\begin{array}{l} \text{from} \\ (5) \\ (9) \end{array} \quad \Delta y = \frac{A^2 \cdot L^2}{x_v + \Delta x} - y_v = -\frac{\Delta x \cdot L^2}{x_v \cdot (x_v + \Delta x)} \quad (183)$$

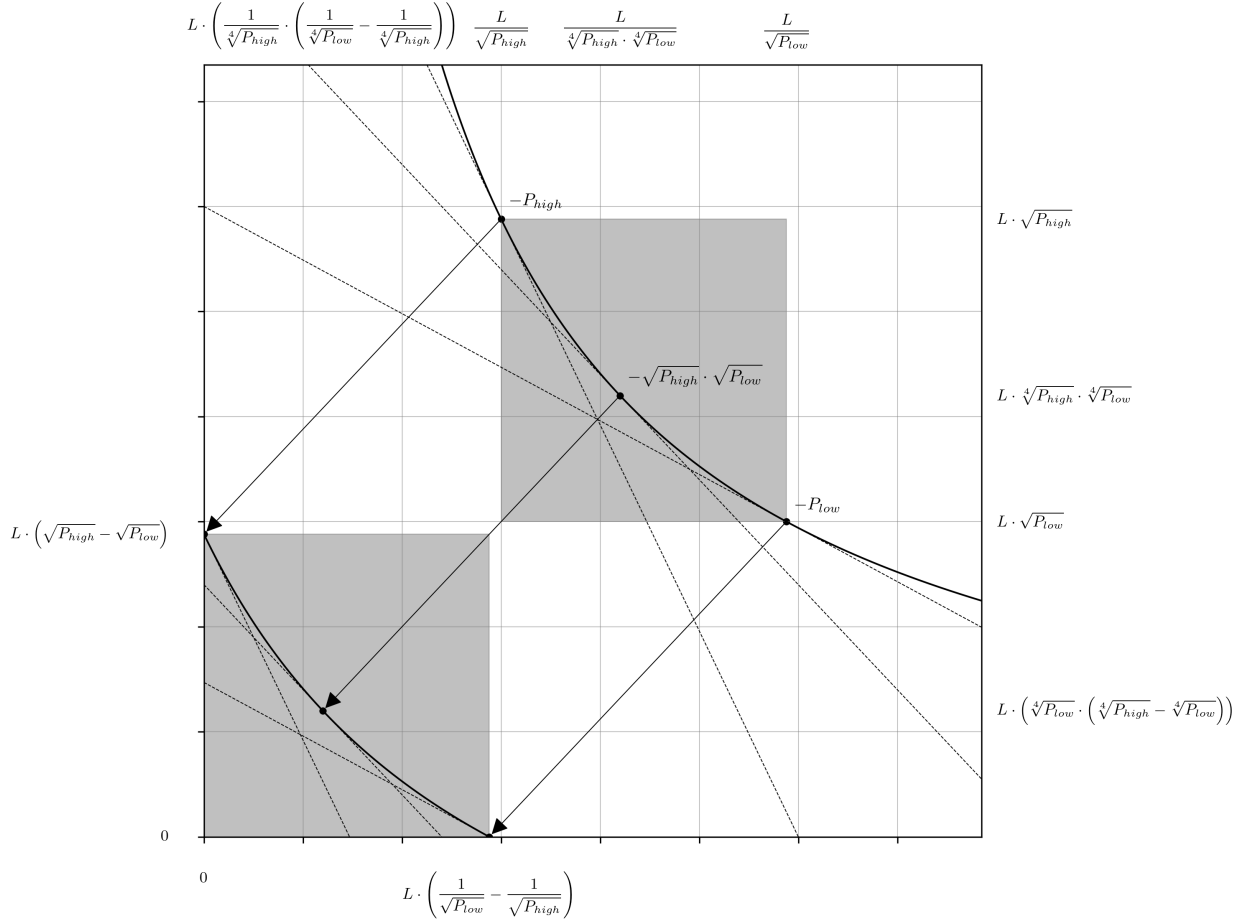


Fig. 29 Reconstruction of the Uniswap v3 real curve is depicted as a map of the virtual curve back to the x- and y-axes.

$$\begin{array}{l} \text{from} \\ (16) \end{array} \quad \frac{\partial x_v}{\partial y_v} = -\frac{L^2}{y_v^2}; \quad \frac{\partial y_v}{\partial x_v} = -\frac{y_v^2}{L^2} \quad (184)$$

$$\begin{array}{l} \text{from} \\ (17) \end{array} \quad \frac{\partial y_v}{\partial x_v} = -\frac{L^2}{x_v^2}; \quad \frac{\partial x_v}{\partial y_v} = -\frac{x_v^2}{L^2} \quad (185)$$

The indifference of the real and virtual curves with respect to the calculated swap quantities is again evident in the analysis (Figures 30, 31). Translocation upon the integrated forms (i.e. the bonding curves, Figure 30) and integration above their implied price curves (Figure 31) yields the same token amounts, Δx and Δy . The only difference is the frame of reference, which is shifted by $(-x_{\text{asym}}, -y_{\text{asym}})$ in the virtual curve compared to the real curve, which has no effect on either the marginal rate, or the effective rate of exchange. Since the L term is exposed directly on the Uniswap v3 smart contracts, legacy infrastructure that was developed to integrate with prior iterations of the canonical $x \cdot y = k$ on-chain liquidity system can be retrofit with relatively little effort. Therefore, the virtual curve is in some aspect the preferred context through which third party software observes and interacts with the Uniswap v3 system, which was likely designed and implemented with $x \cdot y = k$ as a core assumption. It would be naïve to assume that this is an accident. The parameterization is deliberately self-explanatory and allows for legacy software to be quickly patched with conditional arguments regarding the price boundaries, while allowing the core swap functions to remain in-tact.

4.3 The Uniswap v3 Reference Curve

To begin constructing the Uniswap v3 reference curve, first recall that the product of x_0 and y_0 is used as its scaling constant (Equation 2). In other words, $x_0 \cdot y_0$ is equal to k in the proverbial “constant product” equation, $x \cdot y = k$. With

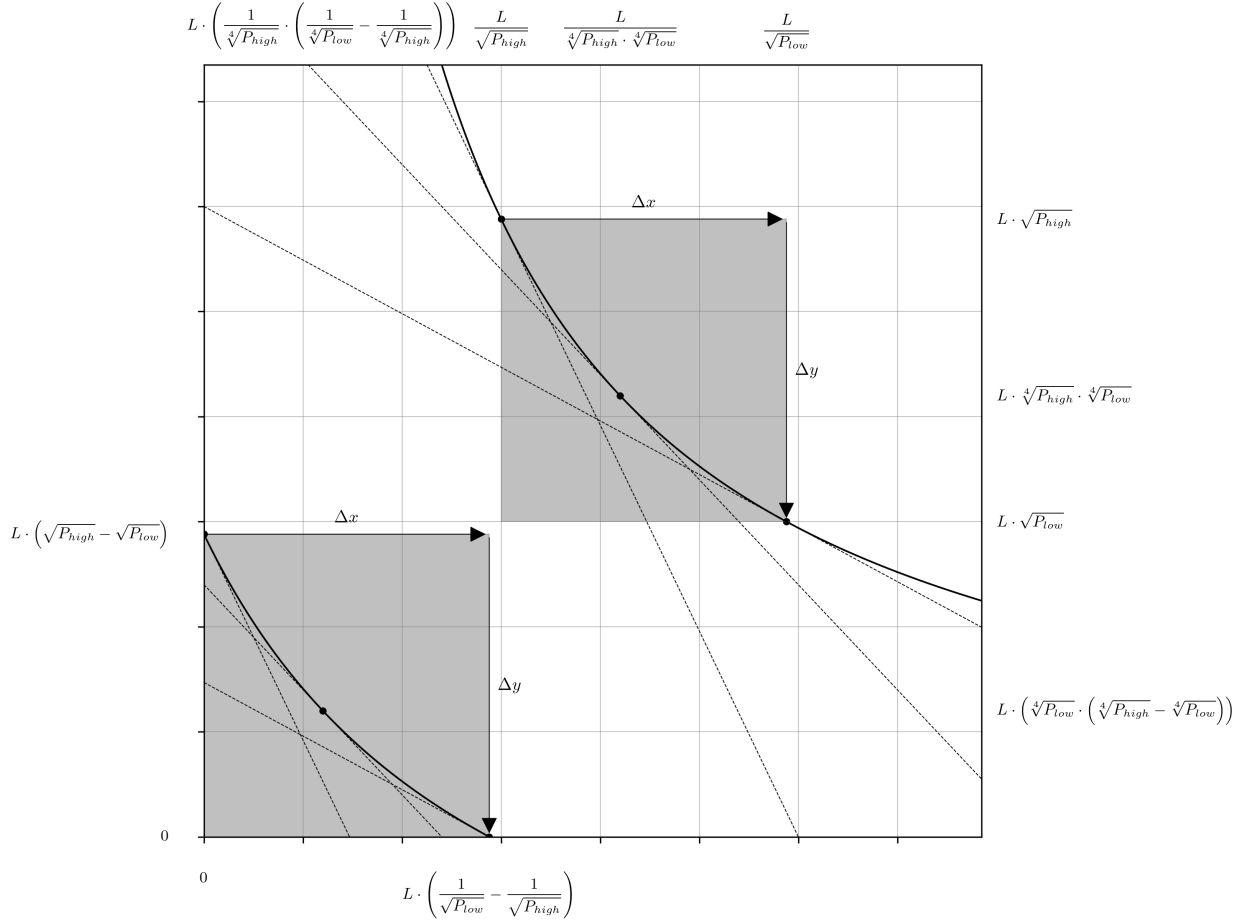


Fig. 30 Traversal upon the rectangular hyperbolas $(x + L/\sqrt{P_{\text{high}}}) \cdot (y + L \cdot \sqrt{P_{\text{low}}}) = L^2$, and $x_v \cdot y_v = L^2$ (Equations 125 and 178), representing a token swap against the Uniswap v3 real and virtual curves, where $\Delta x > 0$ and $\Delta y < 0$. The swap quantities Δx and Δy , and marginal rates of exchange before and after the swap are identical. Therefore, with respect to the outcome of the exchange the difference between the two curve implementations is zero.

the identities of x_0 and y_0 in-hand, this scaling constant can be derived from the product of the RHS of Equations 175 and 177 (Equations 186 and 187). While there are many compelling algebraic rearrangements for this identity, the form in Equation 187 was chosen for its ease of use in the derivations to follow, and as a call-back to the so-called “capital efficiency” term previously isolated in Equation 59.

$$\begin{array}{l} \text{from} \\ (2) \\ (175) \\ (177) \end{array} \quad x \cdot y = L \cdot \left(\frac{1}{\sqrt[4]{P_{\text{high}}}} \cdot \left(\frac{1}{\sqrt[4]{P_{\text{low}}}} - \frac{1}{\sqrt[4]{P_{\text{high}}}} \right) \right) \cdot L \cdot \left(\sqrt[4]{P_{\text{low}}} \cdot \left(\sqrt[4]{P_{\text{high}}} - \sqrt[4]{P_{\text{low}}} \right) \right) \quad (186)$$

$$\begin{array}{l} \text{from} \\ (186) \end{array} \quad x \cdot y = L^2 \cdot \left(1 - 2 \cdot \frac{\sqrt[4]{P_{\text{low}}}}{\sqrt[4]{P_{\text{high}}}} + \left(\frac{\sqrt[4]{P_{\text{low}}}}{\sqrt[4]{P_{\text{high}}}} \right)^2 \right) = L^2 \cdot \left(1 - \frac{\sqrt[4]{P_{\text{low}}}}{\sqrt[4]{P_{\text{high}}}} \right)^2 \quad (187)$$

With the reference curve’s scaling constant now defined in terms of L , P_{high} and P_{low} , the coordinates corresponding to the price bounds, $\min(x)$, $\max(x)$, $\min(y)$, $\max(y)$, can also be expressed with the same parameters. In an earlier demonstration, this process was made trivial by “reversing” the effective amplification of the virtual curve relative to the reference curve by taking the quotients of $\min(x_v)$, $\max(y_v)$, $\max(x_v)$, and $\min(y_v)$, and the amplification constant A (Equations 65, 66, 67, 68). While this process is still possible via the definition of A in terms of P_{high} and P_{low} (Equation 59), it no longer has the same intuitive benefit with respect to the construction process. This is a good excuse

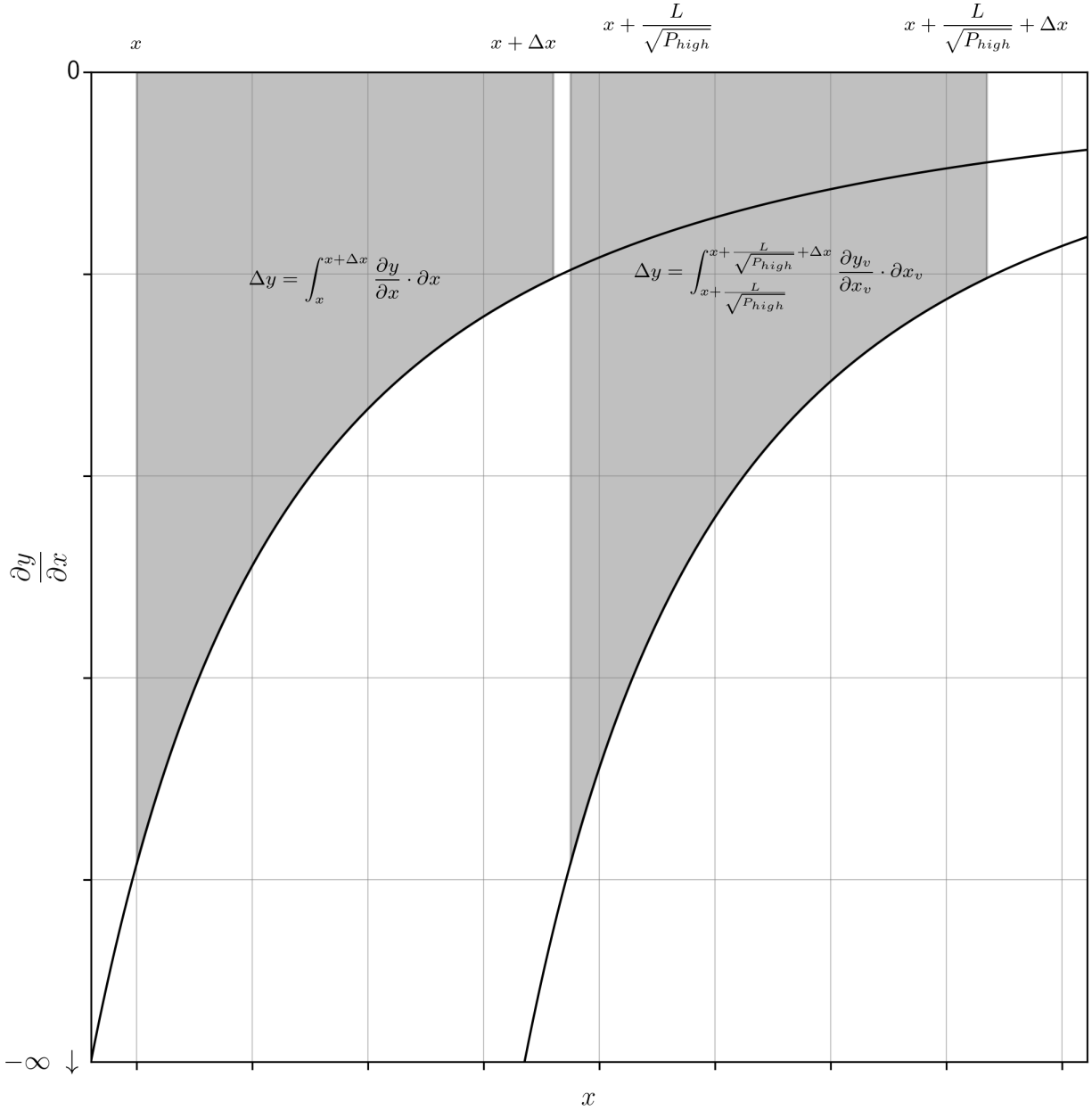


Fig. 31 The integration above $\partial y/\partial x = -L^2/(x + L/\sqrt{P_{\text{high}}})^2$ and $\partial y_v/\partial x_v = -L^2/x_v^2$ (Equations 138 and 185) over the intervals $x \rightarrow x + \Delta x$ and $x + L/\sqrt{P_{\text{high}}} \rightarrow x + L/\sqrt{P_{\text{high}}} + \Delta x$ (i.e. $x_v \rightarrow x_v + \Delta x$) representing a token swap against both the real and virtual curves, where $\Delta x > 0$ and $\Delta y < 0$. Apart from the shift along the x-axis, these are identical in every other aspect. Note that the relationship between the real and virtual price curves is additive (x and Δx versus $x + L/\sqrt{P_{\text{high}}}$ and $x + L/\sqrt{P_{\text{high}}} + \Delta x$).

to explore the more analytical approach. The process is identical to that demonstrated when attempting to add some rigor to the amplification reversal method (Equations 69 and 70); the derivative of the reference curve (Equations 16 and 17) is forced to either P_{high} or P_{low} (native parameters in this case), and the x or y variable is substituted for $\min(x)$, $\max(x)$, $\min(y)$, or $\max(y)$, as appropriate. Then the coordinate of interest is obtained via trivial rearrangements of the resulting expressions (Equations 188, 189, 190, 191, 192, 193, 194 and 195) (Figure 32).

$$\begin{array}{l} \text{from} \\ (17) \\ (177) \end{array} \quad \frac{\partial y}{\partial x} = -P_{\text{high}} = -\frac{L^2 \cdot \left(1 - \frac{\sqrt[4]{P_{\text{low}}}}{\sqrt[4]{P_{\text{high}}}}\right)^2}{\min^2(x)} \quad (188)$$

$$\begin{array}{l} \text{from} \\ (188) \end{array} \quad \min(x) = \frac{L}{\sqrt{P_{\text{high}}}} \cdot \left(1 - \frac{\sqrt[4]{P_{\text{low}}}}{\sqrt[4]{P_{\text{high}}}}\right) \quad (189)$$

$$\begin{array}{l} \text{from} \\ (17) \\ (177) \end{array} \quad \frac{\partial y}{\partial x} = -P_{\text{low}} = -\frac{L^2 \cdot \left(1 - \frac{\sqrt[4]{P_{\text{low}}}}{\sqrt[4]{P_{\text{high}}}}\right)^2}{\max^2(x)} \quad (190)$$

$$\begin{array}{l} \text{from} \\ (190) \end{array} \quad \max(x) = \frac{L}{\sqrt{P_{\text{low}}}} \cdot \left(1 - \frac{\sqrt[4]{P_{\text{low}}}}{\sqrt[4]{P_{\text{high}}}}\right) \quad (191)$$

$$\begin{array}{l} \text{from} \\ (16) \\ (177) \end{array} \quad \frac{\partial y}{\partial x} = -P_{\text{low}} = -\frac{\min^2(y)}{L^2 \cdot \left(1 - \frac{\sqrt[4]{P_{\text{low}}}}{\sqrt[4]{P_{\text{high}}}}\right)^2} \quad (192)$$

$$\begin{array}{l} \text{from} \\ (192) \end{array} \quad \min(y) = L \cdot \sqrt{P_{\text{low}}} \cdot \left(1 - \frac{\sqrt[4]{P_{\text{low}}}}{\sqrt[4]{P_{\text{high}}}}\right) \quad (193)$$

$$\begin{array}{l} \text{from} \\ (16) \\ (177) \end{array} \quad \frac{\partial y}{\partial x} = -P_{\text{high}} = -\frac{\max^2(y)}{L^2 \cdot \left(1 - \frac{\sqrt[4]{P_{\text{low}}}}{\sqrt[4]{P_{\text{high}}}}\right)^2} \quad (194)$$

$$\begin{array}{l} \text{from} \\ (194) \end{array} \quad \max(y) = L \cdot \sqrt{P_{\text{high}}} \cdot \left(1 - \frac{\sqrt[4]{P_{\text{low}}}}{\sqrt[4]{P_{\text{high}}}}\right) \quad (195)$$

As noted above, the analysis of the Uniswap v3 reparameterization and its real, virtual, and reference curves has been necessarily performed in the reverse order compared to the seminal work (Figures 1 to 21). Regardless, the liquidity amplification heuristic applies all the same, and can be represented as before with arrows connecting pairs of points on the reference and virtual curves, where the derivatives evaluated at these points are equal (Figures 33).

The relative trade volumes supported by the reference and virtual curves over the same price interval can now be compared (Figures 34 to 35). As before, note that while the trade action executes from and terminates at the same marginal price values and achieves the same overall effective exchange rate, the trade amounts are significantly greater in the virtual curve. The increased trade volume can be inspected visually from the increased arrow lengths in Figure 34, and the expansion observed for the integrated area in Figure 35.

This concludes our examination of the Uniswap v3 reparameterization.

4.4 The Carbon DeFi Real Curve

Bancor's peer-to-peer trading product, *Carbon DeFi*, also uses a unique, "unnatural" reparameterization of the seminal concentrated liquidity invariant informed by the protocol's specific requirements. Unlike its predecessors, Carbon

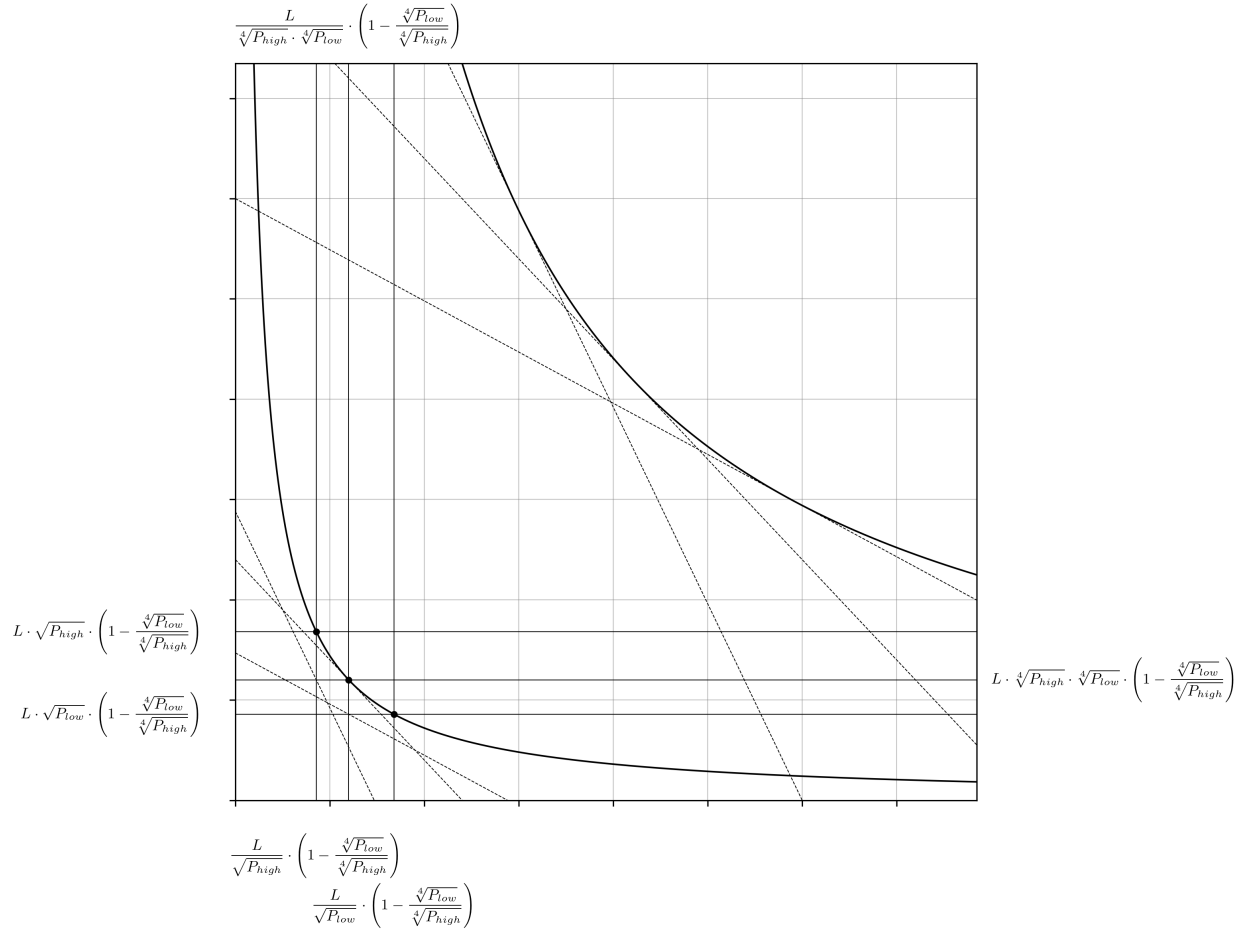


Fig. 32 The algebraic identities of the points where the lines tangent to the Uniswap v3 reference curve and parallel to the tangent lines at the price boundaries of the virtual curve are now elucidated (Equations 175, 177, 189, 191, 193, 195).

DeFi's purpose is not to re-create Bancor's original vision for automatic liquidity systems vis-à-vis continuous pricing methods that attempt to follow the market, but rather to support the arbitrary price quoting behaviours exhibited by market participants. The particulars of the Carbon DeFi design are beyond the scope of this document and deserve a dedicated discourse. However, the necessary context is simple enough to state ad hoc.

In short, Carbon DeFi system must be able to adjust the curve's scaling parameter reliably and accurately as required under certain circumstances to maintain price quote boundaries as dictated by its users. This is potentially a sensitive process. Naïvely shoe-horning either of the implementations previously discussed for Bancor v2 or Uniswap v3 is an inelegant and unnecessarily computationally intensive choice at best, and risks exposing an exploit resulting from precision loss during fixed-point operations at worst. Therefore, Carbon DeFi requires the scaling parameter of the curve to be expressed exclusively in terms of one token balance, which can be adjusted with reference to the same without performing any calculations at all, thus observing best practices in defensive programming. Just as the Uniswap v3 reparameterization is the correct form for the system it represents, the Carbon DeFi reparameterization is correct for its own systems, but *both refer to the same underlying mathematical object*.

As an aside, Carbon DeFi's curves are also unusual because they refer to only one token balance, rather than two. This has no immediate ramifications for the analyses we are about to perform but is worth raising for its own sake and to foreshadow a future publication which will handle these details more thoroughly. The only detail needed is that, by convention, Carbon DeFi treats the y-axis as belonging to the only token its bonding curve describes. Therefore, the derivation of the Carbon DeFi real curve begins from its most conspicuous identity, the y-intercept.

Since Carbon DeFi is a price quoting protocol, the price boundaries represented by P_{high} and P_{low} are obvious choices to encapsulate natively. The objective then becomes to substitute the L term in Equation 125 with a redundant definition expressed in terms of the y-intercept, y_{int} , and the price boundaries, P_{high} and P_{low} . This can be accomplished easily

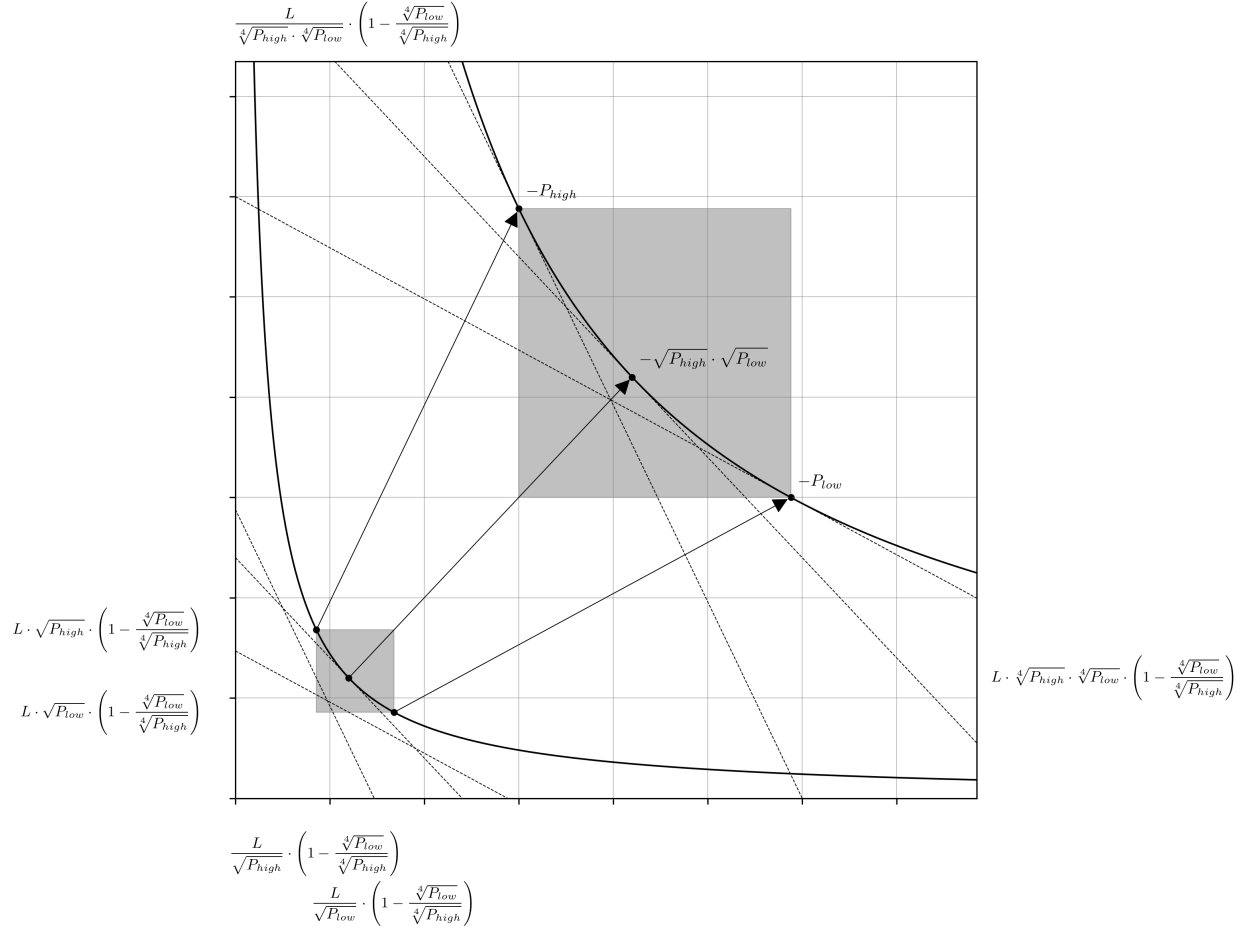


Fig. 33 The amplification process is depicted with corresponding shaded areas of the Uniswap v3 reference and virtual curves, respectively. Points where the first derivative of each curve evaluates to the same result are shown as white dots, and the mapping of these points is depicted with white arrows.

with reference to the work already done. The y-intercept was previously defined in terms of L , P_{high} , and P_{low} in Equation 145; rearrangement of this identity to isolate L (Equation 196), followed by substitution into Equation 125 yields the reparametrized Carbon DeFi real curve invariant (Equation 197). Refactoring the expression into a more presentable phenotype is done by defining the parameters a , b , and z , which are equal to $\sqrt{P_{high}} - \sqrt{P_{low}}$, $\sqrt{P_{low}}$, and the y-intercept, y_{int} , of the real curve, respectively (Equations 198, 199 and 200). Substitution of these definitions into Equation 197 yields Equation 201, and rearrangement yields Equations 202 and 203. Note that the differences between Equations 197, 201, 202 and 203 are only cosmetic. These features are depicted in Figure 36.

$$\begin{array}{l} \text{from} \\ (145) \end{array} \quad L = \frac{y_{int}}{\sqrt{P_{high}} - \sqrt{P_{low}}} \quad (196)$$

$$\begin{array}{l} \text{from} \\ (125) \\ (196) \end{array} \quad \left(x + \frac{y_{int}}{\sqrt{P_{high}} \cdot (\sqrt{P_{high}} - \sqrt{P_{low}})}\right) \cdot \left(y + \frac{\sqrt{P_{low}} \cdot y_{int}}{\sqrt{P_{high}} - \sqrt{P_{low}}}\right) = \frac{y_{int}^2}{(\sqrt{P_{high}} - \sqrt{P_{low}})^2} \quad (197)$$

$$a = \sqrt{P_{high}} - \sqrt{P_{low}} \quad (198)$$

$$b = \sqrt{P_{low}} \quad (199)$$

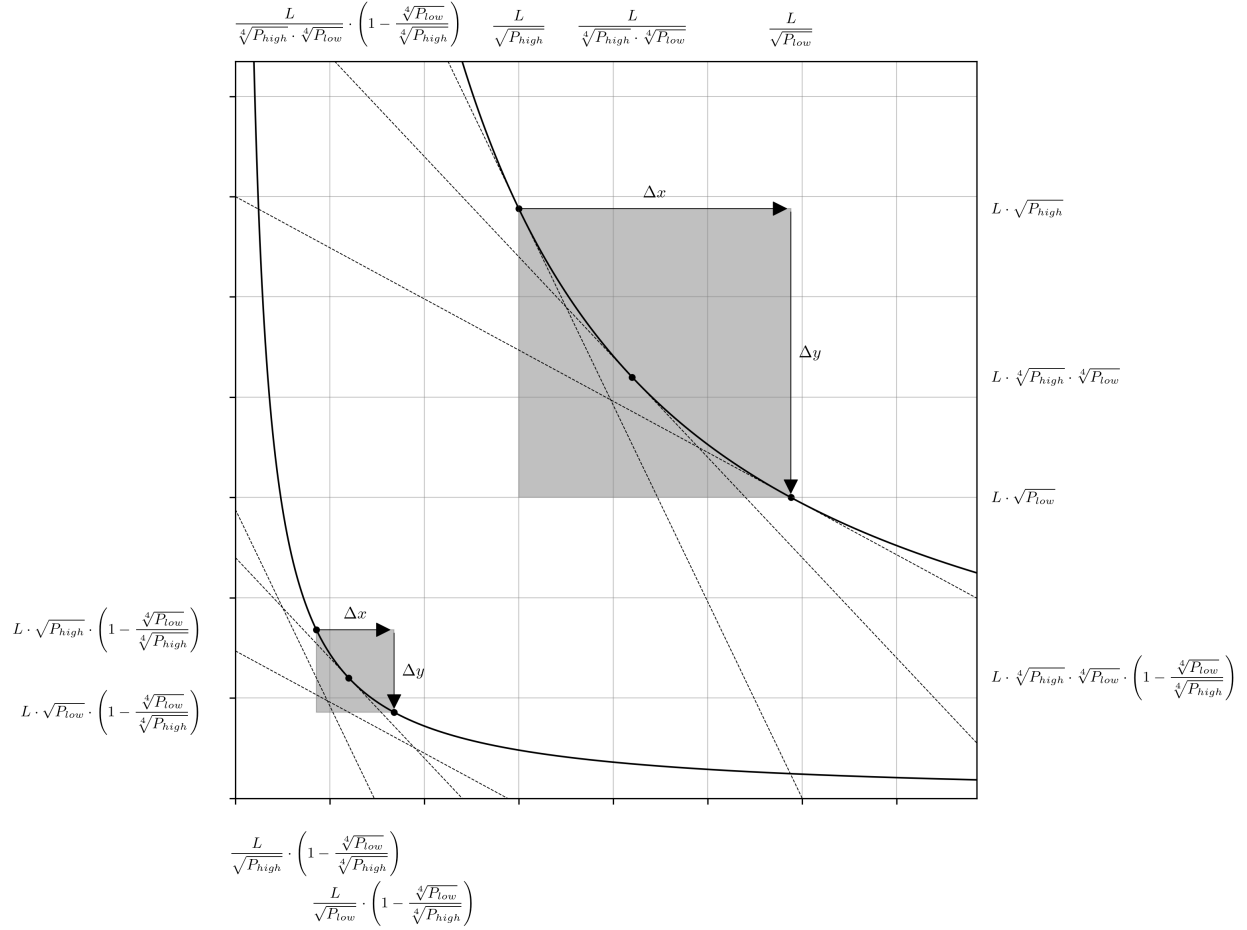


Fig. 34 Traversal upon the rectangular hyperbolas $x_v \cdot y_v = L^2$ and $x \cdot y = L^2 \cdot \left(1 - \frac{\sqrt[4]{P_{low}}}{\sqrt[4]{P_{high}}}\right)^2$ (Equations 178 and 187), representing a token swap against the reference and amplified liquidity pools, where $\Delta x > 0$ and $\Delta y < 0$. The marginal rates of exchange before and after the swap are identical. The ratio of the Δx and Δy arrow lengths for each curve are also identical, and therefore the overall rate of exchange, $\Delta y/\Delta x$ is equal in both cases.

$$z = y_{int} \quad (200)$$

from
(197)
(198)
(199)
(200)

$$\left(x + \frac{z}{a \cdot (a + b)}\right) \cdot \left(y + \frac{z \cdot b}{a}\right) = \frac{z^2}{a^2} \quad (201)$$

from
(201)

$$y \cdot (z + x \cdot a \cdot (a + b)) = z \cdot (z - x \cdot b \cdot (a + b)) \quad (202)$$

from
(201)

$$\frac{y}{z} = \frac{z - x \cdot b \cdot (a + b)}{z + x \cdot a \cdot (a + b)} \quad (203)$$

It might be helpful to consider how this arrangement can be expressed in more familiar terms. The expression $a \cdot (a + b)$ is redundant with $P_{high} - P_0$, and $b \cdot (a + b)$ is redundant with P_0 (Equations 204, 205 and 206). Substitution of these relationships and the identity $z = y_{int}$ into Equation 203 yields Equation 206.

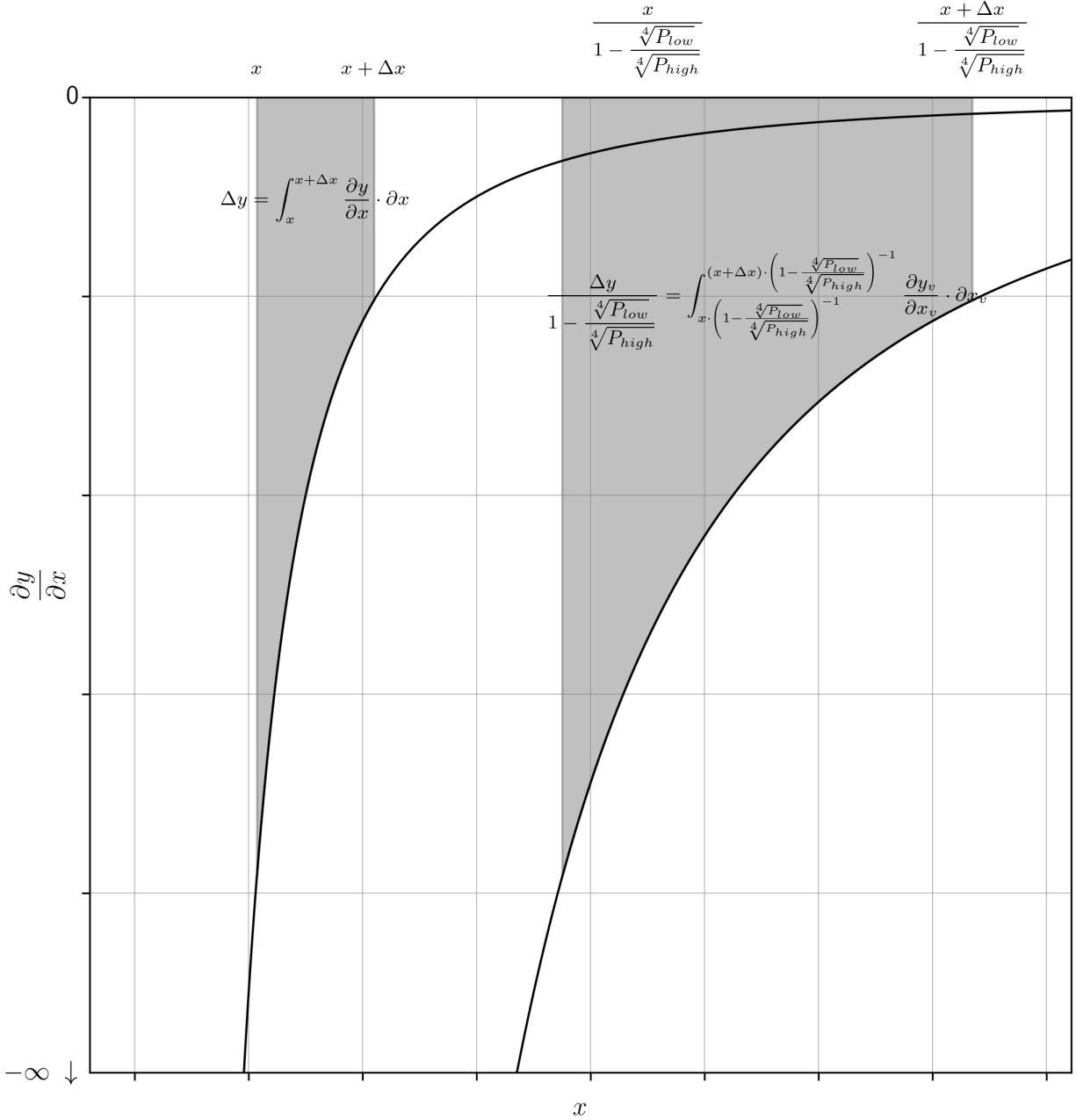


Fig. 35 The integration above $\frac{\partial y}{\partial x} = -L^2 \cdot \left(1 - \frac{\sqrt[4]{P_{low}}}{\sqrt[4]{P_{high}}}\right)^2 / x^2$ (i.e. $\frac{\partial}{\partial x}$ Equation 187) and $\frac{\partial y}{\partial x} = -L^2 / x^2$ (Equation 185) over the intervals $x \rightarrow x + \Delta x$ and $x / \left(1 - \frac{\sqrt[4]{P_{low}}}{\sqrt[4]{P_{high}}}\right) \rightarrow (x + \Delta x) / \left(1 - \frac{\sqrt[4]{P_{low}}}{\sqrt[4]{P_{high}}}\right)$ (i.e. $x_v \rightarrow x_v + \Delta x$) representing a token swap against both the reference and amplified liquidity pools, where $\Delta x > 0$ and $\Delta y < 0$. Note that that the integration areas for the reference and virtual curves are Δy and $\Delta y / \left(1 - \frac{\sqrt[4]{P_{low}}}{\sqrt[4]{P_{high}}}\right)$, respectively. By inference, any token swap against the virtual curve can be calculated from the reference curve by taking its quotient versus the poorly named “capital efficiency” term (Equation 59).

from
(198)
(199)

$$a \cdot (a + b) = \left(\sqrt{P_{high}} - \sqrt{P_{low}}\right) \cdot \left(\sqrt{P_{high}} - \sqrt{P_{low}} + \sqrt{P_{low}}\right) = P_{high} - P_0 \quad (204)$$

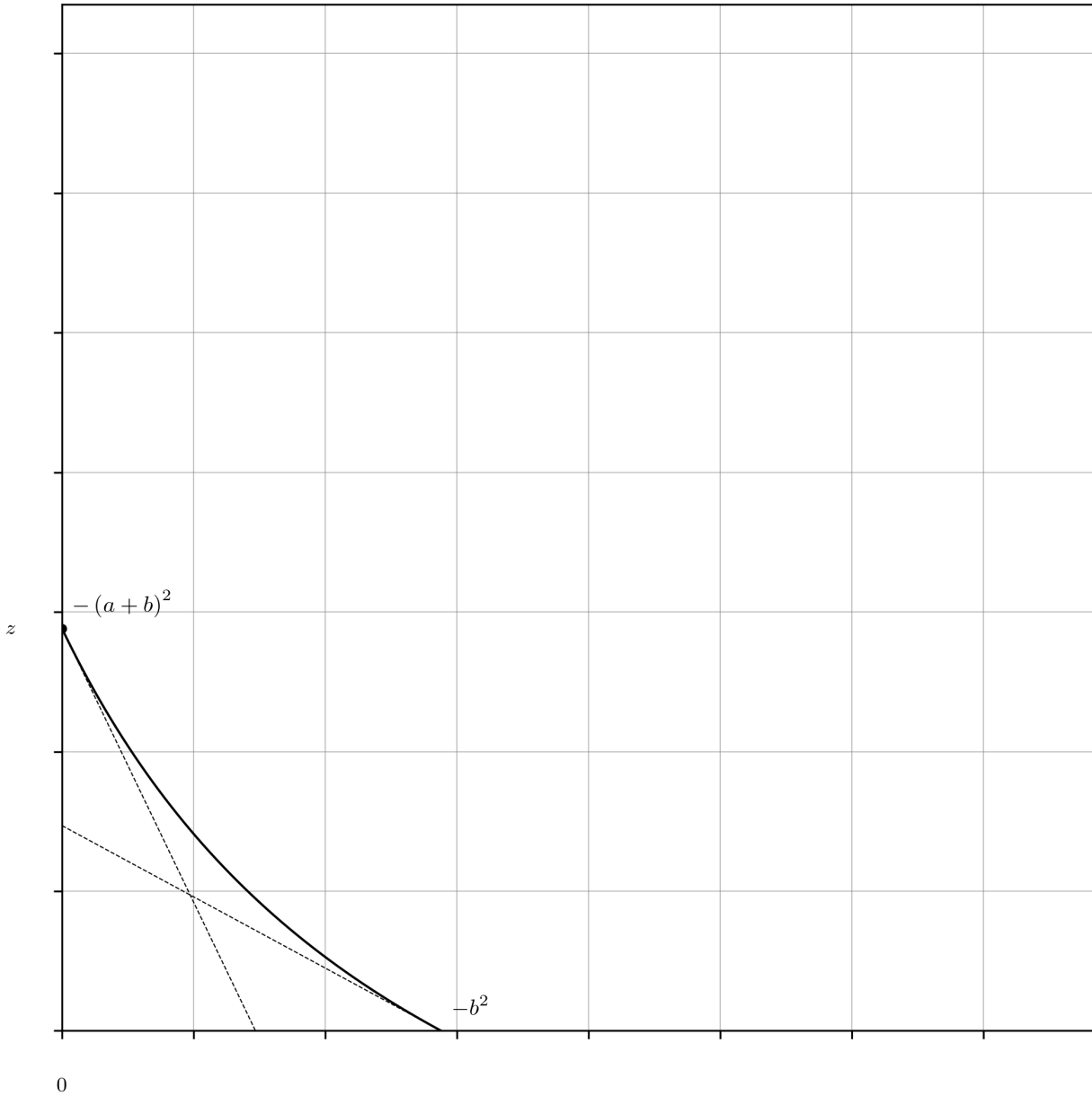


Fig. 36 Initial Carbon DeFi real curve. Due to its parameterization and prior to performing any additional analysis, only the slopes of the tangent lines at the intercepts $-P_{\text{high}} = -(a+b)^2$ and $-P_{\text{low}} = -b^2$, and the y-intercept itself, $y_{\text{int}} = z$, are known.

$$\begin{array}{l} \text{from} \\ (198) \\ (199) \end{array} \quad b \cdot (a+b) = \sqrt{P_{\text{low}}} \cdot \left(\sqrt{P_{\text{high}}} - \sqrt{P_{\text{low}}} + \sqrt{P_{\text{low}}} \right) = P_0 \quad (205)$$

$$\begin{array}{l} \text{from} \\ (201) \\ (202) \\ (203) \end{array} \quad \frac{y}{y_{\text{int}}} = \frac{y_{\text{int}} - x \cdot P_0}{y_{\text{int}} + x \cdot (P_{\text{high}} - P_0)} = \mathbf{Eqn. 194} \quad (206)$$

As was performed for the Uniswap v3 reparameterization, we will now begin the process of completely elucidating the Carbon DeFi model commencing from its real curve description (Equations 201, 202 and 203). The objectives are the same as before – to characterise the real, virtual, and reference curves, and recontextualize them in terms of the general

theory. First, manipulation of the Carbon DeFi invariant (Equation 201) to isolate the x and y terms yields Equations 207 and 208.

$$\begin{array}{l} \text{from} \\ (201) \end{array} \quad x = \frac{z^2}{a^2 \cdot \left(y + \frac{b \cdot z}{a}\right)} - \frac{z}{a \cdot (a + b)} \quad (207)$$

$$\begin{array}{l} \text{from} \\ (201) \end{array} \quad y = \frac{z^2}{a^2 \cdot \left(x + \frac{z}{a \cdot (a + b)}\right)} - \frac{b \cdot z}{a} \quad (208)$$

The token swap equations are obtained via now familiar methods. The x and y terms in Equation 201, or Equations 207 and 208 are substituted for $x + \Delta x$ and $y + \Delta y$ then rearranged to make either Δx or Δy the subject (Equations 209, 210 and 211).

$$\begin{array}{l} \text{from} \\ (201) \end{array} \quad \left(x + \Delta x + \frac{z}{a \cdot (a + b)}\right) \cdot \left(y + \Delta y + \frac{b \cdot z}{a}\right) = \frac{z^2}{a^2} \quad (209)$$

$$\begin{array}{l} \text{from} \\ (207) \\ (209) \end{array} \quad \Delta x = \frac{z^2}{a^2 \cdot \left(y + \Delta y + \frac{b \cdot z}{a}\right)} - \frac{z}{a \cdot (a + b)} - x \quad (210)$$

$$\begin{array}{l} \text{from} \\ (208) \\ (209) \end{array} \quad \Delta y = \frac{z^2}{a^2 \cdot \left(x + \Delta x + \frac{z}{a \cdot (a + b)}\right)} - \frac{b \cdot z}{a} - y \quad (211)$$

Substituting the identities for x and y in Equations 207 and 208 into Equations 210 and 211 (Equations 212 and 214), then simplifying, results in the single-dimension swap equations (Equations 213 and 215).

$$\begin{array}{l} \text{from} \\ (207) \\ (210) \end{array} \quad \Delta x = \frac{z^2}{a^2 \cdot \left(y + \Delta y + \frac{b \cdot z}{a}\right)} - \frac{z}{a \cdot (a + b)} - \frac{z^2}{a^2 \cdot \left(y + \frac{b \cdot z}{a}\right)} + \frac{z}{a \cdot (a + b)} \quad (212)$$

$$\begin{array}{l} \text{from} \\ (212) \end{array} \quad \Delta x = -\frac{\Delta y \cdot z^2}{(a \cdot y + b \cdot z) \cdot (a \cdot (y + \Delta y) + b \cdot z)} \quad (213)$$

$$\begin{array}{l} \text{from} \\ (208) \\ (211) \end{array} \quad \Delta y = \frac{z^2}{a^2 \cdot \left(x + \Delta x + \frac{z}{a \cdot (a + b)}\right)} - \frac{b \cdot z}{a} - \frac{z^2}{a^2 \cdot \left(x + \frac{z}{a \cdot (a + b)}\right)} + \frac{b \cdot z}{a} \quad (214)$$

$$\begin{array}{l} \text{from} \\ (214) \end{array} \quad \Delta y = -\frac{\Delta x \cdot z^2 \cdot (a + b)^2}{(x \cdot a \cdot (a + b) + z) \cdot ((x + \Delta x) \cdot a \cdot (a + b) + z)} \quad (215)$$

The swap formulas Equations 213 and 215 can also be obtained directly from their seminal counterparts, Equations 87 and 89, by substituting the scaling term, $A^2 \cdot x_0 \cdot y_0$, and the horizontal and vertical shift terms, $x_0 \cdot (A - 1)$ and $y_0 \cdot (A - 1)$, for their reparameterized forms z^2 , $z / (a \cdot (a + b))$, and $(b \cdot z) / a$, respectively (Equations 196, 197, 198, 199, 200, 201, 202 and 203). This approach is similarly well-suited to obtaining the effective and marginal rate equations, but as before, these identities will be elaborated according to the previously established methods. Repeating

the process demonstrated in Equations 12, 13, 14 and 15, Equations 92, 93, 94 and 95, and Equations 135, 136, 137 and 138, rearrangement of Equations 213 and 215 gives the *effective rate of exchange* (Equations 216 and 218), followed by determination of the limit as the denominator goes to zero gives the *instantaneous rate of exchange* (i.e. the marginal price) (Equations 217 and 219).

$$\begin{array}{l} \text{from} \\ (211) \end{array} \quad \frac{\Delta x}{\Delta y} = -\frac{z^2}{(a \cdot y + b \cdot z) \cdot (a \cdot (y + \Delta y) + b \cdot z)} \quad (216)$$

$$\begin{array}{l} \text{from} \\ (214) \end{array} \quad \frac{\partial x}{\partial y} = \lim_{\Delta y \rightarrow 0} \frac{\Delta x}{\Delta y} = -\frac{z^2}{(a \cdot y + b \cdot z)^2}; \quad \frac{\partial y}{\partial x} = -\frac{(a \cdot y + b \cdot z)^2}{z^2} \quad (217)$$

$$\begin{array}{l} \text{from} \\ (213) \end{array} \quad \frac{\Delta y}{\Delta x} = -\frac{z^2 \cdot (a + b)^2}{(x \cdot a \cdot (a + b) + z) \cdot ((x + \Delta x) \cdot a \cdot (a + b) + z)} \quad (218)$$

$$\begin{array}{l} \text{from} \\ (216) \end{array} \quad \frac{\partial y}{\partial x} = \lim_{\Delta x \rightarrow 0} \frac{\Delta y}{\Delta x} = -\frac{z^2 \cdot (a + b)^2}{(x \cdot a \cdot (a + b) + z)^2}; \quad \frac{\partial x}{\partial y} = -\frac{(x \cdot a \cdot (a + b) + z)^2}{z^2 \cdot (a + b)^2} \quad (219)$$

The Carbon DeFi marginal rate equations can also be expressed in terms of both the x- and y-dimensions (remember, for Carbon DeFi only the y-dimension is a token balance) via substitution of the x and y terms in Equations 13 and 15 with their horizontally or vertically shifted transformations (Equation 220). Simplifying the fractions in Equation 220 yields Equation 221.

$$\begin{array}{l} \text{from} \\ (125) \\ (136) \\ (138) \end{array} \quad \frac{\partial x}{\partial y} = -\frac{x + \frac{z}{a \cdot (a + b)}}{y + \frac{b \cdot z}{a}}; \quad \frac{\partial y}{\partial x} = -\frac{y + \frac{b \cdot z}{a}}{x + \frac{z}{a \cdot (a + b)}} \quad (220)$$

$$\begin{array}{l} \text{from} \\ (139) \end{array} \quad \frac{\partial x}{\partial y} = -\frac{x \cdot a \cdot (a + b) + z}{(a + b)(a \cdot y + b \cdot z)}; \quad \frac{\partial y}{\partial x} = -\frac{(a + b)(a \cdot y + b \cdot z)}{x \cdot a \cdot (a + b) + z} \quad (221)$$

Continuous summation over the price curves (Equations 217 and 219) over the interval representing the number of tokens being swapped yields results identical to Equations 212, 213, 214 and 215. Be reminded that x and y are functions of each other, so it is a mistake to attempt direct integration of Equation 221 without separating these variables first (not shown).

$$\begin{array}{l} \text{from} \\ (212) \\ (213) \\ (217) \end{array} \quad \Delta x = -\int_y^{y+\Delta y} \frac{z^2}{(a \cdot y + b \cdot z)^2}; \quad \cdot \partial y = \left[\frac{z^2}{a \cdot y + b \cdot z} \right]_y^{y+\Delta y} \Rightarrow \text{Eqns. 212 and 213} \quad (222)$$

$$\begin{array}{l} \text{from} \\ (214) \\ (215) \\ (219) \end{array} \quad \Delta y = -\int_x^{x+\Delta x} \frac{z^2 \cdot (a + b)^2}{(x \cdot a \cdot (a + b) + z)^2} \cdot \partial x = \left[\frac{z^2 \cdot (a + b)^2}{x \cdot a \cdot (a + b) + z} \right]_x^{x+\Delta x} \Rightarrow \text{Eqns. 214 and 215} \quad (223)$$

Both the direct token swap by traversal upon the bonding curve $y \cdot (z + x \cdot a \cdot (a + b)) = z \cdot (z - x \cdot b \cdot (a + b))$ (Equation 202) and the integration above $\partial y/\partial x = -z^2 \cdot (a + b)^2 / (x \cdot a \cdot (a + b) + z)^2$ (Equation 219) over the interval $x \rightarrow x + \Delta x$ are depicted in Figures 37 and 38.

The y-intercept of the Carbon DeFi invariant is one of its parameters, z (Equation 200), and the x-intercept is obtained by direct substitution of y for zero in Equation 207 (Equation 224) (Figure 39). As anticipated, the quotient of y_{int} and x_{int} is equal to P_0 as previously observed in Equations 110 and 146 (Equation 225). The x- and y-asymptotes can be obtained as demonstrated before, either geometrically (subtract from the origin the implied horizontal and vertical shift parameters in Equation 201), or analytically (substitute the y- or x-component required to set the denominator of

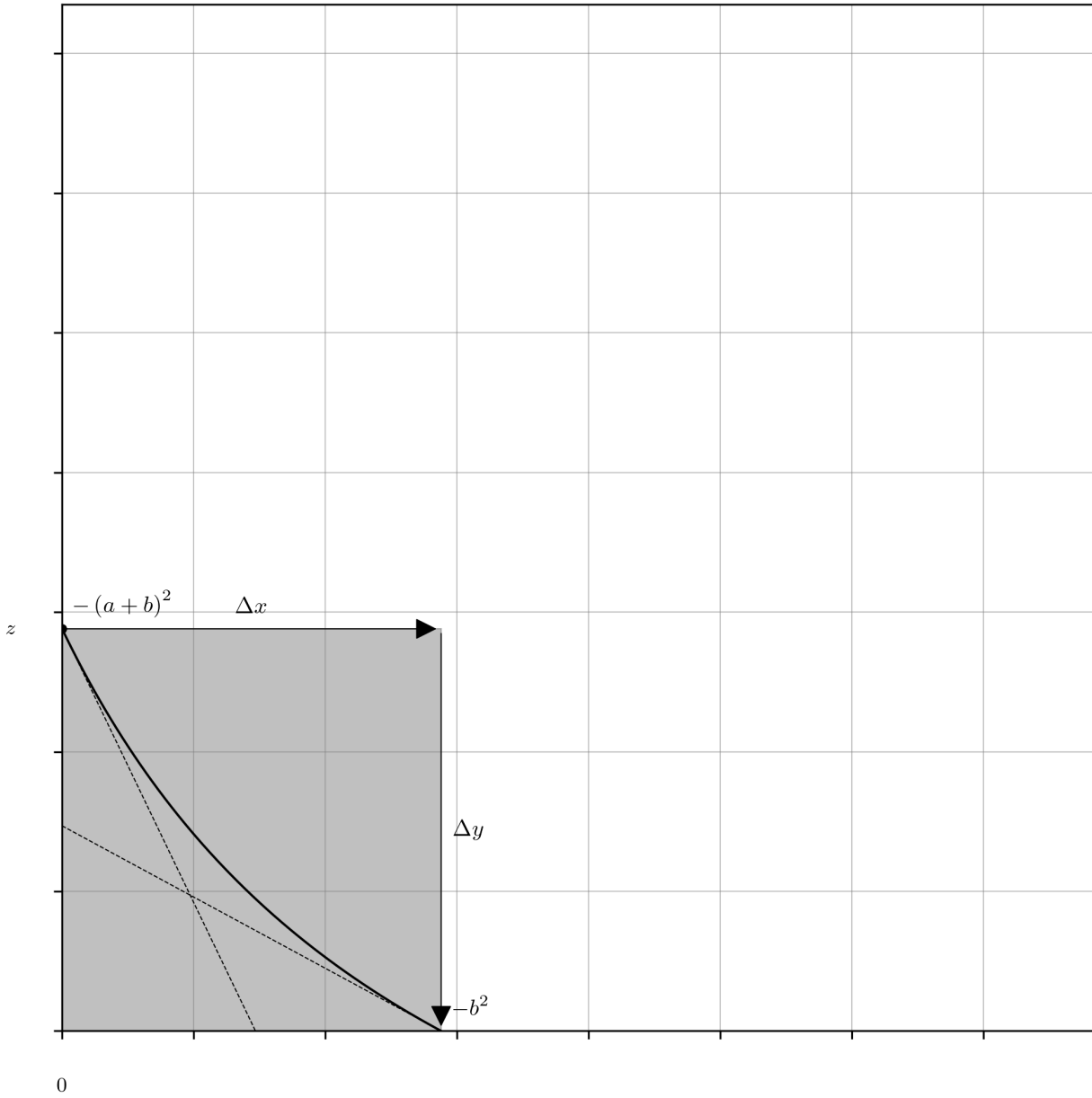


Fig. 37 Traversal upon the rectangular hyperbola $y \cdot (z + x \cdot a \cdot (a + b)) = z \cdot (z - x \cdot b \cdot (a + b))$ (Equation 202), representing a token swap against the Carbon DeFi real curve, where $\Delta x > 0$ and $\Delta y < 0$.

Equations 207 and 208 to zero) (Equations 226 and 227) (Figure 40). Consistent with prior observations (Equations 111 and 147), the quotient of the y- and x-asymptotes is equal to P_0 (Equation 228).

$$\begin{array}{l} \text{from} \\ (207) \end{array} \quad x_{\text{int}} = \frac{z}{a \cdot b} - \frac{z}{a \cdot (a + b)} = \frac{z}{b \cdot (a + b)} \quad (224)$$

$$\begin{array}{l} \text{from} \\ (200) \\ (205) \\ (224) \end{array} \quad \frac{y_{\text{int}}}{x_{\text{int}}} = b \cdot (a + b) = P_0 \quad (225)$$

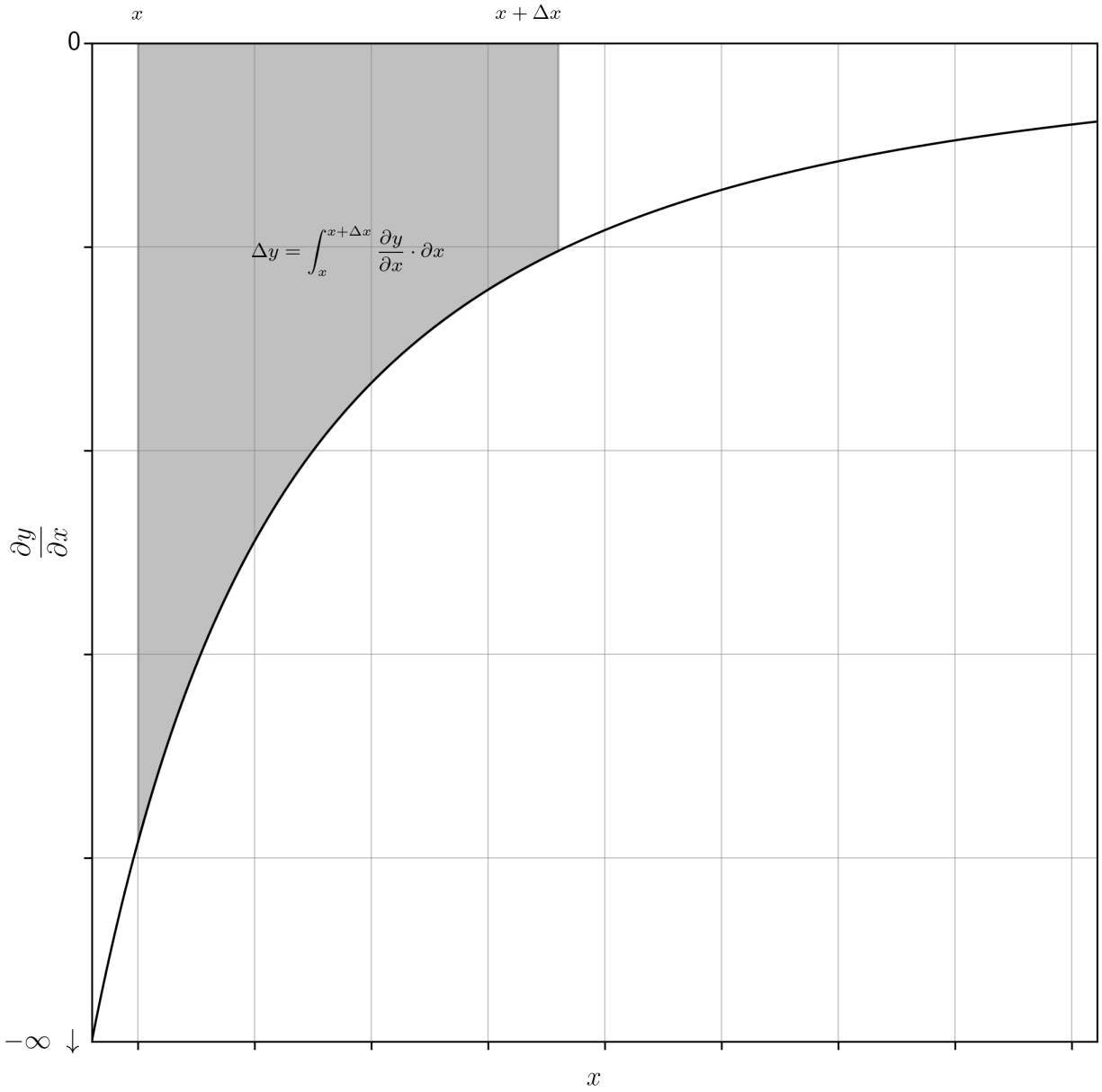


Fig. 38 The integration above $\partial y/\partial x = -z^2 \cdot (a+b)^2 / (x \cdot a \cdot (a+b) + z)^2$ (Equation 219) over the interval $x \rightarrow x + \Delta x$ representing a token swap against the Carbon DeFi real curve, where $\Delta x > 0$ and $\Delta y < 0$.

from (208)
$$x_{\text{asym}} = -\frac{z}{a \cdot (a+b)} \quad (226)$$

from (206)
$$y_{\text{asym}} = -\frac{b \cdot z}{a} \quad (227)$$

from (224) (225)
$$\frac{y_{\text{asym}}}{x_{\text{asym}}} = b \cdot (a+b) = P_0 \quad (228)$$

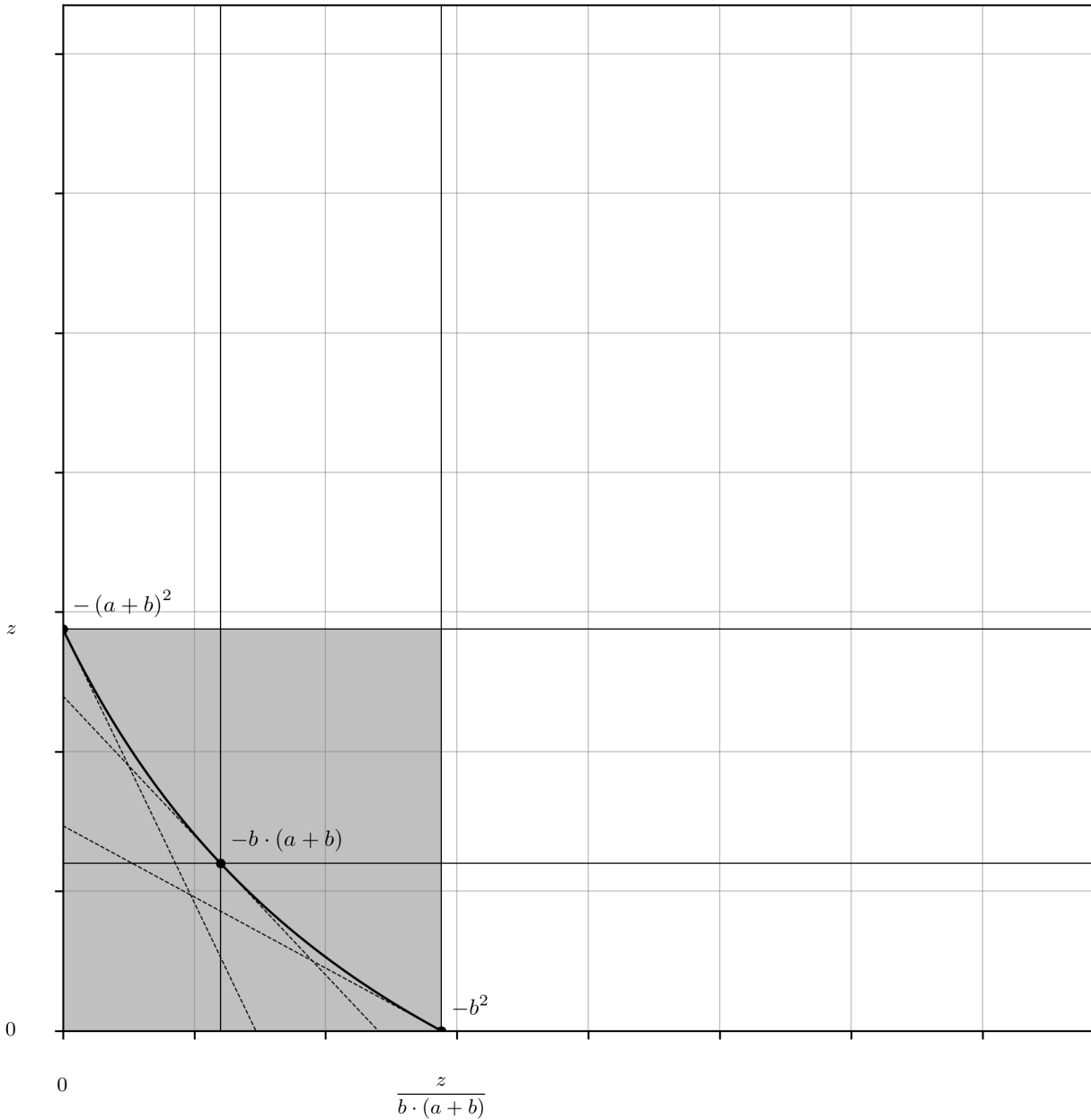


Fig. 39 The x- and y-intercepts of the Carbon DeFi real curve are annotated on the appropriate axes (Equations 200 and 224), and the algebraic identity for the first derivative of the curve evaluated at these points (via Equations 198 and 199), and their geometric mean (Equation 205), are illustrated with annotated tangent lines to the curve.

4.5 The Carbon DeFi Virtual Curve

The process of characterizing the Carbon DeFi virtual curve is essentially identical to that demonstrated for the Bancor v2 and Uniswap v3 virtual curves (Equations 112, 113, 114, and 115; and 160, 161, 162, 163, 164, 165, 166, 167, 168, and 169). First, the $\max(x_v)$, $\min(x_v)$, $\max(y_v)$, and $\min(y_v)$ coordinates are obtained by reversing the horizontal and vertical shifts implied by the real curve description (Equations 229, 230, 233 and 234), then locating “center” by evaluating the geometric means of the virtual curve boundaries (Equations 232 and 236) (Figure 41). Lastly, the mystery constant C is confirmed by taking the quotient of the maximum and minimum bounds in both dimensions (Equations 237 and 238).

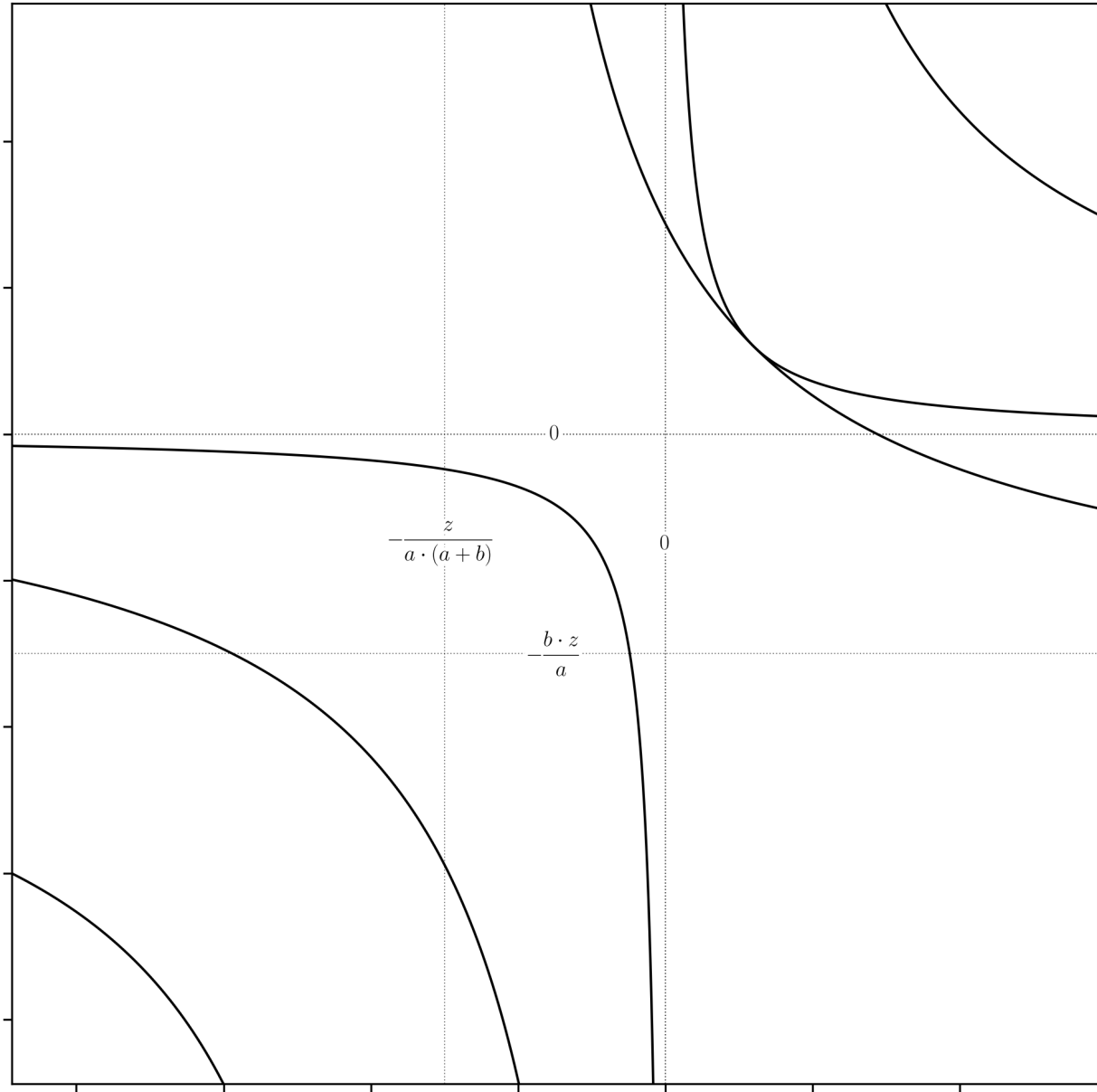


Fig. 40 The horizontal and vertical asymptotes of the Carbon DeFi virtual and reference curves, and its real curve (Equations 226 and 227), are depicted with dotted lines and their coordinates are annotated appropriately. While we have not yet approached the characterization of the reference and virtual curves, it is trivial that their asymptotes are at zero.

$$\begin{array}{l} \text{from} \\ (224) \\ (226) \end{array} \quad \max(x_v) = (x_{\text{int}} - x_{\text{asym}}) = \frac{z}{b \cdot (a + b)} + \frac{z}{a \cdot (a + b)} = \frac{z}{a \cdot b} \quad (229)$$

$$\begin{array}{l} \text{from} \\ (226) \end{array} \quad \min(x_v) = (0 - x_{\text{asym}}) = \frac{z}{a \cdot (a + b)} \quad (230)$$

$$\begin{array}{l} \text{from} \\ (229) \\ (230) \end{array} \quad \max(x_v) \cdot \min(x_v) = \frac{z}{a \cdot b} \cdot \frac{z}{a \cdot (a + b)} = \frac{z^2}{a^2 \cdot b \cdot (a + b)} \quad (231)$$

$$\begin{array}{l} \text{from} \\ (231) \end{array} \quad \sqrt{\max(x_v)} \cdot \sqrt{\min(x_v)} = \frac{z}{a \cdot \sqrt{b \cdot (a+b)}} \quad (232)$$

$$\begin{array}{l} \text{from} \\ (200) \\ (227) \end{array} \quad \max(y_v) = (y_{\text{int}} - y_{\text{asym}}) = z + \frac{b \cdot z}{a} = \frac{z \cdot (a+b)}{a} \quad (233)$$

$$\begin{array}{l} \text{from} \\ (227) \end{array} \quad \min(y_v) = (0 - y_{\text{asym}}) = \frac{b \cdot z}{a} \quad (234)$$

$$\begin{array}{l} \text{from} \\ (233) \\ (234) \end{array} \quad \max(y_v) \cdot \min(y_v) = \frac{z \cdot (a+b)}{a} \cdot \frac{b \cdot z}{a} = \frac{z^2 \cdot b \cdot (a+b)}{a^2} \quad (235)$$

$$\begin{array}{l} \text{from} \\ (235) \end{array} \quad \sqrt{\max(y_v)} \cdot \sqrt{\min(y_v)} = \frac{z \cdot \sqrt{b \cdot (a+b)}}{a} \quad (236)$$

$$\begin{array}{l} \text{from} \\ (229) \\ (230) \end{array} \quad \frac{\max(x_v)}{\min(x_v)} = \frac{\frac{z}{a \cdot b}}{\frac{z}{a \cdot (a+b)}} = \frac{a+b}{b} = \frac{\sqrt{P_{\text{high}}}}{\sqrt{P_{\text{low}}}} = C \quad (237)$$

$$\begin{array}{l} \text{from} \\ (233) \\ (234) \end{array} \quad \frac{\max(y_v)}{\min(y_v)} = \frac{\frac{z \cdot (a+b)}{a}}{\frac{b \cdot z}{a}} = \frac{a+b}{b} = \frac{\sqrt{P_{\text{high}}}}{\sqrt{P_{\text{low}}}} = C \quad (238)$$

To complete the characterization of the real curve (and begin characterizing the reference curve), the identities of x_0 and y_0 must be acquired by compensating for the shift parameter (equivalent to x_{asym} and y_{asym}) with respect to the “center” coordinates of the virtual curve (i.e., the geometric means of $\min(x_v)$ and $\max(x_v)$, and $\min(y_v)$ and $\max(y_v)$). Reversing the shift (Equations 239 and 241) then simplifying (Equations 240 and 242) yields the identities of x_0 and y_0 in terms of a , b , and z . In both cases, the simplified forms, as well as a seemingly unnecessary expansion of $b \cdot (a+b)$ into the square of its square root, are presented. The simplified versions are innocuous with respect to the annotation of the real curve; however, the expanded version reveals a continued pattern with respect to the reference curve capstone identities. Both are used in their appropriate contexts.

With these coordinates, the characterization of the real curve is now complete (Figure 42).

$$\begin{array}{l} \text{from} \\ (226) \\ (232) \end{array} \quad x_0 = \sqrt{\max(x_v)} \cdot \sqrt{\min(x_v)} + x_{\text{asym}} = \frac{z}{a \cdot \sqrt{b \cdot (a+b)}} - \frac{z}{a \cdot (a+b)} \quad (239)$$

$$\begin{array}{l} \text{from} \\ (239) \end{array} \quad x_0 = \frac{z \cdot (\sqrt{b \cdot (a+b)} - b)}{a \cdot b \cdot (a+b)} = \frac{z}{a \cdot \sqrt{b \cdot (a+b)}} \cdot \frac{\sqrt{b \cdot (a+b)} - b}{\sqrt{b \cdot (a+b)}} \quad (240)$$

$$\begin{array}{l} \text{from} \\ (227) \\ (236) \end{array} \quad y_0 = \sqrt{\max(y_v)} \cdot \sqrt{\min(y_v)} + y_{\text{asym}} = \frac{z \cdot \sqrt{b \cdot (a+b)}}{a} - \frac{b \cdot z}{a} \quad (241)$$

$$\begin{array}{l} \text{from} \\ (241) \end{array} \quad y_0 = \frac{z \cdot (\sqrt{b \cdot (a+b)} - b)}{a} = \frac{z \cdot \sqrt{b \cdot (a+b)}}{a} \cdot \frac{\sqrt{b \cdot (a+b)} - b}{\sqrt{b \cdot (a+b)}} \quad (242)$$

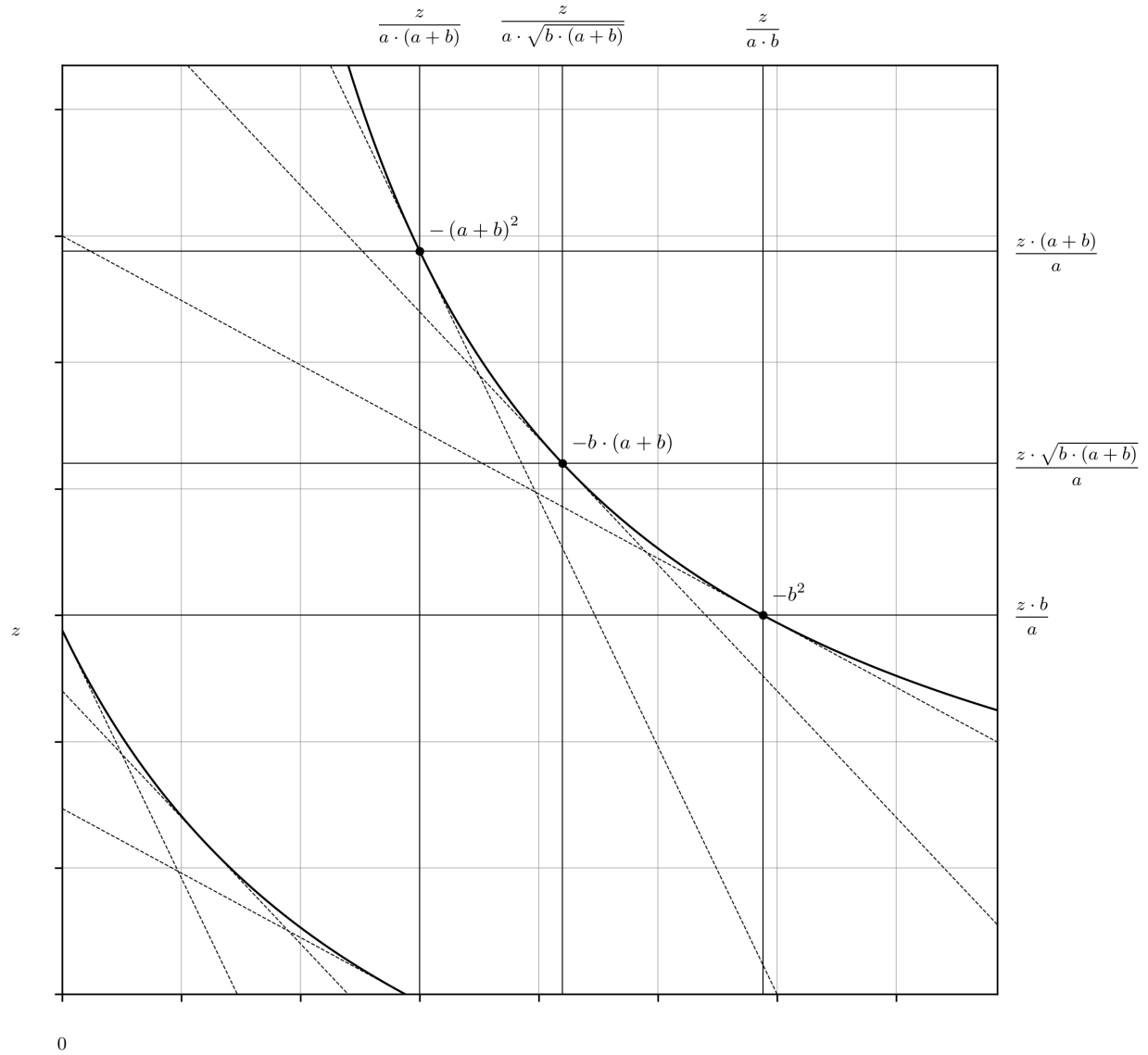


Fig. 41 The completed characterisation of the Carbon DeFi virtual curve, with the coordinates at its price bounds and geometric mean of the price bounds annotated as appropriate (Equations 229, 230, 232, 233, 234 and 236).

Similar to the Uniswap v3 curve constructions and in contrast to the Bancor v2 constructions, we have derived the virtual curve beginning from the shifted real curve. Regardless, it is still appropriate to define the real curve in terms of the virtual curve and the horizontal and vertical shifts (Figure 43).

To complete the virtual curve characterization, recall that it is just a regular rectangular hyperbola. Its scaling constant can be obtained directly from inspection of the RHS of Equation 201, or from the product of any set of coordinates along the curve, (e.g., $\min(x_v) \cdot \max(y_v)$, $\max(x_v) \cdot \min(y_v)$, or $\sqrt{\max(x_v)} \cdot \sqrt{\min(x_v)} \cdot \sqrt{\max(y_v)} \cdot \sqrt{\min(y_v)}$) (Equation 243). Then, elaboration of the marginal price and token swap equations is performed as was done for Equations 26, 27, 28, 29, 30, 31, 32, 33, 34 and 35 and Equations 178, 179, 180, 181, 182, 183, 184, and 185 (Equations 243, 244, 245, 246, 247, 248, 249, and 250).

$$\text{from (2)} \quad x_v \cdot y_v = \frac{z}{a \cdot \sqrt{b \cdot (a+b)}} \cdot \frac{z \cdot \sqrt{b \cdot (a+b)}}{a} = \frac{z^2}{a^2} \quad (243)$$

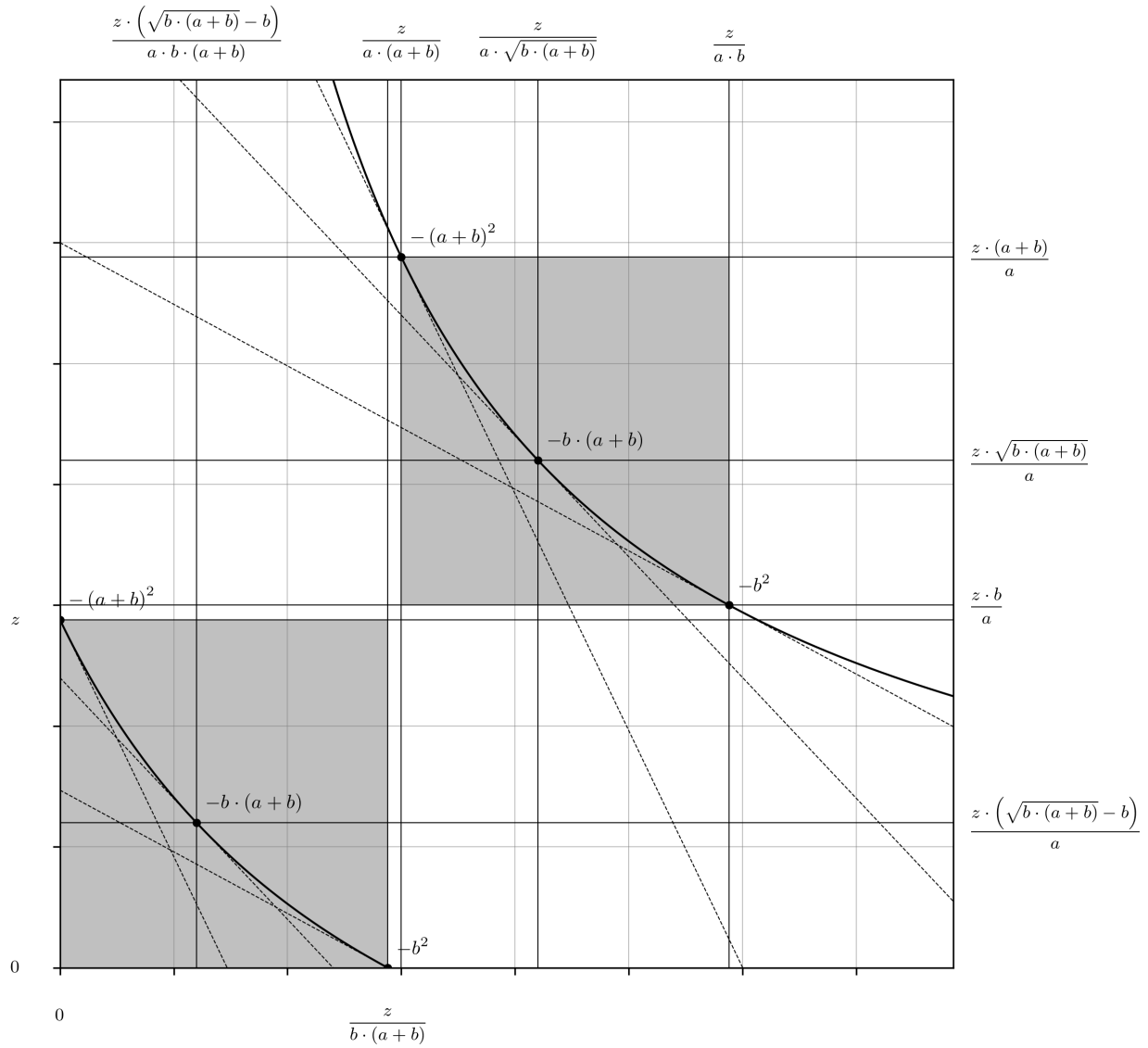


Fig. 42 Completed characterizations of the Carbon DeFi real and virtual curves are depicted and annotated appropriately (Equations 200, 224, 229, 230, 232, 233, 234, 236, 240 and 242).

from (8)
$$y_v = \frac{z^2}{a^2 \cdot x_v} \quad (244)$$

from (6)
$$x_v = \frac{z^2}{a^2 \cdot y_v} \quad (245)$$

from (3)
$$(x_v + \Delta x) \cdot (y_v + \Delta y) = \frac{z^2}{a^2} \quad (246)$$

from (4) (7)
$$\Delta x = \frac{z^2}{a^2 \cdot (y_v + \Delta y)} - x_v = -\frac{\Delta y \cdot z^2}{a^2 \cdot (y_v \cdot (y_v + \Delta y))} \quad (247)$$

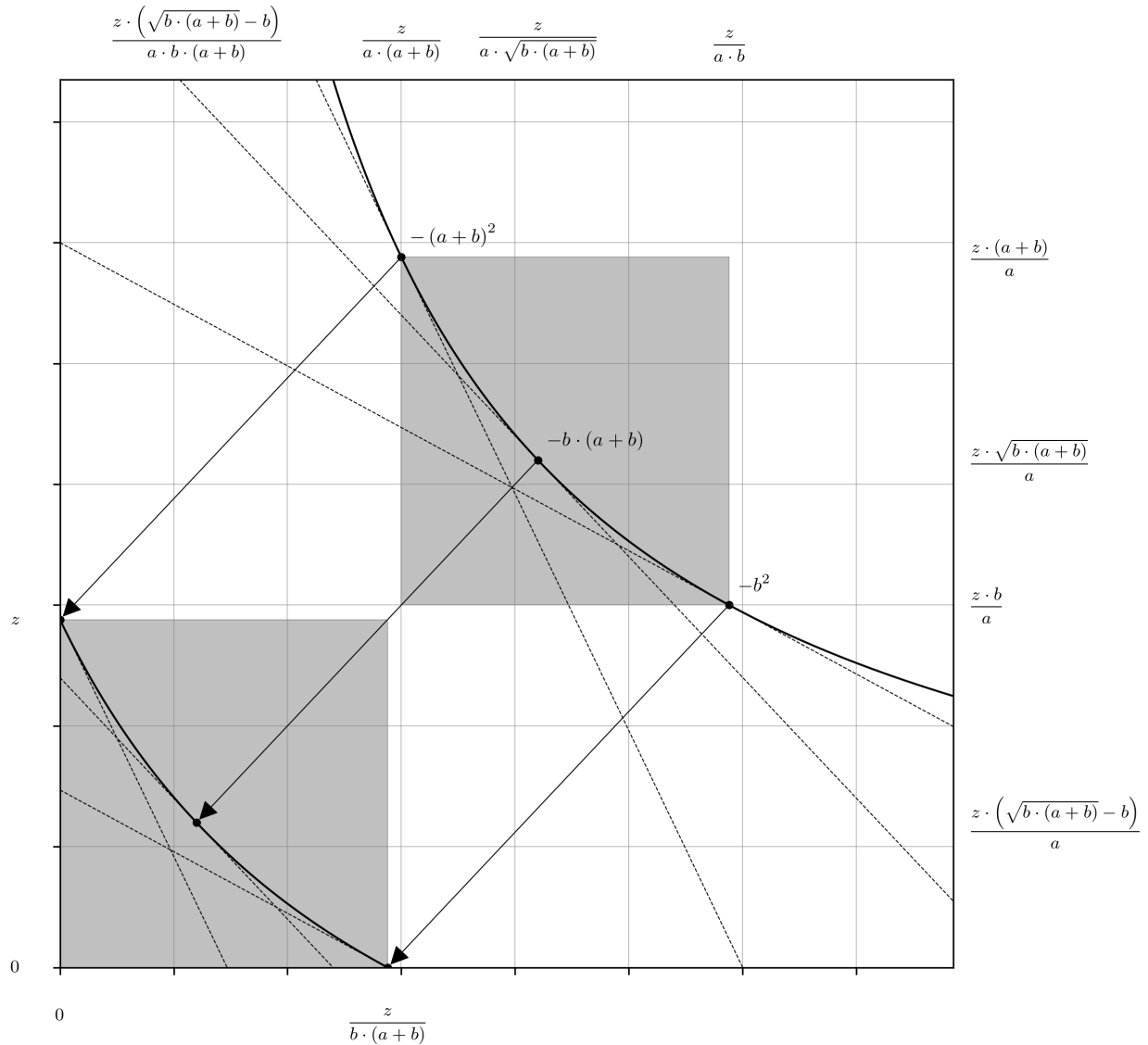


Fig. 43 Reconstruction of the Carbon DeFi real curve is depicted as a map of the virtual curve back to the x- and y-axes.

$$\begin{array}{l} \text{from} \\ (5) \\ (9) \end{array} \quad \Delta y = \frac{A^2 \cdot z^2}{a^2 \cdot (x_v + \Delta x)} - y_v = -\frac{\Delta x \cdot z^2}{a^2 \cdot (x_v \cdot (x_v + \Delta x))} \quad (248)$$

$$\begin{array}{l} \text{from} \\ (16) \end{array} \quad \frac{\partial x_v}{\partial y_v} = -\frac{z^2}{a^2 \cdot y_v^2}; \quad \frac{\partial y_v}{\partial x_v} = -\frac{a^2 \cdot y_v^2}{z^2} \quad (249)$$

$$\begin{array}{l} \text{from} \\ (17) \end{array} \quad \frac{\partial y_v}{\partial x_v} = -\frac{z^2}{a^2 \cdot x_v^2}; \quad \frac{\partial x_v}{\partial y_v} = -\frac{a^2 \cdot x_v^2}{z^2} \quad (250)$$

The indifference of the real and virtual curves with respect the calculated swap quantities is again evident in the analysis (Figures 44 and 45). Translocation upon the integrated forms (i.e. the bonding curves, Figure 44) and integration above their implied price curves (Figure 45) yields the same token amounts, Δx and Δy . The only difference is the frame of

reference, which is shifted by $(-x_{\text{asym}}, -y_{\text{asym}})$ in the virtual curve compared to the real curve, which has no effect on either the marginal rate, or the effective rate of exchange. As with Uniswap v3, Carbon DeFi exposes the terms necessary to adapt legacy software that is dependent on the $x \cdot y = k$ assumption; simply read z and a from the smart contracts and k becomes the square of their quotient, $k = (z/a)^2$.

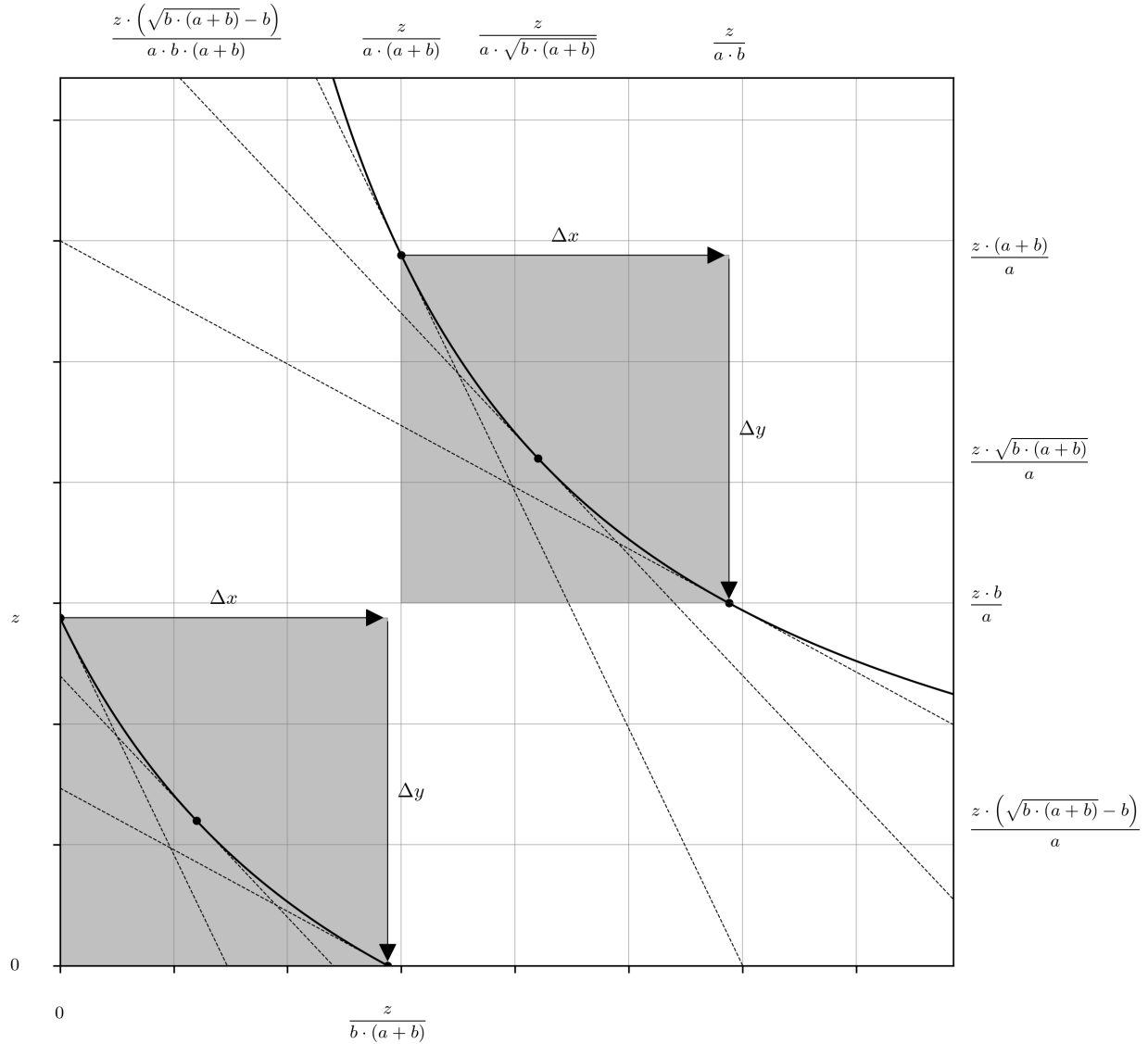


Fig. 44 Traversal upon the rectangular hyperbolas $y \cdot (z + x \cdot a \cdot (a + b)) = z \cdot (z - x \cdot b \cdot (a + b))$ and $x_v \cdot y_v = z^2/a^2$ (Equations 202 and 243), representing a token swap against the Carbon DeFi real and virtual curves, where $\Delta x > 0$ and $\Delta y < 0$. The swap quantities Δx and Δy , and marginal rates of exchange before and after the swap are identical. Therefore, with respect to the outcome of the exchange the difference between the two curve implementations is zero.

4.6 The Carbon DeFi Reference Curve

The Carbon DeFi reference curve is constructed according to the general methods established above. The product of x_0 and y_0 is equal to its scaling constant (i.e. k in the proverbial “constant product” equation, $x \cdot y = k$), and can be obtained from the RHS of Equations 240 and 242 (Equations 251 and 252). The form the expression takes in Equation 252 is to make the re-scaling of the reference curve with respect to the virtual curve obvious, which also allows for the original amplification term, A , to be extracted and represented in terms of a , b , and z (Equations 59, 252 and 253).

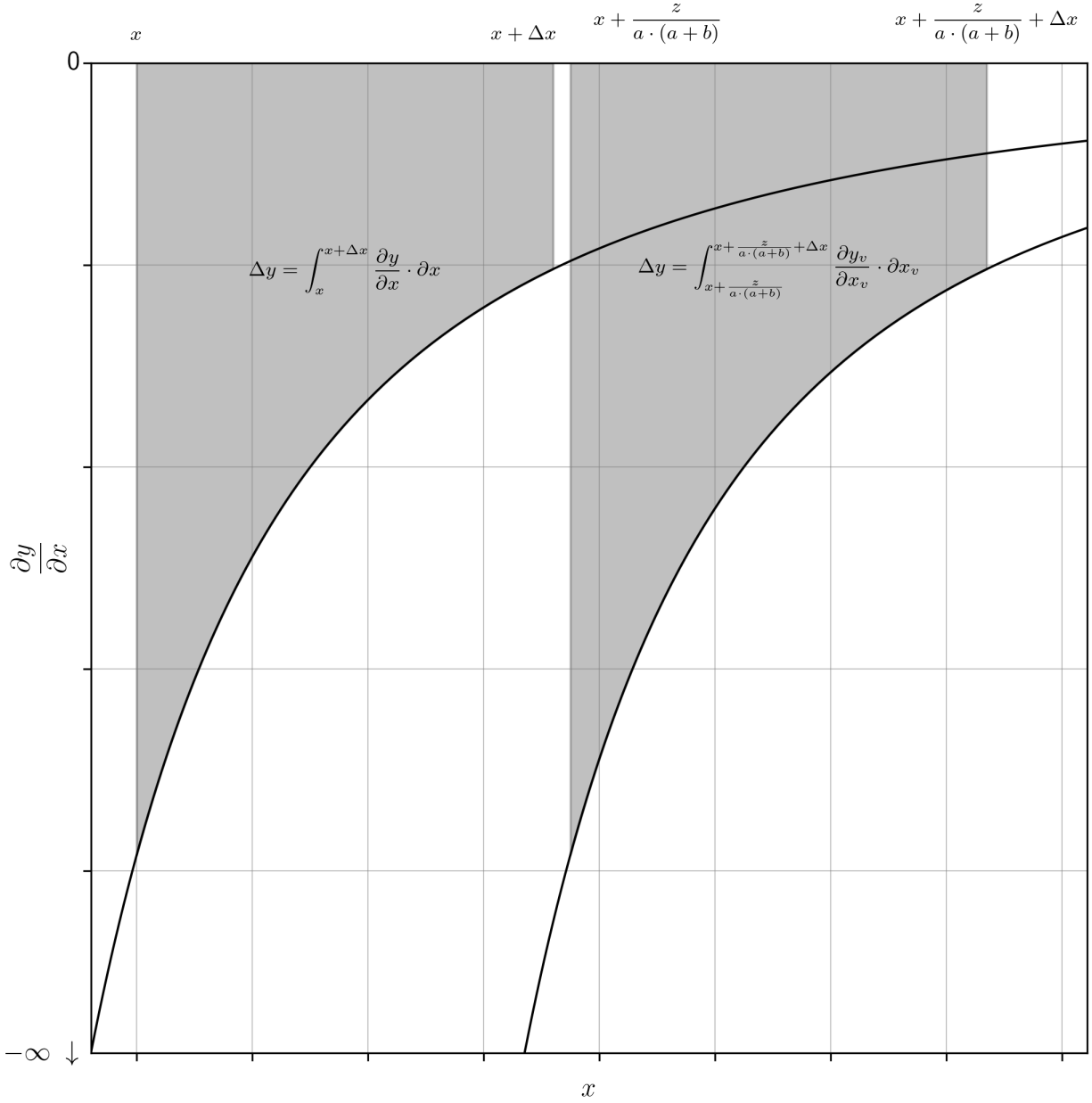


Fig. 45 The integration above $\partial y/\partial x = -z^2 \cdot (a+b)^2 / (x \cdot a \cdot (a+b) + z)^2$ and $\partial y_v/\partial x_v = -z^2 / (a \cdot x_v)^2$ (Equations 219 and 250) over the intervals $x \rightarrow x + \Delta x$ and $x + z/(a \cdot (a+b)) \rightarrow x + z/(a \cdot (a+b)) + \Delta x$ (i.e. $x_v \rightarrow x_v + \Delta x$) representing a token swap against both the real and virtual curves, where $\Delta x > 0$ and $\Delta y < 0$. Apart from the shift along the x-axis, these are identical in every other aspect. Note that the relationship between the real and virtual price curves is additive (x and Δx versus $x + z/(a \cdot (a+b))$ and $x + z/(a \cdot (a+b)) + \Delta x$).

from
(2)
(240)
(242)

$$x \cdot y = \frac{z \cdot (\sqrt{b \cdot (a+b)} - b)}{a \cdot b \cdot (a+b)} \cdot \frac{z \cdot (\sqrt{b \cdot (a+b)} - b)}{a} \quad (251)$$

from
(251)

$$x \cdot y = \frac{z^2 \cdot (\sqrt{b \cdot (a+b)} - b)^2}{a^2 \cdot b \cdot (a+b)} = \frac{z^2}{a^2} \cdot \left(\frac{\sqrt{b \cdot (a+b)} - b}{\sqrt{b \cdot (a+b)}} \right)^2 \quad (252)$$

$$\begin{array}{l} \text{from} \\ (59) \\ (199) \\ (205) \\ (252) \end{array} \quad \frac{\sqrt{b \cdot (a+b)}}{\sqrt{b \cdot (a+b)} - b} = \frac{\sqrt{P_0}}{\sqrt{P_0} - \sqrt{P_{\text{low}}}} \Rightarrow \frac{\sqrt[4]{P_{\text{high}}}}{\sqrt[4]{P_{\text{high}}} - \sqrt[4]{P_{\text{low}}}} = A \quad (253)$$

With the reference curve's scaling constant now defined in terms of a , b , and z , the coordinates corresponding to the price bounds, $\min(x)$, $\max(x)$, $\min(y)$, and $\max(y)$, can also be expressed with the same parameters. As was done for the Uniswap v3 case, we will approach this analytically. First, the derivative of the reference curve (Equations 16 and 17) is forced to either $-P_{\text{high}}$ or $-P_{\text{low}}$; in the Carbon DeFi parameterization, $P_{\text{low}} = b^2$ and $P_{\text{high}} = (a+b)^2$. Then, the x or y variable is substituted for $\min(x)$, $\max(x)$, $\min(y)$, or $\max(y)$, as appropriate, and the coordinate of interest is obtained via trivial rearrangements of the resulting expressions (Equations 254, 255, 256, 257, 258, 259, 260, and 261) (Figure 46).

$$\begin{array}{l} \text{from} \\ (17) \\ (252) \end{array} \quad \frac{\partial y}{\partial x} = -(a+b)^2 = -\frac{z^2 \cdot \left(\frac{\sqrt{b \cdot (a+b)} - b}{\sqrt{b \cdot (a+b)}} \right)^2}{\min^2(x)} \quad (254)$$

$$\begin{array}{l} \text{from} \\ (254) \end{array} \quad \min(x) = \frac{z}{a \cdot (a+b)} \cdot \left(\frac{\sqrt{b \cdot (a+b)} - b}{\sqrt{b \cdot (a+b)}} \right) \quad (255)$$

$$\begin{array}{l} \text{from} \\ (17) \\ (252) \end{array} \quad \frac{\partial y}{\partial x} = -b^2 = -\frac{z^2 \cdot \left(\frac{\sqrt{b \cdot (a+b)} - b}{\sqrt{b \cdot (a+b)}} \right)^2}{\max^2(x)} \quad (256)$$

$$\begin{array}{l} \text{from} \\ (256) \end{array} \quad \max(x) = \frac{z}{a \cdot b} \cdot \left(\frac{\sqrt{b \cdot (a+b)} - b}{\sqrt{b \cdot (a+b)}} \right) \quad (257)$$

$$\begin{array}{l} \text{from} \\ (16) \\ (252) \end{array} \quad \frac{\partial y}{\partial x} = -b^2 = -\frac{\min^2(y)}{\frac{z^2 \cdot \left(\frac{\sqrt{b \cdot (a+b)} - b}{\sqrt{b \cdot (a+b)}} \right)^2}{a^2}} \quad (258)$$

$$\begin{array}{l} \text{from} \\ (258) \end{array} \quad \min(y) = \frac{z \cdot b}{a} \cdot \left(\frac{\sqrt{b \cdot (a+b)} - b}{\sqrt{b \cdot (a+b)}} \right) \quad (259)$$

$$\begin{array}{l} \text{from} \\ (16) \\ (252) \end{array} \quad \frac{\partial y}{\partial x} = -(a+b)^2 = -\frac{\max^2(y)}{\frac{z^2 \cdot \left(\frac{\sqrt{b \cdot (a+b)} - b}{\sqrt{b \cdot (a+b)}} \right)^2}{a^2}} \quad (260)$$

$$\begin{array}{l} \text{from} \\ (260) \end{array} \quad \max(y) = \frac{z \cdot (a+b)}{a} \cdot \left(\frac{\sqrt{b \cdot (a+b)} - b}{\sqrt{b \cdot (a+b)}} \right) \quad (261)$$

As with the Uniswap v3 constructions, the Carbon DeFi constructions have been performed in the reverse order compared to the seminal work (Figures 1 to 21). However, the liquidity amplification heuristic is still useful, and can be

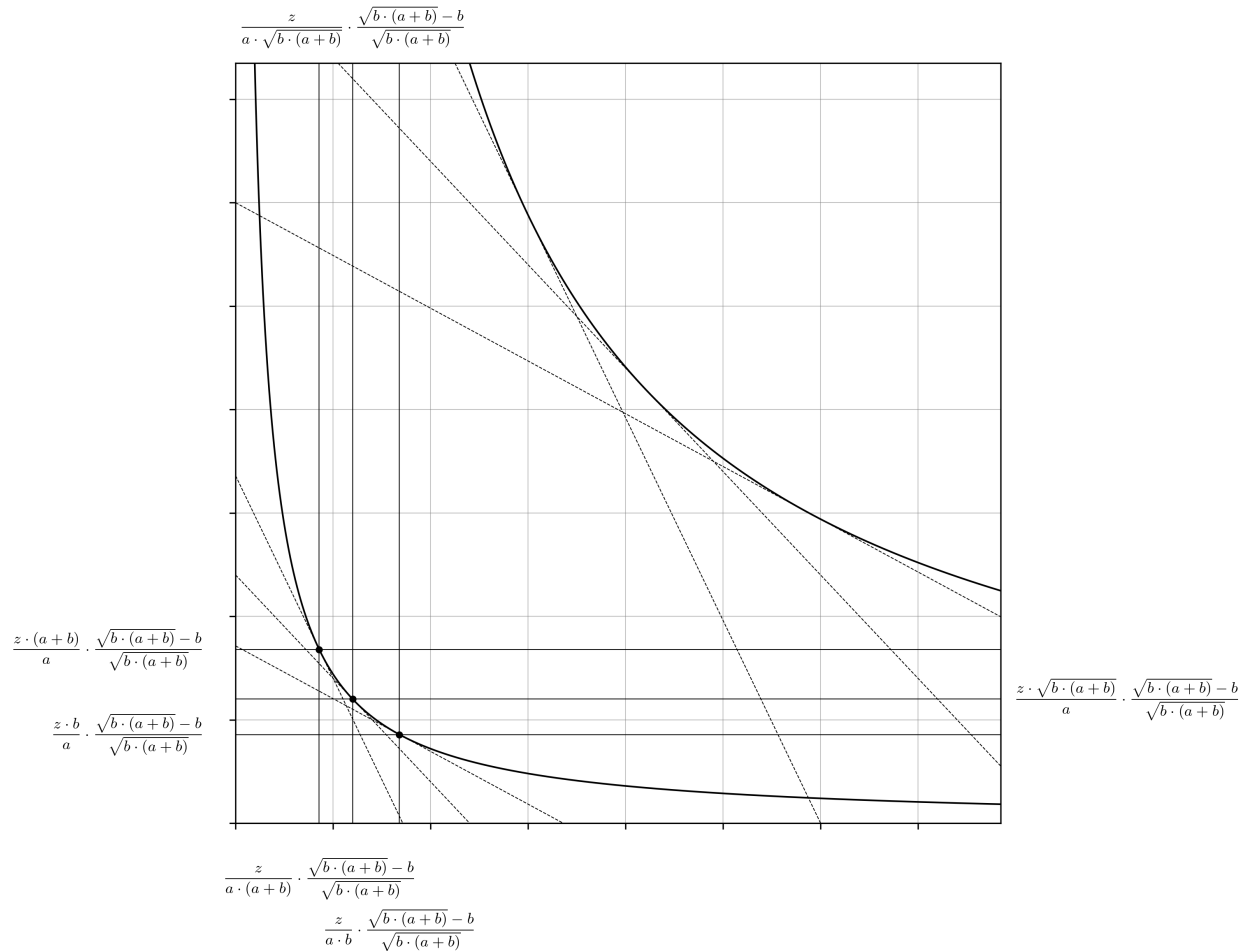


Fig. 46 The algebraic identities of the points where the lines tangent to the Carbon DeFi reference curve and parallel to the tangent lines at the price boundaries of the virtual curve are now elucidated (Equations 240, 242, 255, 257, 259 and 261).

depicted as before with arrows connecting pairs of points on the reference and virtual curves, where the derivatives evaluated at these points are equal (Figure 47).

Trade volumes between reference and virtual curves within the same price range are compared (Figures 48 and 49). Despite trading at the same marginal and effective exchange rates, the virtual curve shows significantly higher trade volumes, as seen by longer arrows in Figure 48 and a larger integrated area in Figure 49.

This concludes our examination of the Carbon DeFi curves, and the section on “unnatural” parameterizations. The critical algebraic identities for all three protocols examined here (Bancor’s v2 and Carbon DeFi, and Uniswap’s v3) are tabulated in Table 1, which provides something akin to a concentrated liquidity Rosetta stone, allowing for direct translation of key parameters between the contexts wherein each protocol resides. Remember - from the analytical and geometric perspectives, *all three descriptions are mathematically redundant*. Their apparent differences emerge from the choice of notation and parameterization, which only reflects their smart contract implementation; the underlying pricing algorithm remains unchanged in all three.

5 The “Natural” Reparameterizations of the Concentrated Liquidity Invariant Function

The previous sections are referred to as the “unnatural” parameterizations because the way they are constructed is artificial; they are created by deliberately asserting something, such as the relative amplification of the virtual curve compared to the reference curve, the price bounds, or one of the intercepts of the real curve, whereas a “natural” construction might begin at a more fundamental level, free from the context of the protocol for which it is being defined.

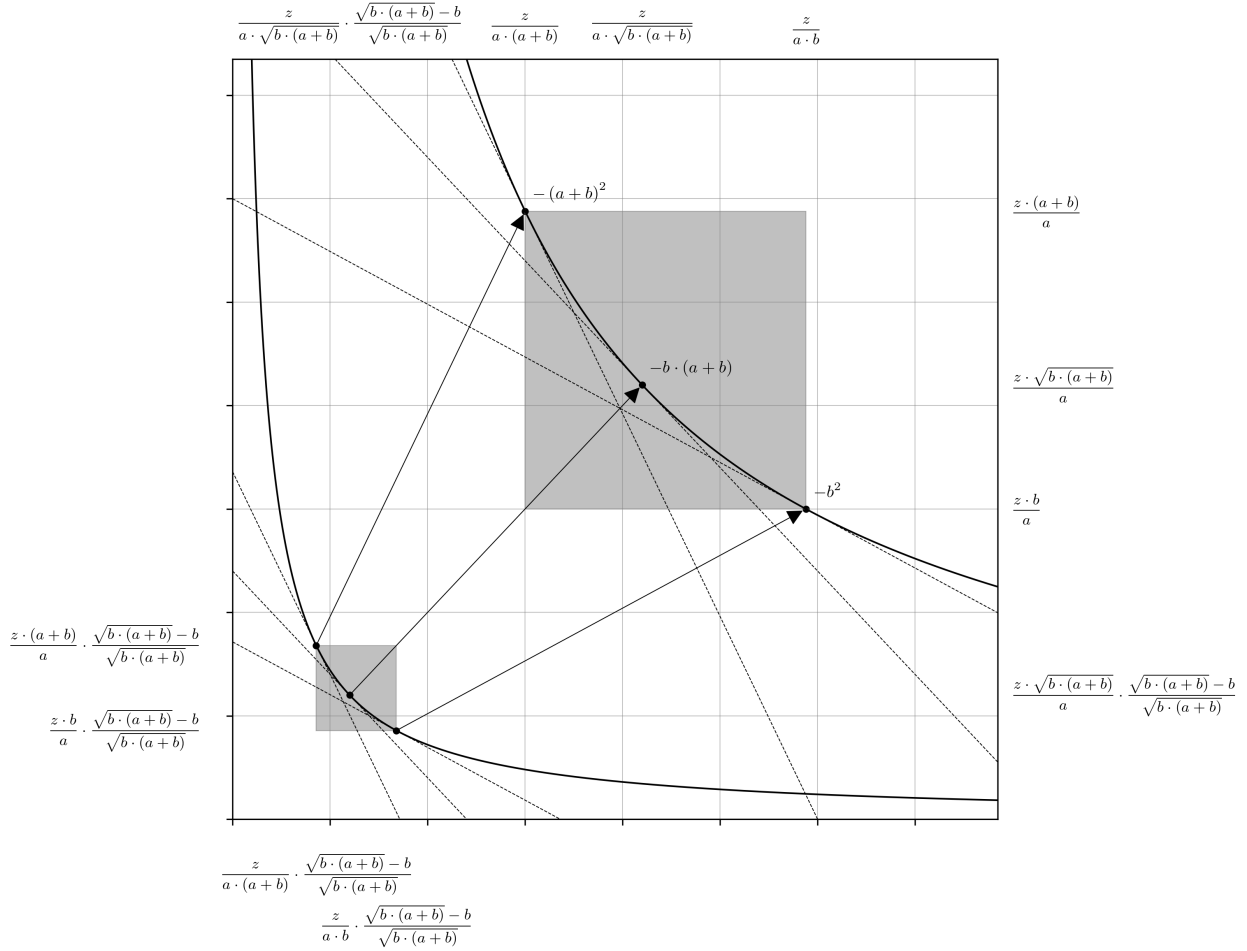


Fig. 47 The amplification process is depicted with corresponding shaded areas of the Carbon DeFi reference and virtual curves, respectively. Points where the first derivative of each curve evaluates to the same result are shown as white dots, and the mapping of these points is depicted with white arrows.

With that said, it is not immediately clear how to go about obtaining the natural description of these objects. Contributions of an academic nature are often presented as though one already possessed the intuition and depth of understanding to have arrived at what is disclosed, effortlessly. That was not the case here. In fact the opposite is true – a conspicuously compact set of equations for the concentrated real curve was discovered first, and their connection to more fundamental concepts was found later while investigating their significance.

The following sections are [mostly] presented in chronological order with respect to the investigation of this topic material, which has the benefit of a top-down trajectory towards the underlying hyperbolic trigonometry of these curves.

5.1 Three “Pretty” Invariants

In Section 3.1, following the discussion of amplification term, A , expressed with respect to the price boundaries, P_{high} and P_{low} , (Equations 57, 58 and 59), it was stated that there is a more conspicuous identity, C , which almost seems as though it wants to assert its own existence (Equations 60, 61, 62, 63 and 64). This term itches, and its persistence motivates a refactorization which includes it as a native parameter. Beginning from the seminal concentrated liquidity function (Equation 80), and the x_{int} , y_{int} , x_{asym} , and y_{asym} identities derived therefrom (Equations 106, 107, 108 and 109), it is a relatively easy task to identify A , $A - 1$, and $2A - 1$ as key terms which will need to be defined with respect to C . Note that this process alone begins to reveal a symmetry that was hidden there all along (Equations 262, 263 and 264).

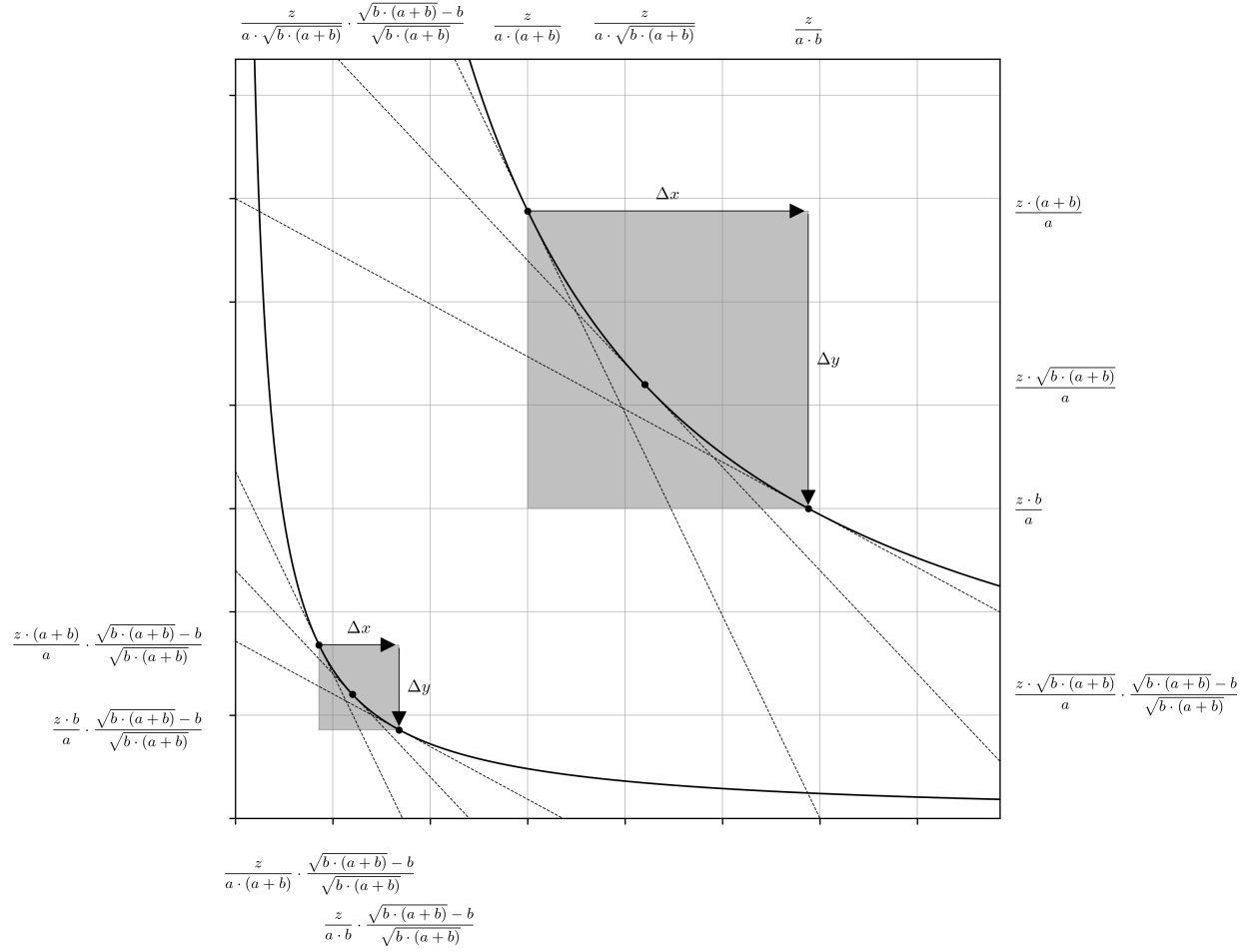


Fig. 48 Traversal upon the rectangular hyperbolas $x_v \cdot y_v = z^2/a^2$ and $x \cdot y = z^2 \cdot (\sqrt{b}\sqrt{a+b} - b)^2 / (a^2 \cdot b \cdot (a+b))$ (Equations 243 and 252), representing a token swap against the reference and amplified liquidity pool, where $\Delta x > 0$ and $\Delta y < 0$. The marginal rates of exchange before and after the swap are identical. The ratio of the Δx and Δy arrow lengths for each curve are also identical. Therefore the overall rate of exchange, $\Delta y/\Delta x$ is equal in both cases.

from
(60)
(61)
(62)
(63)
(64)

$$A = \frac{1}{1 - \frac{\sqrt[4]{P_{\text{low}}}}{\sqrt[4]{P_{\text{high}}}}} = \frac{\sqrt[4]{P_{\text{high}}}}{\sqrt[4]{P_{\text{high}}} - \sqrt[4]{P_{\text{low}}}} = \frac{\sqrt{C} + 1}{C - 1} + 1 = \frac{\sqrt{C}}{\sqrt{C} - 1} \quad (262)$$

from
(60)
(61)
(62)
(63)
(64)

$$A - 1 = \frac{1}{\frac{\sqrt[4]{P_{\text{high}}}}{\sqrt[4]{P_{\text{low}}}} - 1} = \frac{\sqrt[4]{P_{\text{low}}}}{\sqrt[4]{P_{\text{high}}} - \sqrt[4]{P_{\text{low}}}} = \frac{\sqrt{C} + 1}{C - 1} = \frac{1}{\sqrt{C} - 1} \quad (263)$$

from
(262)
(263)

$$2A - 1 = \frac{1}{1 - \frac{\sqrt[4]{P_{\text{low}}}}{\sqrt[4]{P_{\text{high}}}}} + \frac{1}{\frac{\sqrt[4]{P_{\text{high}}}}{\sqrt[4]{P_{\text{low}}}} - 1} = \frac{\sqrt[4]{P_{\text{high}}} + \sqrt[4]{P_{\text{low}}}}{\sqrt[4]{P_{\text{high}}} - \sqrt[4]{P_{\text{low}}}} = \frac{(\sqrt{C} + 1)^2}{C - 1} = \frac{\sqrt{C} + 1}{\sqrt{C} - 1} \quad (264)$$

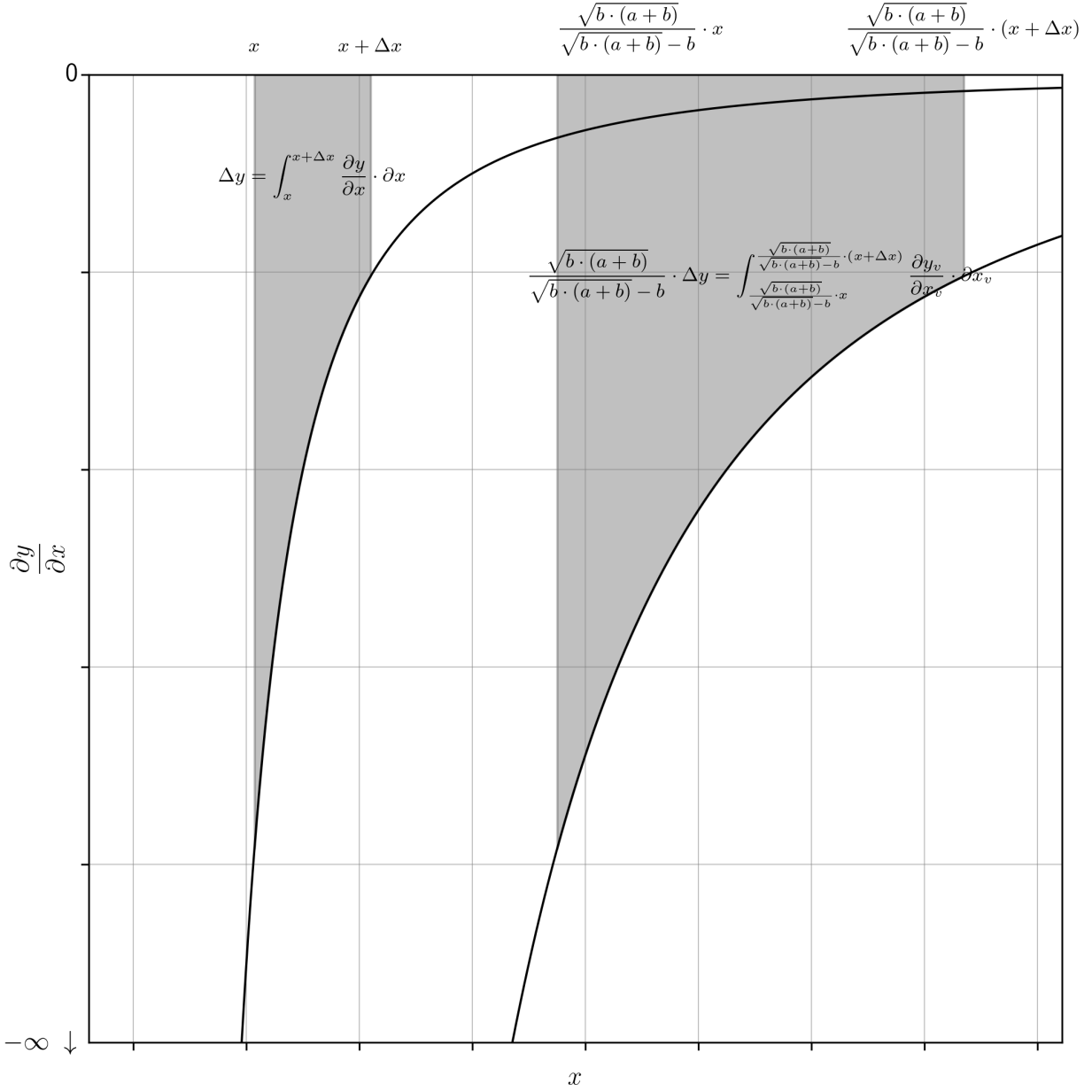


Fig. 49 The integration above $\partial y/\partial x = -z^2 \cdot (\sqrt{b} \cdot \sqrt{a+b} - b)^2 / (a^2 \cdot b \cdot (a+b) \cdot x^2)$ and $\partial y_v/\partial x_v = -z^2 / (a \cdot x_v)^2$ over the intervals $x \rightarrow x + \Delta x$ and $x \cdot \sqrt{b} \cdot \sqrt{a+b} / (\sqrt{b} \cdot \sqrt{a+b} - b) \rightarrow (x + \Delta x) \cdot \sqrt{b} \cdot \sqrt{a+b} / (\sqrt{b} \cdot \sqrt{a+b} - b)$ (i.e. $x_v \rightarrow x_v + \Delta x$) representing a token swap against both the reference and amplified liquidity pools, where $\Delta x > 0$ and $\Delta y < 0$ ($\partial/\partial x$ Equation 252 and Equation 250). Note that that the integration areas for the reference and virtual curves are Δy and $\Delta y \cdot \sqrt{b} \cdot \sqrt{a+b} / (\sqrt{b} \cdot \sqrt{a+b} - b)$, respectively. By inference, any token swap against the virtual curve can be calculated from the reference curve by applying the amplification term (Equations 59 and 253).

Incorporating the identities of A and $A - 1$ in terms of C (Equations 262 and 263) from above into the seminal Bancor v2 invariant (Equation 80) yields Equation 265, and its rearrangement to isolate C yields Equation 266.

Real Invariant Equation (Bonding Curve)				
Bancor v2	$(x + x_0 \cdot (A - 1)) \cdot (y + y_0 \cdot (A - 1)) = A^2 \cdot x_0 \cdot y_0$			
Uniswap v3	$\left(x + \frac{L}{\sqrt{P_{\text{high}}}}\right) \cdot \left(y + L \cdot \sqrt{P_{\text{low}}}\right) = L^2$			
Carbon DeFi	$\left(x + \frac{z}{a \cdot (a + b)}\right) \cdot \left(y + \frac{z \cdot b}{a}\right) = \frac{z^2}{a^2}$			
	Amplification Term	Reference Center x	Reference Center y	
Bancor v2	A	x_0	y_0	
Uniswap v3	$\frac{1}{1 - \frac{\sqrt[4]{P_{\text{low}}}}{\sqrt[4]{P_{\text{high}}}}}$	$\frac{L}{\sqrt[4]{P_{\text{high}}} \cdot \sqrt[4]{P_{\text{low}}}} \cdot \left(1 - \frac{\sqrt[4]{P_{\text{low}}}}{\sqrt[4]{P_{\text{high}}}}\right)$	$L \cdot \sqrt[4]{P_{\text{high}}} \cdot \sqrt[4]{P_{\text{low}}} \cdot \left(1 - \frac{\sqrt[4]{P_{\text{low}}}}{\sqrt[4]{P_{\text{high}}}}\right)$	
Carbon DeFi	$\frac{\sqrt{b} \cdot \sqrt{a + b}}{\sqrt{b} \cdot \sqrt{a + b} - b}$	$\frac{z}{a \cdot \sqrt{b} \cdot \sqrt{a + b}} \cdot \frac{\sqrt{b} \cdot \sqrt{a + b} - b}{\sqrt{b} \cdot \sqrt{a + b}}$	$\frac{z \cdot \sqrt{b} \cdot \sqrt{a + b}}{a} \cdot \frac{\sqrt{b} \cdot \sqrt{a + b} - b}{\sqrt{b} \cdot \sqrt{a + b}}$	
	High Price Boundary	Low Price Boundary	Geometric Mean Price	
Bancor v2	$\frac{A^2}{(A - 1)^2} \cdot \frac{y_0}{x_0}$	$\frac{(A - 1)^2}{A^2} \cdot \frac{y_0}{x_0}$	$\frac{y_0}{x_0}$	
Uniswap v3	P_{high}	P_{low}	$\sqrt{P_{\text{high}}} \cdot \sqrt{P_{\text{low}}}$	
Carbon DeFi	$(a + b)^2$	b^2	$b \cdot (a + b)$	
	x Asymptote	y Asymptote	x Intercept	y Intercept
Bancor v2	$-x_0 \cdot (A - 1)$	$-y_0 \cdot (A - 1)$	$\frac{x_0 \cdot (2A - 1)}{A - 1}$	$\frac{y_0 \cdot (2A - 1)}{A - 1}$
Uniswap v3	$-\frac{L}{\sqrt{P_{\text{high}}}}$	$-L \cdot \sqrt{P_{\text{low}}}$	$L \cdot \left(\frac{1}{\sqrt{P_{\text{low}}}} - \frac{1}{\sqrt{P_{\text{high}}}}\right)$	$L \cdot \left(\sqrt{P_{\text{high}}} - \sqrt{P_{\text{low}}}\right)$
Carbon DeFi	$-\frac{z}{a \cdot (a + b)}$	$-\frac{z \cdot b}{a}$	$\frac{z}{b \cdot (a + b)}$	z

Table 1 Summary of the real curve capstone identities for Bancor v2, Uniswap v3, and Carbon DeFi, in their native parameterizations.

from
(80)
(262)
(263)

$$\left(x + \frac{x_0}{\sqrt{C} - 1}\right) \cdot \left(y + \frac{y_0}{\sqrt{C} - 1}\right) = \frac{x_0 \cdot y_0 \cdot C}{(\sqrt{C} - 1)^2} \quad (265)$$

from
(265)

$$\frac{(x - x_0)^2 \cdot (y - y_0)^2}{(x \cdot y - x_0 \cdot y_0)^2} = C \quad (266)$$

After that, rearrangement of Equations 106 and 107 to express x_0 and y_0 in terms of A , x_{int} and y_{int} (Equation 267) followed by their substitution into the general invariant (Equation 80) yields Equation 268. Then, substitution of the A , $A - 1$ and $2A - 1$ terms from Equations 262, 263 and 264 as needed yields Equation 269, which after rearrangement to isolate C yields Equation 270.

$$\begin{array}{l} \text{from} \\ (106) \\ (107) \end{array} \quad x_0 = x_{\text{int}} \cdot \frac{(A-1)}{(2A-1)}; \quad y_0 = y_{\text{int}} \cdot \frac{(A-1)}{(2A-1)} \quad (267)$$

$$\begin{array}{l} \text{from} \\ (80) \\ (267) \end{array} \quad \left(x + x_{\text{int}} \cdot \frac{(A-1)^2}{(2A-1)} \right) \cdot \left(y + y_{\text{int}} \cdot \frac{(A-1)^2}{(2A-1)} \right) = x_{\text{int}} \cdot y_{\text{int}} \cdot \frac{A^2 \cdot (A-1)^2}{(2A-1)^2} \quad (268)$$

$$\begin{array}{l} \text{from} \\ (262) \\ (263) \\ (264) \\ (268) \end{array} \quad \left(x + \frac{x_{\text{int}}}{C-1} \right) \cdot \left(y + \frac{y_{\text{int}}}{C-1} \right) = \frac{x_{\text{int}} \cdot y_{\text{int}} \cdot C}{(C-1)^2} \quad (269)$$

$$\begin{array}{l} \text{from} \\ (269) \end{array} \quad \frac{(x_{\text{int}} - x) \cdot (y_{\text{int}} - y)}{x \cdot y} = C \quad (270)$$

Lastly, rearrangement of Equations 108 and 109 to express x_{asym} and y_{asym} in terms of A , x_{int} and y_{int} (Equation 271) followed by their substitution into the general invariant (Equation 80) yields Equation 272. In contrast to Equations 80 and 268, Equation 272 features $A^2 / (A-1)^2$ as the only term requiring substitution, which has already been proved to be equal to C (Equations 60, 61, 62, 63 and 64). Therefore, effective replacement of the A terms to yield Equation 273 can be performed without reference to Equations 262, 263 and 264. Then, rearrangement to isolate C yields Equation 274.

$$\begin{array}{l} \text{from} \\ (108) \\ (109) \end{array} \quad x_0 = -\frac{x_{\text{asym}}}{(A-1)}; \quad y_0 = -\frac{y_{\text{asym}}}{(A-1)} \quad (271)$$

$$\begin{array}{l} \text{from} \\ (80) \\ (271) \end{array} \quad (x - x_{\text{asym}}) \cdot (y - y_{\text{asym}}) = x_{\text{asym}} \cdot y_{\text{asym}} \cdot \frac{A^2}{(A-1)^2} \quad (272)$$

$$\begin{array}{l} \text{from} \\ (60) \\ (61) \\ (62) \\ (63) \\ (64) \\ (272) \end{array} \quad (x - x_{\text{asym}}) \cdot (y - y_{\text{asym}}) = x_{\text{asym}} \cdot y_{\text{asym}} \cdot C \quad (273)$$

$$\begin{array}{l} \text{from} \\ (273) \end{array} \quad \frac{(x - x_{\text{asym}}) \cdot (y - y_{\text{asym}})}{x_{\text{asym}} \cdot y_{\text{asym}}} = C \quad (274)$$

Note that Equations 266, 270 and 274 are conspicuously simple, even “pretty”, at least compared to the status quo for the “unnatural” archetypes in the previous sections. Moreover, *they are all equal to each other* (Equation 275). Combined with the other identities already proven (and implied) earlier in Equations 63, 64, 77, 78, 116, 117, 170, 171, 237 and 238 (Equation 276), we are starting to approach something akin to an algebraic universal translator for *any* concentrated real curve, regardless of its parameterization. While this is certainly not the only way to achieve this (e.g. Table 1), there is something peculiarly terse about this one, and its prettiness hints at something more fundamental.

$$\begin{array}{l} \text{from} \\ (273) \end{array} \quad \frac{(x - x_0)^2 \cdot (y - y_0)^2}{(x \cdot y - x_0 \cdot y_0)^2} = \frac{(x_{\text{int}} - x) \cdot (y_{\text{int}} - y)}{x \cdot y} = \frac{(x - x_{\text{asym}}) \cdot (y - y_{\text{asym}})}{x_{\text{asym}} \cdot y_{\text{asym}}} = C \quad (275)$$

$$\begin{array}{l} \text{from} \\ (273) \end{array} \quad \frac{y_{\text{asym}} - y_{\text{int}}}{y_{\text{asym}}} = \frac{x_{\text{asym}} - x_{\text{int}}}{x_{\text{asym}}} = \frac{(y_{\text{asym}} - y_0)^2}{y_{\text{asym}}^2} = \frac{(x_{\text{asym}} - x_0)^2}{x_{\text{asym}}^2} = \frac{\sqrt{P_{\text{high}}}}{\sqrt{P_{\text{low}}}} = C \quad (276)$$

5.2 Transforming and Normalizing the Curves in a New Coordinate System

The analysis in the following section employs the hyperbolic trigonometry functions. However, these functions are only defined for a unit hyperbola, which opens to the left and the right, with its vertices at $(-1, +1)$. Therefore, we have two options. Either we redefine these functions to operate in the native parameter space of the bonding curves, or transform the bonding curves into a compatible representation. There is fundamentally no difference between either option, only a difference of perspective and intuition. Since the hyperbolic trigonometry functions are relatively exotic and given that transforming the curves is a core theme of this exploration, we are going to operate on the curves themselves and then apply the trigonometric analysis on their transformed versions.

This part of the exercise begins by first returning to the standard $x \cdot y = x_0 \cdot y_0$ curve. Prior to the hyperbolic trigonometric analysis, we must first perform a rotation about the origin and then re-scale to create a unit hyperbola. The rotation is -45° (a clockwise rotation is negative), or $-\pi/4$ radians. Therefore, the transformation matrix, R_{-45° , is derived from the general rotation matrix (Equation 277) by substituting $\theta = -\pi/4$ (Equation 278).

$$R = \begin{bmatrix} \cos(\theta) & -\sin(\theta) \\ \sin(\theta) & \cos(\theta) \end{bmatrix} \quad (277)$$

$$\begin{array}{l} \text{from} \\ (277) \end{array} \quad R_{-45^\circ} = \begin{bmatrix} \cos\left(-\frac{\pi}{4}\right) & -\sin\left(-\frac{\pi}{4}\right) \\ \sin\left(-\frac{\pi}{4}\right) & \cos\left(-\frac{\pi}{4}\right) \end{bmatrix} = \begin{bmatrix} \frac{1}{\sqrt{2}} & -\frac{1}{\sqrt{2}} \\ \frac{1}{\sqrt{2}} & \frac{1}{\sqrt{2}} \end{bmatrix} \quad (278)$$

The above matrix can be used to apply the transformation on all points (x, y) on the curve $x \cdot y = x_0 \cdot y_0$ as follows (Equation 279):

$$\begin{array}{l} \text{from} \\ (278) \end{array} \quad \begin{bmatrix} t \\ u \end{bmatrix} = R_{-45^\circ} \cdot \begin{bmatrix} x \\ y \end{bmatrix} = \begin{bmatrix} \frac{1}{\sqrt{2}} & -\frac{1}{\sqrt{2}} \\ \frac{1}{\sqrt{2}} & \frac{1}{\sqrt{2}} \end{bmatrix} \cdot \begin{bmatrix} x \\ y \end{bmatrix} = \begin{bmatrix} \frac{x}{\sqrt{2}} + \frac{y}{\sqrt{2}} \\ -\frac{x}{\sqrt{2}} + \frac{y}{\sqrt{2}} \end{bmatrix} \quad (279)$$

Therefore, any set of coordinates (x, y) is transformed to (t, u) , thus rotating the $x \cdot y = x_0 \cdot y_0$ curve 45° clockwise (Equations 280 and 281). The overall process is depicted in Figure 50.

$$\begin{array}{l} \text{from} \\ (279) \end{array} \quad t = f_{x,y \rightarrow t}(x, y) = \frac{x + y}{\sqrt{2}} \quad (280)$$

$$\begin{array}{l} \text{from} \\ (279) \end{array} \quad u = f_{x,y \rightarrow u}(x, y) = \frac{y - x}{\sqrt{2}} \quad (281)$$

As we have done previously in the context of swap equations and marginal price formulas, we can reduce the dimensions needed for performing the rotation such that the transformation can be performed with reference only to one coordinate in the set by substituting the identities of x and y (Equations 6 and 8) as required to eliminate the opposite dimension, denoted by $f_{x \rightarrow t}$ and $f_{y \rightarrow u}$. In other words, t can be expressed entirely as a function of x (Equation 282) and u can be expressed entirely as a function of y (Equation 283).

$$\begin{array}{l} \text{from} \\ (8) \\ (280) \end{array} \quad t = f_{x \rightarrow t}(x) = \frac{x + \frac{x_0 \cdot y_0}{x}}{\sqrt{2}} = \frac{x^2 + x_0 \cdot y_0}{x \cdot \sqrt{2}} \quad (282)$$

$$\begin{array}{l} \text{from} \\ (6) \\ (281) \end{array} \quad u = f_{y \rightarrow u}(y) = \frac{y - \frac{x_0 \cdot y_0}{y}}{\sqrt{2}} = \frac{y^2 - x_0 \cdot y_0}{y \cdot \sqrt{2}} \quad (283)$$

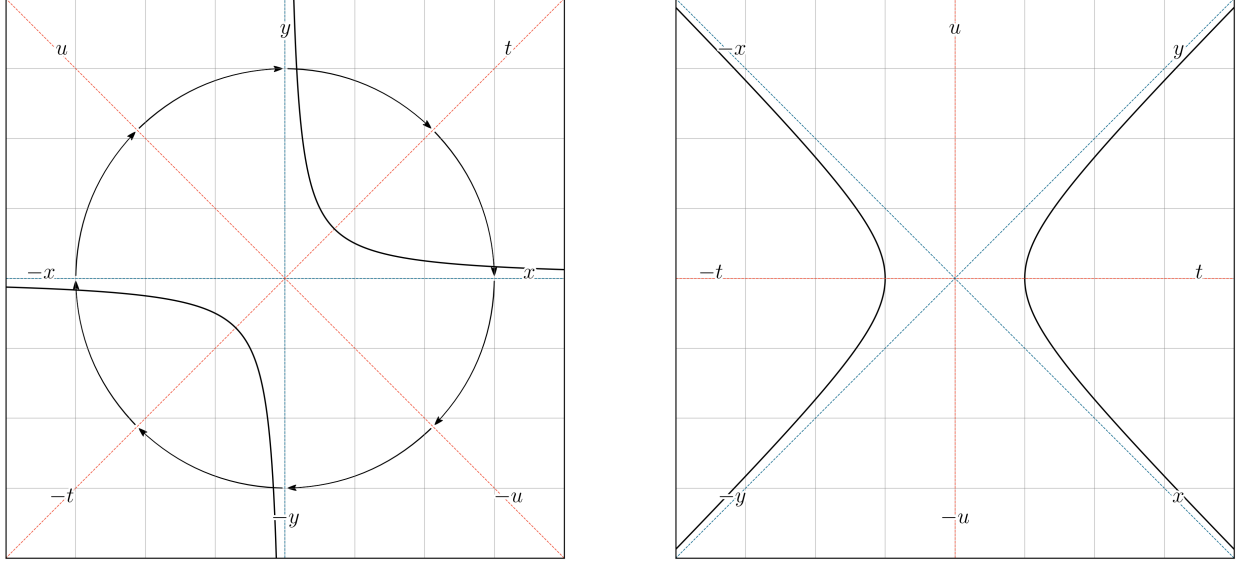


Fig. 50 A general depiction of coordinate system transformation and rotation. This figure visualizes the transformation and rotation of a coordinate system from the standard Cartesian x - and y -axes to a rotated system denoted by t - and u - axes. Arrows indicate the direction of rotation from each of the Cartesian axes (x, y) to the new rotated axes (t, u), mimicking the motion of a steering wheel as it turns to the right. Note that the hyperbola drawn in the left panel opens towards the bottom-left and top-right quadrants, whereas the hyperbola drawn in the right panel opens towards the left and right. The equation of the hyperbola in the left subplot is of the form $x \cdot y = k$, which after the linear transform becomes $t^2 - u^2 = 2 \cdot k$.

We can also map y to t ($f_{y \rightarrow t}$), and x to u ($f_{x \rightarrow u}$) (Equations 282 and 283); we can use both forms to prove the invariant equation of the transformed hyperbola, which opens to the left and right in the t dimension.

$$\begin{array}{l} \text{from} \\ (6) \\ (280) \end{array} \quad t = f_{y \rightarrow t}(y) = \frac{\frac{x_0 \cdot y_0}{y} + y}{\sqrt{2}} = \frac{x_0 \cdot y_0 + y^2}{y \cdot \sqrt{2}} \quad (284)$$

$$\begin{array}{l} \text{from} \\ (8) \\ (281) \end{array} \quad u = f_{x \rightarrow u}(x) = \frac{\frac{x_0 \cdot y_0}{x} - x}{\sqrt{2}} = \frac{x_0 \cdot y_0 - x^2}{x \cdot \sqrt{2}} \quad (285)$$

Then, to obtain the identity of the transformed hyperbola, which has the form $t^2 - u^2 = 2 \cdot k$, we can substitute the reduced-dimensions expressions for t and u from either Equations 282 and 285, or Equations 283 and 284; the pair of expressions used must eliminate the remaining x or y dimension, which yields the transformed invariant equation entirely in its native dimensions t and u (Equations 286 and 287). Alternatively, the $x_0 \cdot y_0$ terms can be substituted for its identity $x \cdot y$ Equation 2, which delivers the same result. Remember, x_0 and y_0 are constants; while the notation references the x and y dimensions, the values themselves are not dependent on them. Therefore Equations 286 and 287 are truly two-dimensional, *not* four-dimensional expressions.

$$\begin{array}{l} \text{from} \\ (282) \\ (285) \end{array} \quad t^2 - u^2 = \frac{(x^2 + x_0 \cdot y_0)^2}{2 \cdot x^2} - \frac{(x_0 \cdot y_0 - x^2)^2}{2 \cdot x^2} = 2 \cdot x_0 \cdot y_0 \quad (286)$$

$$\begin{array}{l} \text{from} \\ (283) \\ (284) \end{array} \quad t^2 - u^2 = \frac{(x_0 \cdot y_0 + y^2)^2}{2 \cdot y^2} - \frac{(y^2 - x_0 \cdot y_0)^2}{2 \cdot y^2} = 2 \cdot x_0 \cdot y_0 \quad (287)$$

Our objective is now to apply this rotation to the key points defining the reference and virtual curves (Figure 51). The elements of the real curve that inform this analysis are implicit; to incorporate the real curve into the following

derivations, simply scale it down in-place (i.e. without moving the point at (x_0, y_0)) to become the reference curve or reverse its horizontal and vertical shifts to become the virtual curve as we have done previously (Equations 160, 162, 164, 165, 167, 169, 229, 230, 232, 233, 234 and 236). The analysis being performed here for either of the reference or virtual curves, individually, generalize to each other, and by extension, also to the real curve. Therefore, as with much of the work demonstrated in this document, performing these steps for both the reference and virtual curves is done for its pedagogical benefit and not necessarily because it is required by the analysis. The analysis can be completed with only one of these.

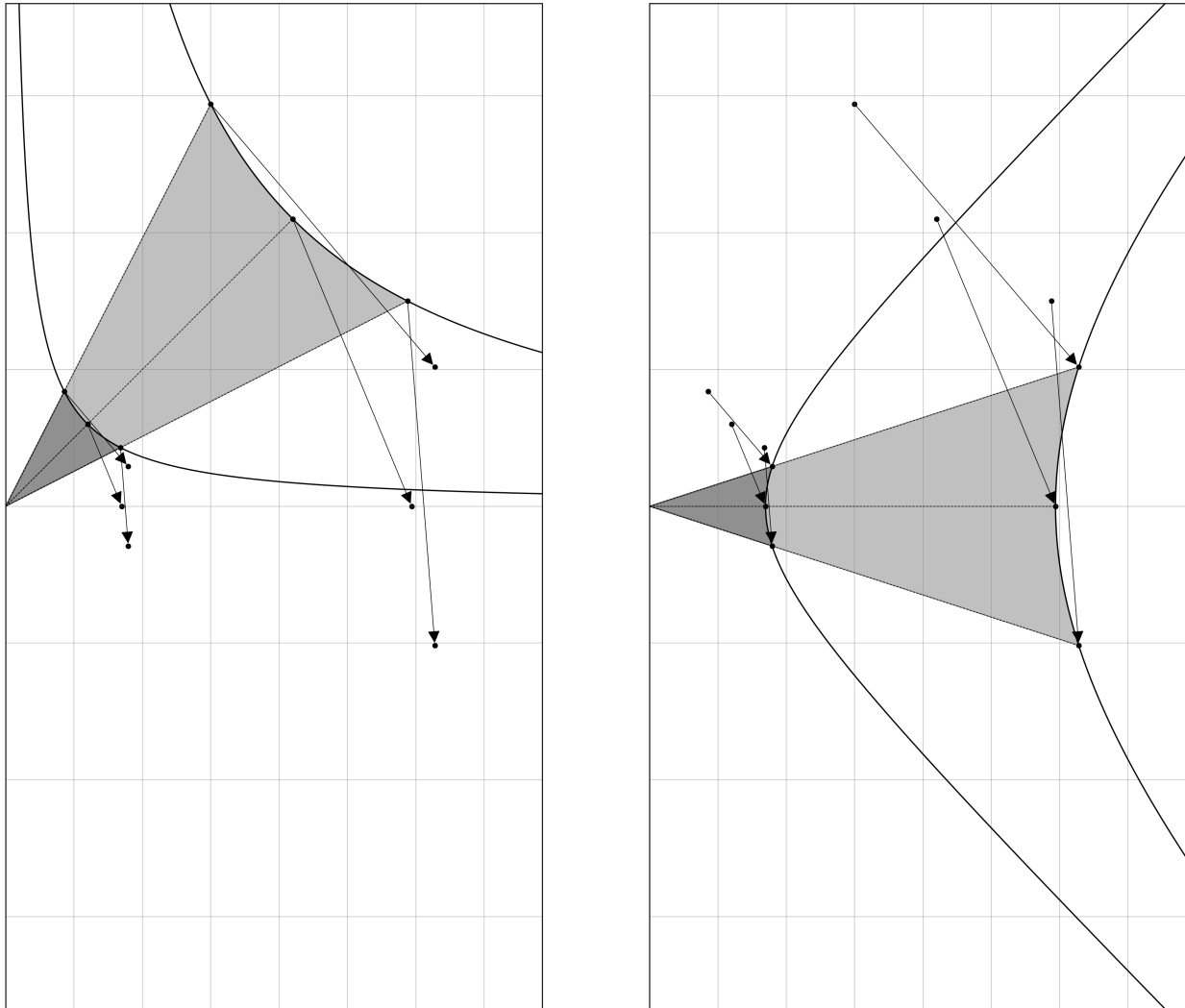


Fig. 51 The key identities associated with the reference and virtual curves are drawn with rays emanating from the origin, which enclose a shaded region. The desired linear transformation (Equation 279) is depicted with arrows beginning from these same points in the Cartesian (x, y) plane, and ending at their implied destinations in the new coordinate system (t, u) . The transformation from the (x, y) to the (t, u) coordinates is represented as an apparent -45° rotation between the left and right panels of the figure.

The redundancy produced by the dimension reduction in Equations 284, 285, 286 and 287 means that the transformation from the Cartesian (x, y) plane to the new (t, u) coordinate system can be performed in at least three different ways. Either both the x and y coordinates can be used as arguments (Equations 280 and 281), or only one of the x or y coordinates can be used as arguments (Equations 282 and 285, and Equations 283 and 284, respectively). This is easily demonstrated. Recall that the point (x_0, y_0) lies on the reference curve (Figure 2). To obtain its transformed t coordinate, the result of passing both x_0 and y_0 as arguments to Equation 280 is identical to passing only x_0 to Equation 282 and passing only y_0 to Equation 284 (Equation 288). Similarly, to obtain its transformed u coordinate, the result of passing both x_0 and y_0 as arguments to Equation 281 is identical to passing only x_0 to Equation 283 and passing only y_0 to Equation 285 (Equation 289).

$$\begin{array}{l} \text{from} \\ (280) \\ (282) \\ (284) \end{array} \quad f_{x,y \rightarrow t}(x_0, y_0) = f_{x \rightarrow t}(x_0) = f_{y \rightarrow t}(y_0) = \frac{x_0 + y_0}{\sqrt{2}} \quad (288)$$

$$\begin{array}{l} \text{from} \\ (281) \\ (283) \\ (285) \end{array} \quad f_{x,y \rightarrow u}(x_0, y_0) = f_{x \rightarrow u}(x_0) = f_{y \rightarrow u}(y_0) = \frac{y_0 - x_0}{\sqrt{2}} \quad (289)$$

The remainder of this part of the exercise will use the two-argument functions, Equations 280 and 281. Just know this is a completely arbitrary decision and it makes no difference whatsoever if you would prefer to use the single-argument alternatives. Substituting the other key identities previously obtained for the reference curve (Equations 65, 66, 67 and 68) into Equations 280 and 281 yields their transformed (u, t) coordinates (Equations 290, 291, 292 and 293).

$$\begin{array}{l} \text{from} \\ (65) \\ (66) \\ (280) \end{array} \quad f_{x,y \rightarrow t}(\min(x), \max(y)) = \frac{\frac{x_0 \cdot (A-1)}{A} + \frac{A \cdot y_0}{A-1}}{\sqrt{2}} = \frac{x_0 \cdot (A-1)^2 + A^2 \cdot y_0}{\sqrt{2} \cdot A \cdot (A-1)} \quad (290)$$

$$\begin{array}{l} \text{from} \\ (65) \\ (66) \\ (281) \end{array} \quad f_{x,y \rightarrow u}(\min(x), \max(y)) = \frac{\frac{A \cdot y_0}{A-1} - \frac{x_0 \cdot (A-1)}{A}}{\sqrt{2}} = \frac{A^2 \cdot y_0 - x_0 \cdot (A-1)^2}{\sqrt{2} \cdot A \cdot (A-1)} \quad (291)$$

$$\begin{array}{l} \text{from} \\ (67) \\ (68) \\ (280) \end{array} \quad f_{x,y \rightarrow t}(\max(x), \min(y)) = \frac{\frac{A \cdot x_0}{A-1} + \frac{y_0 \cdot (A-1)}{A}}{\sqrt{2}} = \frac{A^2 \cdot x_0 + y_0 \cdot (A-1)^2}{\sqrt{2} \cdot A \cdot (A-1)} \quad (292)$$

$$\begin{array}{l} \text{from} \\ (67) \\ (68) \\ (281) \end{array} \quad f_{x,y \rightarrow u}(\max(x), \min(y)) = \frac{\frac{y_0 \cdot (A-1)}{A} - \frac{A \cdot x_0}{A-1}}{\sqrt{2}} = \frac{y_0 \cdot (A-1)^2 - A^2 \cdot x_0}{\sqrt{2} \cdot A \cdot (A-1)} \quad (293)$$

Then, via the same process, substituting the other key identities previously obtained for the virtual curve (Equations 36, 37, 38, 39, 52 and 54) into Equations 280 and 281 yields their transformed (u, t) coordinates (Equations 294, 295, 296, 297, 298 and 299).

$$\begin{array}{l} \text{from} \\ (52) \\ (54) \\ (280) \end{array} \quad f_{x_v, y_v \rightarrow t_v}(A \cdot x_0, A \cdot y_0) = \frac{A \cdot (x_0 + y_0)}{\sqrt{2}} \quad (294)$$

$$\begin{array}{l} \text{from} \\ (52) \\ (54) \\ (281) \end{array} \quad f_{x_v, y_v \rightarrow u_v}(A \cdot x_0, A \cdot y_0) = \frac{A \cdot (y_0 - x_0)}{\sqrt{2}} \quad (295)$$

$$\begin{array}{l} \text{from} \\ (36) \\ (37) \\ (280) \end{array} \quad f_{x_v, y_v \rightarrow t_v}(\min(x_v), \max(y_v)) = \frac{\frac{x_0 \cdot (A-1)}{A} + \frac{A^2 \cdot y_0}{A-1}}{\sqrt{2}} = \frac{x_0 \cdot (A-1)^2 + A^2 \cdot y_0}{\sqrt{2} \cdot (A-1)} \quad (296)$$

$$\begin{array}{l} \text{from} \\ (36) \\ (37) \\ (281) \end{array} \quad f_{x_v, y_v \rightarrow u_v}(\min(x_v), \max(y_v)) = \frac{\frac{A^2 \cdot y_0}{A-1} - \frac{x_0 \cdot (A-1)}{A}}{\sqrt{2}} = \frac{A^2 \cdot y_0 - x_0 \cdot (A-1)^2}{\sqrt{2} \cdot (A-1)} \quad (297)$$

$$\begin{array}{l} \text{from} \\ (38) \\ (39) \\ (280) \end{array} \quad f_{x_v, y_v \rightarrow t_v}(\max(x_v), \min(y_v)) = \frac{\frac{A^2 \cdot x_0}{A-1} + y_0 \cdot (A-1)}{\sqrt{2}} = \frac{A^2 \cdot x_0 + y_0 \cdot (A-1)^2}{\sqrt{2} \cdot (A-1)} \quad (298)$$

$$\begin{array}{l} \text{from} \\ (38) \\ (39) \\ (281) \end{array} \quad f_{x_v, y_v \rightarrow u_v}(\max(x_v), \min(y_v)) = \frac{y_0 \cdot (A-1) - \frac{A^2 \cdot x_0}{A-1}}{\sqrt{2}} = \frac{y_0 \cdot (A-1)^2 - A^2 \cdot x_0}{\sqrt{2} \cdot (A-1)} \quad (299)$$

Turning our attention back to the plot, the algebraic identities derived in Equations 290, 291, 292, 293, 294, 295, 296, 297, 298 and 299 have been appended as point annotations in Figure 52.

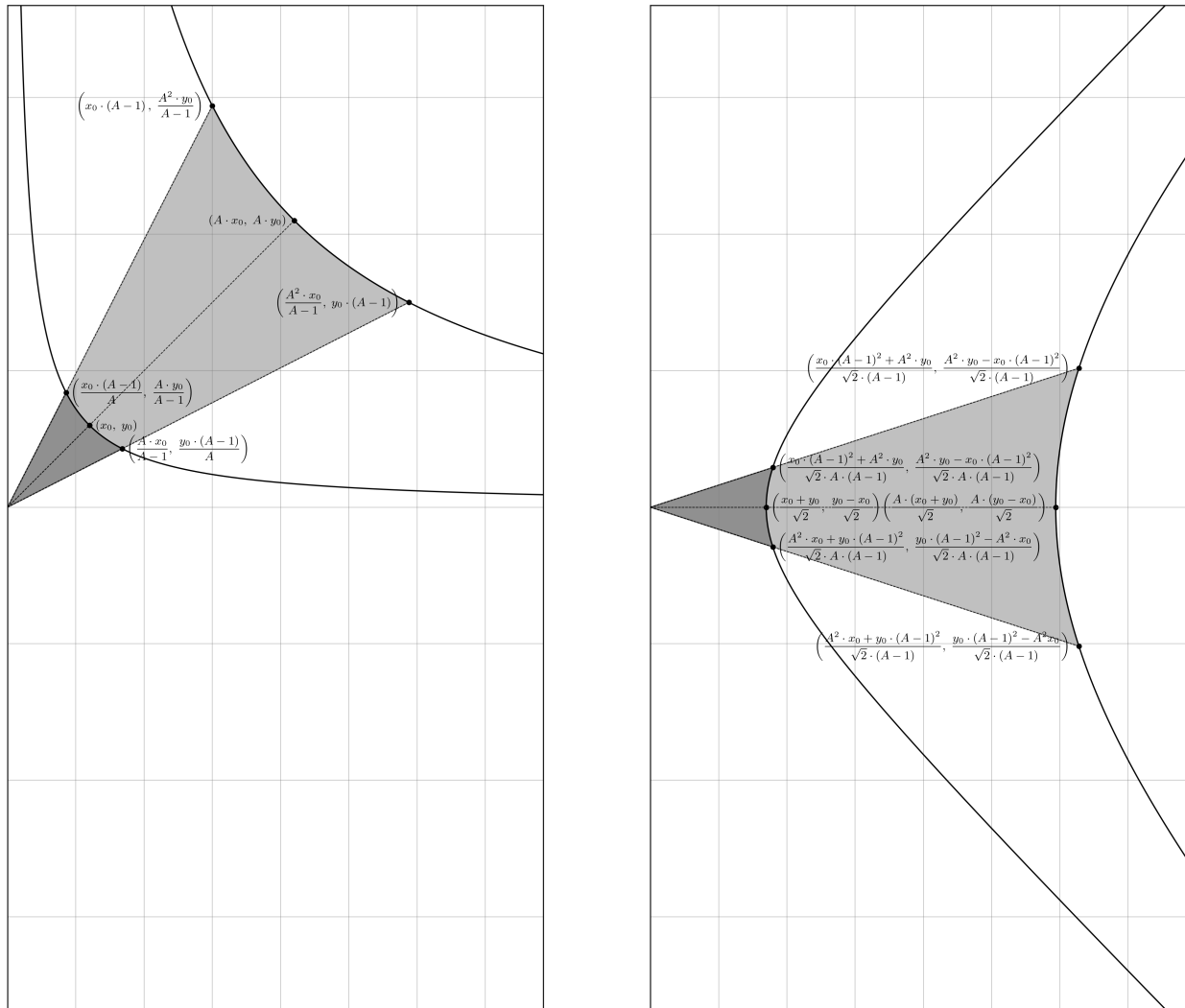


Fig. 52 The reference and virtual curves are depicted before and after the linear -45° transformation has been applied. The capstone identities from both curves appear as annotations in (x, y) and (u, t) format in the left and right panels, respectively (Equations 288, 289, 290, 291, 292, 293, 294, 295, 296, 297, 298 and 299).

Unsurprisingly, even in the transformed coordinate system, the difference between corresponding points on the virtual and reference curves is a factor of A (because of course it is!). For completeness, the invariant for the transformed virtual curve is proved by substitution of the reference curve $x \cdot y = x_0 \cdot y_0$ (Equation 2) for the virtual curve $x \cdot y = A^2 \cdot x_0 \cdot y_0$

(Equation 26) while repeating the process detailed in Equations 282, 283, 284, 285, 286 and 287, which yields Equation 300.

$$\begin{array}{l} \text{from} \\ (282) \\ (285) \end{array} \quad t_v^2 - u_v^2 = 2 \cdot A^2 \cdot x_0 \cdot y_0 \quad (300)$$

Following the rotation, the hyperbola must then be rescaled (i.e. normalized) into unit format such that its vertices lie at $t \pm 1$. To capture this re-scaling in situ, let the re-scaled t and u coordinates be \hat{t} and \hat{u} , respectively. Then, the goal is to define \hat{t} and \hat{u} in terms of x and y , and x_v , and y_v , respectively, such that $\hat{t}^2 - \hat{u}^2 = 1$ in both cases. This is easily achieved by taking the quotient of the LHS and RHS of Equation 286 or Equation 287 for x and y , and the quotient of the LHS and RHS of Equation 286 for x_v and y_v (Equation 301). Distributing the division and leveraging the properties of exponents and radicals yields Equations 302 and 303. In both cases, the LHS and RHS of the equality are expressed as a difference of squares and the identities of \hat{t} and \hat{u} can be obtained by asserting a literal 1:1 correspondence between the minuends and subtrahends on either side. In our context this is okay – but note that the abstraction $a - b = c - d$, therefore $a = c$ and $b = d$ is not always true. The equation for the hyperbola in its rescaled form directly leads to the new definitions of \hat{t} and \hat{u} , and because we are applying the transformation uniformly to both sides of the equation, the equality and the relationship between the variables is maintained in this case (Equations 304 and 305).

$$\begin{array}{l} \text{from} \\ (286) \\ (287) \\ (300) \end{array} \quad \hat{t}^2 - \hat{u}^2 = 1 = \frac{t^2 - u^2}{2 \cdot x_0 \cdot y_0} = \frac{t_v^2 - u_v^2}{2 \cdot A^2 \cdot x_0 \cdot y_0} \quad (301)$$

$$\begin{array}{l} \text{from} \\ (286) \\ (287) \\ (301) \end{array} \quad \hat{t}^2 - \hat{u}^2 = \left(\frac{t}{\sqrt{2} \cdot \sqrt{x_0} \cdot \sqrt{y_0}} \right)^2 - \left(\frac{u}{\sqrt{2} \cdot \sqrt{x_0} \cdot \sqrt{y_0}} \right)^2 \quad (302)$$

$$\begin{array}{l} \text{from} \\ (300) \\ (301) \end{array} \quad \hat{t}^2 - \hat{u}^2 = \left(\frac{t_v}{\sqrt{2} \cdot A \cdot \sqrt{x_0} \cdot \sqrt{y_0}} \right)^2 - \left(\frac{u_v}{\sqrt{2} \cdot A \cdot \sqrt{x_0} \cdot \sqrt{y_0}} \right)^2 \quad (303)$$

$$\begin{array}{l} \text{from} \\ (302) \\ (303) \end{array} \quad \hat{t} = \frac{t}{\sqrt{2} \cdot \sqrt{x_0} \cdot \sqrt{y_0}} = \frac{t_v}{\sqrt{2} \cdot A \cdot \sqrt{x_0} \cdot \sqrt{y_0}} \quad (304)$$

$$\begin{array}{l} \text{from} \\ (302) \\ (303) \end{array} \quad \hat{u} = \frac{u}{\sqrt{2} \cdot \sqrt{x_0} \cdot \sqrt{y_0}} = \frac{u_v}{\sqrt{2} \cdot A \cdot \sqrt{x_0} \cdot \sqrt{y_0}} \quad (305)$$

By establishing this correspondence, we effectively align the structure of the hyperbola's equation in its original and transformed states. This allows for the direct inference of \hat{t} and \hat{u} from x and y , and x_v , and y_v , respectively, adhering to the normalization criterion $\hat{t}^2 - \hat{u}^2 = 1$. From here, the new single-argument mapping functions, $f_{x \rightarrow \hat{t}}$, $f_{y \rightarrow \hat{u}}$, $f_{y \rightarrow \hat{t}}$, $f_{x \rightarrow \hat{u}}$, $f_{x_v \rightarrow \hat{t}}$, $f_{y_v \rightarrow \hat{u}}$, $f_{y_v \rightarrow \hat{t}}$, and $f_{x_v \rightarrow \hat{u}}$ can be derived from the previous mapping functions without any trouble (Equations 306, 307, 308, 309, 310, 311, 312 and 313). The two-argument expressions, $f_{x,y \rightarrow \hat{t}}$, $f_{x,y \rightarrow \hat{u}}$, $f_{x_v,y_v \rightarrow \hat{t}}$, and $f_{x_v,y_v \rightarrow \hat{u}}$ can be recomposed from their single-argument counterparts by substitution of $x_0 \cdot y_0$ for $x \cdot y$ in the reference curve transformation, and substitution of $A^2 \cdot x_0 \cdot y_0$ for $x \cdot y$ in the virtual curve transformation, via Equations 2 and 26 (Equations 314 and 315). Rather pleasingly, the two-argument reference- and virtual-to-unit hyperbola mapping functions are identical. You won't have to think about it for too long to convince yourself that this is an obvious result.

$$\begin{array}{l} \text{from} \\ (282) \\ (304) \end{array} \quad \hat{t} = f_{x \rightarrow \hat{t}}(x) = \frac{f_{x \rightarrow t}}{\sqrt{2} \cdot \sqrt{x_0} \cdot \sqrt{y_0}} = \frac{x^2 + x_0 \cdot y_0}{2 \cdot x \cdot \sqrt{x_0} \cdot \sqrt{y_0}} \quad (306)$$

$$\begin{array}{l} \text{from} \\ (283) \\ (305) \end{array} \quad \hat{u} = f_{y \rightarrow \hat{u}}(y) = \frac{f_{y \rightarrow u}}{\sqrt{2} \cdot \sqrt{x_0} \cdot \sqrt{y_0}} = \frac{y^2 - x_0 \cdot y_0}{2 \cdot y \cdot \sqrt{x_0} \cdot \sqrt{y_0}} \quad (307)$$

$$\begin{array}{l} \text{from} \\ (284) \\ (304) \end{array} \quad \hat{t} = f_{y \rightarrow \hat{t}}(y) = \frac{f_{y \rightarrow t}}{\sqrt{2} \cdot \sqrt{x_0} \cdot \sqrt{y_0}} = \frac{x_0 \cdot y_0 + y^2}{2 \cdot y \cdot \sqrt{x_0} \cdot \sqrt{y_0}} \quad (308)$$

$$\begin{array}{l} \text{from} \\ (285) \\ (305) \end{array} \quad \hat{u} = f_{x \rightarrow \hat{u}}(x) = \frac{f_{x \rightarrow u}}{\sqrt{2} \cdot \sqrt{x_0} \cdot \sqrt{y_0}} = \frac{x_0 \cdot y_0 - x^2}{2 \cdot x \cdot \sqrt{x_0} \cdot \sqrt{y_0}} \quad (309)$$

$$\begin{array}{l} \text{from} \\ (284) \\ (302) \end{array} \quad \hat{t} = f_{x_v \rightarrow \hat{t}}(x_v) = \frac{f_{x_v \rightarrow t_v}}{\sqrt{2} \cdot A \cdot \sqrt{x_0} \cdot \sqrt{y_0}} = \frac{x_v^2 + A^2 \cdot x_0 \cdot y_0}{2 \cdot x_v \cdot A \cdot \sqrt{x_0} \cdot \sqrt{y_0}} \quad (310)$$

$$\begin{array}{l} \text{from} \\ (285) \\ (302) \end{array} \quad \hat{u} = f_{y_v \rightarrow \hat{u}}(y_v) = \frac{f_{y_v \rightarrow u_v}}{\sqrt{2} \cdot A \cdot \sqrt{x_0} \cdot \sqrt{y_0}} = \frac{y_v^2 - A^2 \cdot x_0 \cdot y_0}{2 \cdot y_v \cdot A \cdot \sqrt{x_0} \cdot \sqrt{y_0}} \quad (311)$$

$$\begin{array}{l} \text{from} \\ (284) \\ (302) \end{array} \quad \hat{t} = f_{y_v \rightarrow \hat{t}}(y_v) = \frac{f_{y_v \rightarrow t_v}}{\sqrt{2} \cdot A \cdot \sqrt{x_0} \cdot \sqrt{y_0}} = \frac{A^2 \cdot x_0 \cdot y_0 - y_v^2}{2 \cdot y_v \cdot A \cdot \sqrt{x_0} \cdot \sqrt{y_0}} \quad (312)$$

$$\begin{array}{l} \text{from} \\ (285) \\ (302) \end{array} \quad \hat{u} = f_{x_v \rightarrow \hat{u}}(x_v) = \frac{f_{x_v \rightarrow u_v}}{\sqrt{2} \cdot A \cdot \sqrt{x_0} \cdot \sqrt{y_0}} = \frac{A^2 \cdot x_0 \cdot y_0 - x_v^2}{2 \cdot x_v \cdot A \cdot \sqrt{x_0} \cdot \sqrt{y_0}} \quad (313)$$

$$\begin{array}{l} \text{from} \\ (2) \\ (26) \\ (306) \\ (308) \\ (310) \\ (312) \end{array} \quad \hat{t} = f_{x,y \rightarrow \hat{t}}(x, y) = f_{x_v, y_v \rightarrow \hat{t}}(x_v, y_v) = \frac{x + y}{2 \cdot \sqrt{x} \cdot \sqrt{y}} = \frac{x_v + y_v}{2 \cdot \sqrt{x_v} \cdot \sqrt{y_v}} \quad (314)$$

$$\begin{array}{l} \text{from} \\ (2) \\ (26) \\ (307) \\ (309) \\ (311) \\ (313) \end{array} \quad \hat{u} = f_{x,y \rightarrow \hat{u}}(x, y) = f_{x_v, y_v \rightarrow \hat{u}}(x, y) = \frac{y - x}{2 \cdot \sqrt{x} \cdot \sqrt{y}} = \frac{y_v - x_v}{2 \cdot \sqrt{x_v} \cdot \sqrt{y_v}} \quad (315)$$

To conclude this section, we will derive the algebraic identities for the key points on the unit hyperbola by passing the corresponding points on the reference and virtual curves to the $f_{x,y \rightarrow \hat{t}}$ and $f_{x,y \rightarrow \hat{u}}$ mapping functions, Equations 314 and 315. First, the mapping is performed for the reference curve (Equations 316, 317, 318, 319, 320 and 321).

$$\begin{array}{l} \text{from} \\ (314) \end{array} \quad \hat{t} = f_{x,y \rightarrow \hat{t}}(x_0, y_0) = \frac{x_0 + y_0}{2 \cdot \sqrt{x_0} \cdot \sqrt{y_0}} \quad (316)$$

$$\begin{array}{l} \text{from} \\ (315) \end{array} \quad \hat{u} = f_{x,y \rightarrow \hat{u}}(x_0, y_0) = \frac{y_0 - x_0}{2 \cdot \sqrt{x_0} \cdot \sqrt{y_0}} \quad (317)$$

$$\begin{array}{l} \text{from} \\ (65) \\ (66) \\ (314) \end{array} \quad \hat{t} = f_{x,y \rightarrow \hat{t}}(\min(x), \max(y)) = \frac{\frac{x_0 \cdot (A-1)}{A} + \frac{A \cdot y_0}{A-1}}{2 \cdot \sqrt{\frac{x_0 \cdot (A-1)}{A}} \cdot \sqrt{\frac{A \cdot y_0}{A-1}}} = \frac{x_0 \cdot (A-1)^2 + A^2 \cdot y_0}{2 \cdot A \cdot \sqrt{x_0} \cdot \sqrt{y_0} \cdot (A-1)} \quad (318)$$

$$\begin{array}{l} \text{from} \\ (65) \\ (66) \\ (315) \end{array} \quad \hat{u} = f_{x,y \rightarrow \hat{u}}(\min(x), \max(y)) = \frac{\frac{A \cdot y_0}{A-1} - \frac{x_0 \cdot (A-1)}{A}}{2 \cdot \sqrt{\frac{x_0 \cdot (A-1)}{A}} \cdot \sqrt{\frac{A \cdot y_0}{A-1}}} = \frac{A^2 \cdot y_0 - x_0 \cdot (A-1)^2}{2 \cdot A \cdot \sqrt{x_0} \cdot \sqrt{y_0} \cdot (A-1)} \quad (319)$$

$$\begin{array}{l} \text{from} \\ (67) \\ (68) \\ (314) \end{array} \quad \hat{t} = f_{x,y \rightarrow \hat{t}}(\max(x), \min(y)) = \frac{\frac{A \cdot x_0}{A-1} + \frac{y_0 \cdot (A-1)}{A}}{2 \cdot \sqrt{\frac{A \cdot x_0}{A-1}} \cdot \sqrt{\frac{y_0 \cdot (A-1)}{A}}} = \frac{A^2 \cdot x_0 + y_0 \cdot (A-1)^2}{2 \cdot A \cdot \sqrt{x_0} \cdot \sqrt{y_0} \cdot (A-1)} \quad (320)$$

$$\begin{array}{l} \text{from} \\ (67) \\ (68) \\ (315) \end{array} \quad \hat{u} = f_{x,y \rightarrow \hat{u}}(\max(x), \min(y)) = \frac{\frac{y_0 \cdot (A-1)}{A} - \frac{A \cdot x_0}{A-1}}{2 \cdot \sqrt{\frac{A \cdot x_0}{A-1}} \cdot \sqrt{\frac{y_0 \cdot (A-1)}{A}}} = \frac{y_0 \cdot (A-1)^2 - A^2 \cdot x_0}{2 \cdot A \cdot \sqrt{x_0} \cdot \sqrt{y_0} \cdot (A-1)} \quad (321)$$

The expectation is that both the reference and virtual curves should map to the same coordinates on the unit hyperbola, since the difference in the relative scaling has been appropriately and separately accounted for in the derivations presented in this section. The fact that the final, two-argument mapping functions for both the reference and virtual coordinates are identical is irrelevant; the output for passing key points on the reference and virtual curves should be the same. Indeed, this is now shown to be true (Equations 322, 323, 324, 325, 326 and 327).

$$\begin{array}{l} \text{from} \\ (314) \end{array} \quad \hat{t} = f_{x_v, y_v \rightarrow \hat{t}}(A \cdot x_0, A \cdot y_0) = \frac{A \cdot x_0 + A \cdot y_0}{2 \cdot \sqrt{A \cdot x_0} \cdot \sqrt{A \cdot y_0}} = \frac{x_0 + y_0}{2 \cdot \sqrt{x_0} \cdot \sqrt{y_0}} \quad (322)$$

$$\begin{array}{l} \text{from} \\ (315) \end{array} \quad \hat{u} = f_{x_v, y_v \rightarrow \hat{u}}(A \cdot x_0, A \cdot y_0) = \frac{A \cdot y_0 - A \cdot x_0}{2 \cdot \sqrt{A \cdot x_0} \cdot \sqrt{A \cdot y_0}} = \frac{y_0 - x_0}{2 \cdot \sqrt{x_0} \cdot \sqrt{y_0}} \quad (323)$$

$$\begin{array}{l} \text{from} \\ (36) \\ (37) \\ (314) \end{array} \quad \hat{t} = f_{x_v, y_v \rightarrow \hat{t}}(\min(x_v), \max(y_v)) = \frac{x_0 \cdot (A-1) + \frac{A^2 \cdot y_0}{A-1}}{2 \cdot \sqrt{x_0 \cdot (A-1)} \cdot \sqrt{\frac{A^2 \cdot y_0}{A-1}}} = \frac{x_0 \cdot (A-1)^2 + A^2 \cdot y_0}{2 \cdot A \cdot \sqrt{x_0} \cdot \sqrt{y_0} \cdot (A-1)} \quad (324)$$

$$\begin{array}{l} \text{from} \\ (36) \\ (37) \\ (315) \end{array} \quad \hat{u} = f_{x_v, y_v \rightarrow \hat{u}}(\min(x_v), \max(y_v)) = \frac{\frac{A^2 \cdot y_0}{A-1} - x_0 \cdot (A-1)}{2 \cdot \sqrt{x_0 \cdot (A-1)} \cdot \sqrt{\frac{A^2 \cdot y_0}{A-1}}} = \frac{A^2 \cdot y_0 - x_0 \cdot (A-1)^2}{2 \cdot A \cdot \sqrt{x_0} \cdot \sqrt{y_0} \cdot (A-1)} \quad (325)$$

$$\begin{array}{l} \text{from} \\ (38) \\ (39) \\ (314) \end{array} \quad \hat{t} = f_{x_v, y_v \rightarrow \hat{t}}(\max(x_v), \min(y_v)) = \frac{\frac{A^2 \cdot x_0}{A-1} + y_0 \cdot (A-1)}{2 \cdot \sqrt{\frac{A^2 \cdot x_0}{A-1}} \cdot \sqrt{y_0 \cdot (A-1)}} = \frac{A^2 \cdot x_0 + y_0 \cdot (A-1)^2}{2 \cdot A \cdot \sqrt{x_0} \cdot \sqrt{y_0} \cdot (A-1)} \quad (326)$$

$$\begin{array}{l} \text{from} \\ (38) \\ (39) \\ (315) \end{array} \quad \hat{u} = f_{x_v, y_v \rightarrow \hat{u}}(\max(x_v), \min(y_v)) = \frac{y_0 \cdot (A-1) - \frac{A^2 \cdot x_0}{A-1}}{2 \cdot \sqrt{\frac{A^2 \cdot x_0}{A-1}} \cdot \sqrt{y_0 \cdot (A-1)}} = \frac{y_0 \cdot (A-1)^2 - A^2 \cdot x_0}{2 \cdot A \cdot \sqrt{x_0} \cdot \sqrt{y_0} \cdot (A-1)} \quad (327)$$

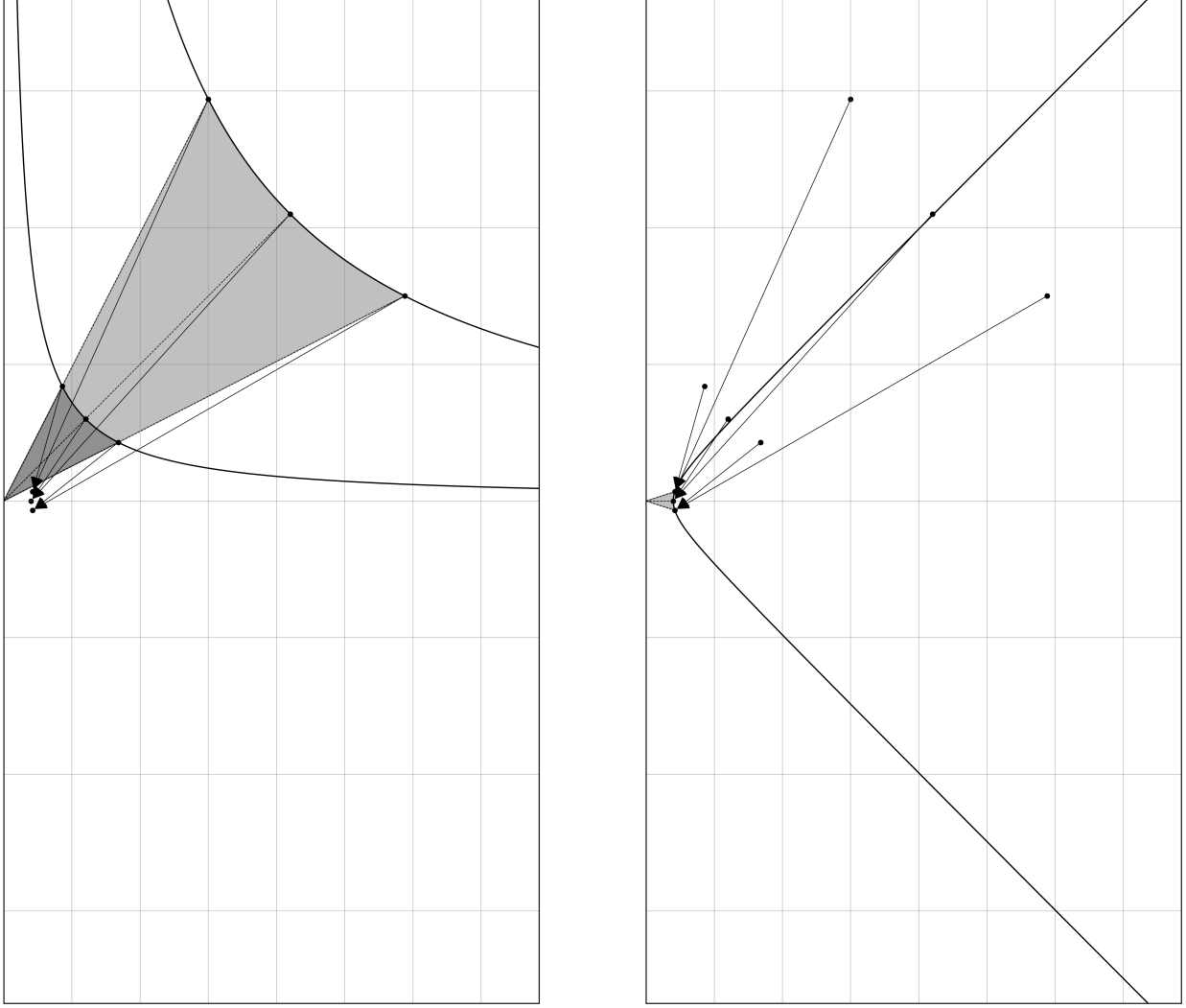


Fig. 53 The new linear transformation, which incorporates both a -45° rotation and normalization is depicted with arrows beginning from the key points on both the reference and virtual curves in the Cartesian (x, y) plane, and ending at their implied destinations in the new coordinate system (\hat{t}, \hat{u}) . Both the reference and virtual curves appear in the left panel, which after the -45° rotation and normalization converge on the same points, the unit hyperbola, which appears in the right panel.

Therefore, we now have the functions which both rotate and normalize either of the reference or virtual curves, and they are the same functions in both cases. After rotating and re-scaling, both the reference and virtual curves are consolidated into each other; the overall process is summarized in Figure 53.

The expressions obtained that describe the transformed and normalized curve, $\hat{t}^2 - \hat{u}^2 = 1$ via Equations 316, 317, 318, 319, 320, 321, 322, 323, 324, 325, 326 and 327, are a little cumbersome. The process for refactoring all of these is the same. First, remove a common factor of $1/2$ before distributing the division, which produces a sum (for \hat{t}) or difference (for \hat{u}) of two quotients, where these quotient identities have previously been established as the square roots of the price boundaries, the square root of the geometric mean of the price boundaries, or the reciprocals of the same (Equations 43, 45 and 47). Substitution allows for all three parameters, x_0 , y_0 , and A to be replaced for single terms, either P_0 , P_{high} or P_{low} , depending on the context (Equations 328, 329, 330, 331, 332 and 333) (Figure 54).

from
(45)
(322)

$$\hat{t}_0 = \frac{1}{2} \cdot \left(\frac{\sqrt{y_0}}{\sqrt{x_0}} + \frac{\sqrt{x_0}}{\sqrt{y_0}} \right) = \frac{1}{2} \cdot \left(\sqrt{P_0} + \frac{1}{\sqrt{P_0}} \right) = \frac{P_0 + 1}{2 \cdot \sqrt{P_0}} \quad (328)$$

$$\begin{array}{l} \text{from} \\ (45) \\ (323) \end{array} \quad \hat{u}_0 = \frac{1}{2} \cdot \left(\frac{\sqrt{y_0}}{\sqrt{x_0}} - \frac{\sqrt{x_0}}{\sqrt{y_0}} \right) = \frac{1}{2} \cdot \left(\sqrt{P_0} - \frac{1}{\sqrt{P_0}} \right) = \frac{P_0 - 1}{2 \cdot \sqrt{P_0}} \quad (329)$$

$$\begin{array}{l} \text{from} \\ (43) \\ (324) \end{array} \quad \min(\hat{t}) = \frac{1}{2} \cdot \left(\frac{A}{A-1} \cdot \frac{\sqrt{y_0}}{\sqrt{x_0}} + \frac{A-1}{A} \cdot \frac{\sqrt{x_0}}{\sqrt{y_0}} \right) = \frac{1}{2} \cdot \left(\sqrt{P_{\text{high}}} + \frac{1}{\sqrt{P_{\text{high}}}} \right) = \frac{P_{\text{high}} + 1}{2 \cdot \sqrt{P_{\text{high}}}} \quad (330)$$

$$\begin{array}{l} \text{from} \\ (43) \\ (325) \end{array} \quad \max(\hat{u}) = \frac{1}{2} \cdot \left(\frac{A}{A-1} \cdot \frac{\sqrt{y_0}}{\sqrt{x_0}} - \frac{A-1}{A} \cdot \frac{\sqrt{x_0}}{\sqrt{y_0}} \right) = \frac{1}{2} \cdot \left(\sqrt{P_{\text{high}}} - \frac{1}{\sqrt{P_{\text{high}}}} \right) = \frac{P_{\text{high}} - 1}{2 \cdot \sqrt{P_{\text{high}}}} \quad (331)$$

$$\begin{array}{l} \text{from} \\ (53) \\ (326) \end{array} \quad \max(\hat{t}) = \frac{1}{2} \cdot \left(\frac{A-1}{A} \cdot \frac{\sqrt{y_0}}{\sqrt{x_0}} + \frac{A}{A-1} \cdot \frac{\sqrt{x_0}}{\sqrt{y_0}} \right) = \frac{1}{2} \cdot \left(\sqrt{P_{\text{low}}} + \frac{1}{\sqrt{P_{\text{low}}}} \right) = \frac{P_{\text{low}} + 1}{2 \cdot \sqrt{P_{\text{low}}}} \quad (332)$$

$$\begin{array}{l} \text{from} \\ (47) \\ (327) \end{array} \quad \min(\hat{u}) = \frac{1}{2} \cdot \left(\frac{A-1}{A} \cdot \frac{\sqrt{y_0}}{\sqrt{x_0}} - \frac{A}{A-1} \cdot \frac{\sqrt{x_0}}{\sqrt{y_0}} \right) = \frac{1}{2} \cdot \left(\sqrt{P_{\text{low}}} - \frac{1}{\sqrt{P_{\text{low}}}} \right) = \frac{P_{\text{low}} - 1}{2 \cdot \sqrt{P_{\text{low}}}} \quad (333)$$

The notation above deserves a brief note. The terms \hat{t}_0 , \hat{u}_0 , $\min(\hat{t})$, $\max(\hat{t})$, $\min(\hat{u})$, and $\max(\hat{u})$ inherit the syntax of their Cartesian counterparts, x_0 , y_0 , $\min(x)$, $\max(x)$, $\min(y)$, and $\max(y)$. The choice of notation here was made to preserve a sense of provenance. For \hat{u}_0 , $\min(\hat{u})$, and $\max(\hat{u})$, the implicit meaning of the notation is guaranteed to be preserved after the transformation and scaling; $\min(\hat{u}) \leq \hat{u}_0 \leq \max(\hat{u})$, always and with no exceptions. However, the same cannot be said for \hat{t}_0 , $\min(\hat{t})$, and $\max(\hat{t})$. Due to the -45° rotation about the origin, there is no general inequality that applies for the relative sizes of \hat{t}_0 , $\min(\hat{t})$, and $\max(\hat{t})$, and all permutations are possible. This is both briefly annoying, but also ultimately irrelevant, as the remainder of the exercise will focus exclusively on \hat{u} . The justification for this is coming in due course.

The $\max(\hat{u})$ and $\min(\hat{u})$ coordinates represent points along the vertical axis of the unit hyperbola, and the area enclosed by the curve and the rays drawn from these points through the origin defines one half the hyperbolic angle, denoted here as ϕ . This is not the familiar angle from circle trigonometry; it is something else (*vide infra*).

5.3 The Trigonometric Description of Liquidity Concentration

In both Euclidean and hyperbolic geometry, angles serve as fundamental measures of separation between intersecting lines. For the unit circle in Euclidean geometry, the angle θ is commonly understood to represent a rotation (indeed, we have already used this intuition in the linear transformation of the curves). However, θ is equally well described as representing an area. Specifically, θ corresponds to the area of the sector enclosed by the unit circle itself and two rays that originate from the circle's centre and intersect its perimeter.

Consider the unit circle, $x^2 + y^2 = 1$. The angle, θ , measured in radians, directly corresponds to the area of the sector formed by the radius of the circle and two rays extending from the origin to two different points on the circle's boundary. This area is equal to one half the angle, $\theta/2$. This relationship arises because the full circle, having an area of π (the area of a circle is $2\pi \cdot r^2$, and $r = 1$ for the unit circle) is spread across 2π radians. Thus, the area covered by any angle θ is proportionally $\theta / (2\pi)$ times the total area of the circle, which simplifies to half the angle, $\theta/2$, for a unit circle.

This is the intuition you should have when considering hyperbolic angles – not as a rotation, but as an area. Specifically, half the hyperbolic angle, $\phi/2$, is precisely the area enclosed by two rays emanating from the origin and intersecting the unit hyperbola, just as half the circular angle, $\theta/2$, is precisely the area enclosed by two rays emanating from the origin and intersecting the unit circle. Circle and hyperbola trigonometry also share some common ground. The most important for our purpose is that the coordinates for a point on both curves can be expressed with respect to the trigonometric functions, sine and cosine (\sin and \cos , respectively) for a circle, and their hyperbola counterparts, the hyperbolic sine and hyperbolic cosine (\sinh and \cosh , respectively) (Figure 55).

The angle that we are interested to determine in the context of concentrated liquidity is the one that measures the separation between P_{high} and P_{low} ; that is, the size of the sector of the hyperbola wherein exchange can occur between tokens. We have the algebraic identities for these points in the (t, u) plane; to measure ϕ , we turn to the inverse

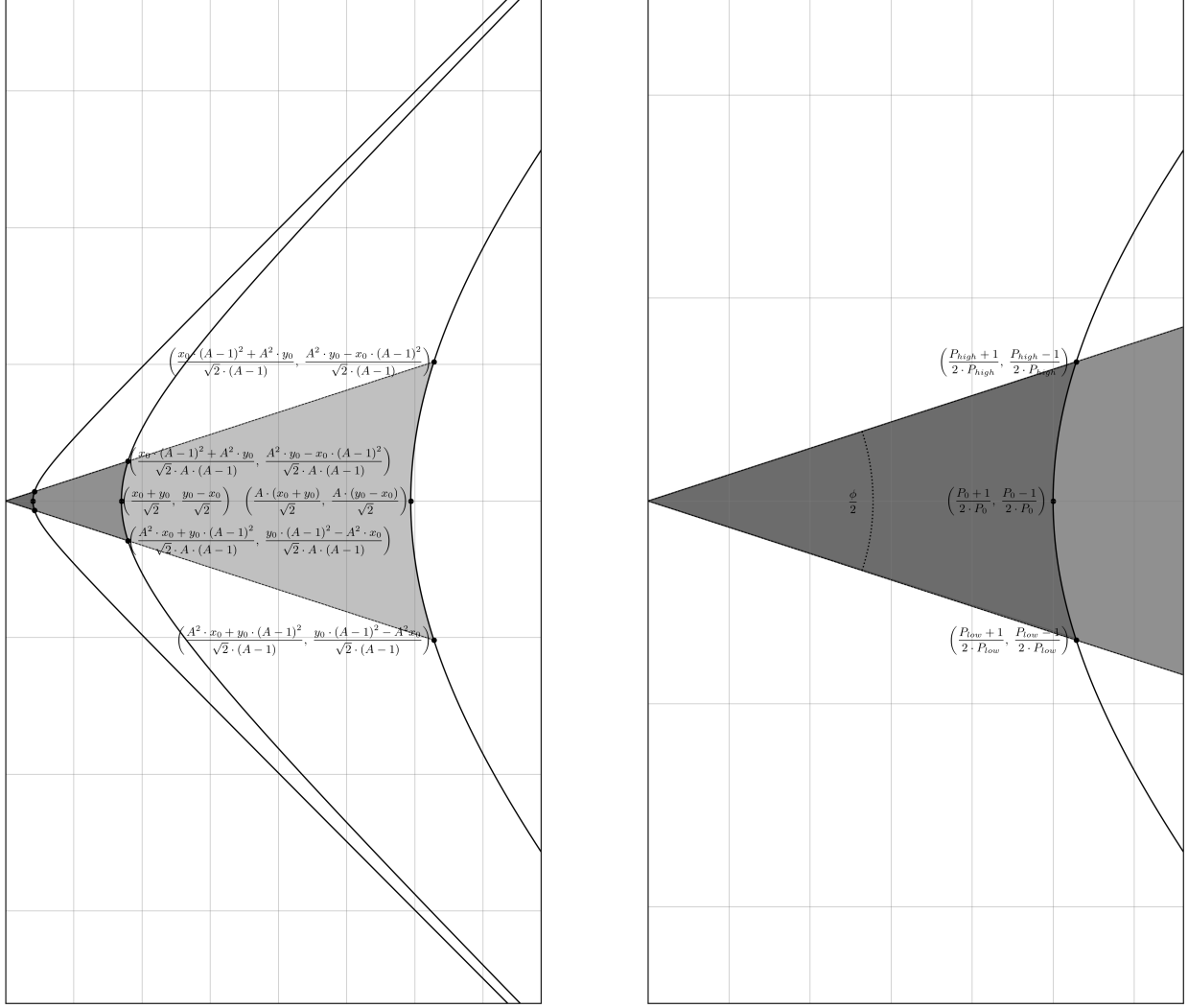


Fig. 54 The transformed reference and virtual curves, $t^2 - u^2 = 2 \cdot x_0 \cdot y_0$ and $t_v^2 - u_v^2 = 2 \cdot A^2 \cdot x_0 \cdot y_0$ are depicted alongside their normalized counterpart, $\hat{t}^2 - \hat{u}^2 = 1$. The point annotations correspond to the capstone identities for all three curves, and appear in (u, t) format in both panels. The scale of the first panel is sufficient to include all three curves and their key points, whereas the second panel is zoomed-in such that the detail around the unit curve can be inspected. The area of the shaded region enclosed by the outer-most rays and the unit hyperbola in the second panel is equal to half its hyperbolic angle, $\phi/2$, annotated accordingly and depicted with a circular arc between its enclosing rays (Equations 328, 329, 330, 331, 332, 333).

hyperbolic sine function, arsinh (or \sinh^{-1}), which takes the vertical displacement from the origin, \hat{u} as an argument, and returns the value ϕ (Equation 334).

$$\text{arsinh}(\hat{u}) = \sinh^{-1}(\hat{u}) = \ln\left(\hat{u} + \sqrt{\hat{u}^2 + 1}\right) \quad (334)$$

While Equation 334 is the form you are likely to have shown to you as *The Arsinh Function*, it is also an incomplete description.

The output for any value of \hat{u} passed to Equation 334 returns a value for ϕ with an implicit reference to $\hat{u} = 0$. It might be helpful to think of the above form of the arsinh (or \sinh^{-1}) function as being the definite integral evaluated from 0 to some upper bound, \hat{u} , rather than evaluated specifically *at* \hat{u} . Fortunately, or unfortunately, we need to explore this a little bit before we can progress any further.

The function $\sinh(\hat{u})$ is continuously differentiable over the reals; it is smooth everywhere and there exists a derivative at all points in its domain (i.e. it is a C^1 function). Since $\text{arsinh}(\hat{u})$ is the inverse of $\sinh(\hat{u})$, it inherits similar

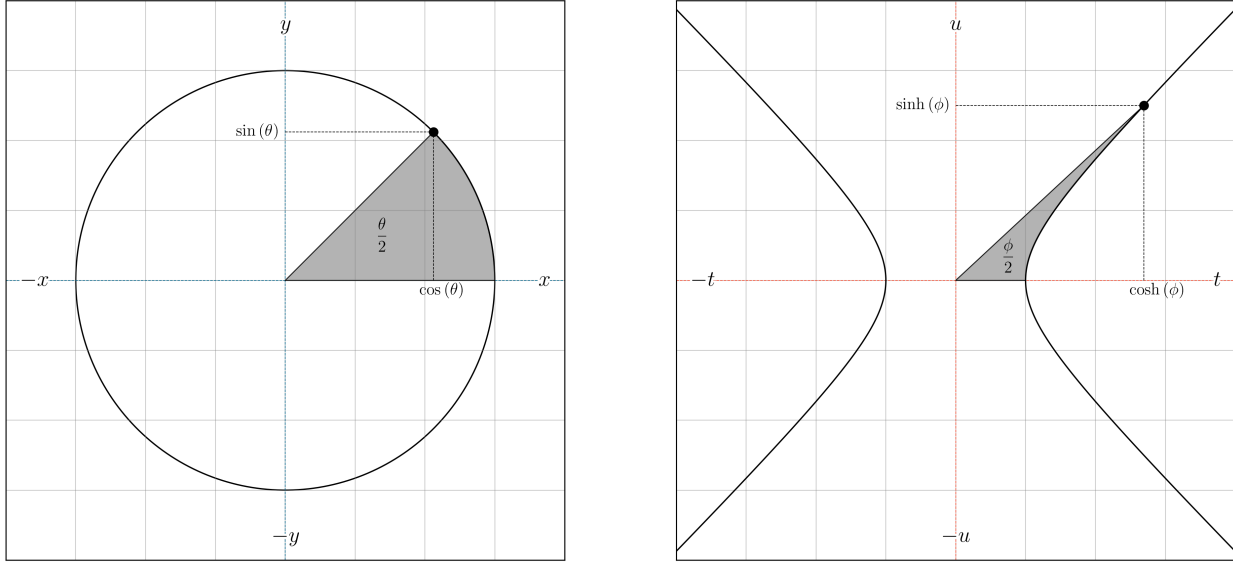


Fig. 55 The circle (first panel) and hyperbola (second panel) trigonometric functions, \sin and \cos , and \sinh and \cosh , respectively, and their relationships to the vertical and horizontal axes of their cognate coordinate systems is presented for clarity's sake. Note the convention used here is that θ refers to the angle measured for a circle, and ϕ refers to the angle measured for a hyperbola. Elsewhere, you will likely encounter other symbols to represent the hyperbolic angle; θ and ψ are common, and so are a and x , but there is no prevailing standard, it seems.

differentiability properties through the inverse function theorem. Therefore, both $\operatorname{arsinh}(\hat{u})$ and its derivative (Equation 335) are well-defined over the real number line as well, $-\infty < \hat{u} < +\infty$. This is the reason we are using $\operatorname{arsinh}(\hat{u})$ and not $\operatorname{arcosh}(\hat{t})$, which is only well-defined for $\hat{t} > 1$ and is ambiguously multi-valued in this domain. We have already observed this behavior. Recall that there is an annoying lack of a general inequality that applies for the relative sizes of \hat{t}_0 , $\min(\hat{t})$, and $\max(\hat{t})$, mentioned above (Equations 328, 330 and 332). The fact that $\operatorname{arsinh}(\hat{u})$ provides all the information we require, unambiguously, is the justification for why such a lack of a general inequality in the \hat{t} notation can safely be ignored; we have no use for \hat{t} because the functions that accept it as an argument are simply not general enough to be useful in this context.

$$\frac{\partial \phi}{\partial \hat{u}} = \frac{\partial}{\partial \hat{u}} \cdot \operatorname{arsinh}(\hat{u}) = \frac{1}{\sqrt{\hat{u}^2 + 1}}, \quad \forall \hat{u} \in \mathbb{R} \quad (335)$$

With that out of the way, we can define a more general $\operatorname{arsinh}(\hat{u})$ function (which yields the hyperbolic angle, ϕ) as the definite integral of its derivative (Equation 335) evaluated from $\min(\hat{u})$ to $\max(\hat{u})$ (Equation 336). Note that forcing $\min(\hat{u})$ in Equation 336 to zero yields Equation 334; however, we can now pass any value for $\min(\hat{u})$ and $\max(\hat{u})$ and measure the hyperbolic angle, ϕ , relative to any positions we want. Much better!

$$\phi = \int_{\min(\hat{u})}^{\max(\hat{u})} \frac{1}{\sqrt{\hat{u}^2 + 1}} \cdot \partial \hat{u} = \left[\ln \left(\hat{u} + \sqrt{\hat{u}^2 + 1} \right) \right]_{\min(\hat{u})}^{\max(\hat{u})} \quad (336)$$

Then, evaluation of the definite integral begins with substitution of the identities for $\max(\hat{u})$ and $\min(\hat{u})$ from Equations 331 and 333, respectively, into the integration bounds in Equation 336 yields a rather grotesque expression for ϕ (Equation 337). However, this can be refactored and simplified into at least three very pleasing redundant forms (Equation 339).

$$\begin{array}{l} \text{from} \\ (331) \\ (333) \\ (336) \end{array} \quad \phi = \ln \left(\frac{P_{\text{high}} - 1}{2 \cdot \sqrt{P_{\text{high}}}} + \sqrt{\left(\frac{P_{\text{high}} - 1}{2 \cdot \sqrt{P_{\text{high}}}} \right)^2 + 1} \right) - \ln \left(\frac{P_{\text{low}} - 1}{2 \cdot \sqrt{P_{\text{low}}}} + \sqrt{\left(\frac{P_{\text{low}} - 1}{2 \cdot \sqrt{P_{\text{low}}}} \right)^2 + 1} \right) \quad (337)$$

$$\text{from (337)} \quad \phi = \ln \left(\frac{\frac{P_{\text{high}} - 1}{2 \cdot \sqrt{P_{\text{high}}}} + \sqrt{\left(\frac{P_{\text{high}} - 1}{2 \cdot \sqrt{P_{\text{high}}}}\right)^2 + 1}}{\frac{P_{\text{low}} - 1}{2 \cdot \sqrt{P_{\text{low}}}} + \sqrt{\left(\frac{P_{\text{low}} - 1}{2 \cdot \sqrt{P_{\text{low}}}}\right)^2 + 1}} \right) = \ln \left(\frac{\sqrt{P_{\text{low}}} \cdot \left(P_{\text{high}} + \sqrt{(P_{\text{high}} + 1)^2 - 1}\right)}{\sqrt{P_{\text{high}}} \cdot \left(P_{\text{low}} + \sqrt{(P_{\text{low}} + 1)^2 - 1}\right)} \right) \quad (338)$$

$$\text{from (338)} \quad \phi = \ln \left(\frac{\sqrt{P_{\text{high}}}}{\sqrt{P_{\text{low}}}} \right) = \ln \left(\sqrt{P_{\text{high}}} \right) - \ln \left(\sqrt{P_{\text{low}}} \right) = \frac{\ln(P_{\text{high}}) - \ln(P_{\text{low}})}{2} \quad (339)$$

At long last, the “natural” parametrization for concentrated liquidity becomes evident. Passing ϕ as an argument to the exponential function, (i.e. e^ϕ) yields the square root of the quotient of P_{high} and P_{low} , which is equal to the [no longer a mystery] constant C , from which the three “pretty” invariant equations emerged (see Section 5.1), which brings this part of the exercise full-circle (Equations 340, 341 and 342).

$$\text{from (339)} \quad e^\phi = C \quad (340)$$

$$\text{from (275) (340)} \quad e^\phi = \frac{(x - x_0)^2 \cdot (y - y_0)^2}{(x \cdot y - x_0 \cdot y_0)^2} = \frac{(x_{\text{int}} - x) \cdot (y_{\text{int}} - y)}{x \cdot y} = \frac{(x - x_{\text{asym}}) \cdot (y - y_{\text{asym}})}{x_{\text{asym}} \cdot y_{\text{asym}}} \quad (341)$$

$$\text{from (276) (340)} \quad e^\phi = \frac{y_{\text{asym}} - y_{\text{int}}}{y_{\text{asym}}} = \frac{x_{\text{asym}} - x_{\text{int}}}{x_{\text{asym}}} = \frac{(y_{\text{asym}} - y_0)^2}{y_{\text{asym}}^2} = \frac{(x_{\text{asym}} - x_0)^2}{x_{\text{asym}}^2} = \frac{\sqrt{P_{\text{high}}}}{\sqrt{P_{\text{low}}}} \quad (342)$$

The remaining trigonometric identities are easily elucidated from the defining relationships of the hyperbolic sine, cosine, and tangent functions (\sinh , \cosh , and \tanh , respectively) (Equations 343, 344, 345 and 346). Curiously, $\cosh(\phi)$ is equal to the quotient of the arithmetic mean and the geometric mean of the price boundaries, which despite being a meaningless coincidence, is a surprising and potentially useful result in and of itself.

$$\text{from (339)} \quad e^\phi = \sinh(\phi) + \cosh(\phi) = \frac{\sqrt{P_{\text{high}}}}{\sqrt{P_{\text{low}}}} \quad (343)$$

$$\text{from (339)} \quad \sinh(\phi) = \frac{e^\phi - e^{-\phi}}{2} = \frac{1}{2} \cdot \left(\frac{\sqrt{P_{\text{high}}}}{\sqrt{P_{\text{low}}}} - \frac{\sqrt{P_{\text{low}}}}{\sqrt{P_{\text{high}}}} \right) = \frac{P_{\text{high}} - P_{\text{low}}}{2 \cdot \sqrt{P_{\text{high}}} \cdot \sqrt{P_{\text{low}}}} \quad (344)$$

$$\text{from (339)} \quad \cosh(\phi) = \frac{e^\phi + e^{-\phi}}{2} = \frac{1}{2} \cdot \left(\frac{\sqrt{P_{\text{high}}}}{\sqrt{P_{\text{low}}}} + \frac{\sqrt{P_{\text{low}}}}{\sqrt{P_{\text{high}}}} \right) = \frac{P_{\text{high}} + P_{\text{low}}}{2 \cdot \sqrt{P_{\text{high}}} \cdot \sqrt{P_{\text{low}}}} \quad (345)$$

$$\text{from (339)} \quad \tanh(\phi) = \frac{\sinh(\phi)}{\cosh(\phi)} = \frac{e^\phi - e^{-\phi}}{e^\phi + e^{-\phi}} = \frac{P_{\text{high}} - P_{\text{low}}}{P_{\text{high}} + P_{\text{low}}} \quad (346)$$

This concludes both our examination of the “natural” concentrated liquidity curve reparameterizations, and our examination of concentrated liquidity in general.

6 Conclusion

This document provides a detailed elaboration of the three preeminent descriptions of concentrated liquidity from Bancor and Uniswap, as well as three additional descriptions informed by their trigonometric analysis in a transformed and normalized coordinate system. Importantly, the equivalence of all six parameterizations is rigorously demonstrated with a view to establish necessary reference standards, and ameliorate an apparent confusion exhibited by fledgling developers as to how to wield the underlying theory.